

**RAPID IMMUNOASSAYS BY  
CAPILLARY ZONE ELECTROPHORESIS WITH  
LASER-INDUCED FLUORESCENCE DETECTION**

**By**

**NICOLE M. SCHULTZ**

**A DISSERTATION PRESENTED TO THE GRADUATE SCHOOL  
OF THE UNIVERSITY OF FLORIDA IN PARTIAL FULFILLMENT  
OF THE REQUIREMENTS FOR THE DEGREE OF  
DOCTOR OF PHILOSOPHY**

**UNIVERSITY OF FLORIDA**

**1994**

*This dissertation is dedicated to my two best friends who are my parents,*

*Richard and Sandra,*

*for all the love and support they have given me over the years.*

## ACKNOWLEDGMENTS

Special note goes to my family for all the encouragement and enthusiasm throughout this experience. They are the greatest fan club a person could have. A special thank you to Aunt Sharon and Uncle George for the endless bull sessions. A particular note goes to George for giving me the courage to begin this endeavor.

Sincere thanks go to the ever-expanding Kennedy group especially Laura Cole the other Kennedy first student. She always seemed to be able to add a fresh insight to my problems. Thanks also go to Dr. Kathryn Williams for allowing me access to the instrumental facilities. An eternal appreciation goes to my roommate, Monica Escobar, for all the friendship and listening. Also, a note to Sunday Brooks who's support and friendship has made this experience much more bearable.

Finally, tremendous gratitude goes to Bob (Dr. Kennedy) for all the ideas and support. His enthusiasm for research truly had a great effect.

## TABLE OF CONTENTS

	<u>page</u>
ACKNOWLEDGEMENTS.....	iii
LIST OF TABLES.....	vi
ABSTRACT.....	vii
<b>CHAPTERS</b>	
1      INTRODUCTION.....	1
Immunoassays.....	1
CZE.....	7
Fluorescence Detection.....	11
Insulin.....	15
Antibodies.....	16
2      NONCOMPETITIVE ASSAY.....	25
Introduction.....	25
Experimental.....	28
Results and Discussion.....	34
Labeling of Fab'.....	46
3      COMPETITIVE ASSAY.....	61
Introduction.....	61
Experimental.....	63
Results and Discussion.....	67
4      APPLICATION I - MEASUREMENT OF INSULIN FROM SINGLE ISLETS OF LANGERHANS.....	89
Introduction.....	89
Experimental.....	90

Results and Discussion.....	93
<b>5 APPLICATION II - DETERMINATION OF BINDING CONSTANTS.....</b>	<b>103</b>
Introduction.....	103
Experimental.....	106
Results and Discussion.....	108
<b>6 CONCLUSIONS AND FUTURE WORK.....</b>	<b>114</b>
<b>APPENDICES</b>	
A PREPARATION OF Fab FRAGMENTS.....	117
B ADSORPTION.....	121
C DETECTOR OPTIMIZATION.....	127
D FITC-INSULIN PURIFICATION.....	134
REFERENCES.....	137
BIOGRAPHICAL SKETCH.....	142

## LIST OF TABLES

<u>Table</u>		<u>page</u>
1-1	Schematic of immunoaffinity interactions.....	9
1-2	Variants in insulin structure.....	16
2-1	Antibody buffer systems.....	35
2-2	Interference study data.....	44
3-1	Electrophoresis buffers.....	69
3-2	Capillary coatings.....	69
4-1	Islet insulin content results.....	94
4-2	Comparison of results of insulin content of rat islets.....	94
4-3	Results of the effects of glucose concentration.....	96
4-4	Results of time release study.....	96
4-5	Ca <sup>+2</sup> release data.....	97
D-1	FITC-insulin absorbance readings.....	135

Abstract of Dissertation Presented to the Graduate School  
of the University of Florida in Partial Fulfillment of the  
Requirements for the Degree of Doctor of Philosophy

RAPID IMMUNOASSAYS BY CAPILLARY ZONE ELECTROPHORESIS  
WITH LASER-INDUCED FLUORESCENCE DETECTION

By

Nicole M. Schultz

December 1994

Chairman: Robert T. Kennedy

Major Department: Chemistry

Two immunoassay techniques utilizing capillary zone electrophoresis with laser-induced fluorescence detection (CZE-LIF) are designed and optimized. Both theoretical and practical aspects of performing a noncompetitive or a competitive assay by CZE are discussed. Benefits of performing such assays include speed and a high mass sensitivity. Run times as short as 30 seconds are achieved with mass limits of detection as low as 30 zeptomoles injected. Applications which benefit from these attributes are also demonstrated.

A noncompetitive assay is demonstrated by detecting the antibody binding fragment (Fab) of a monoclonal anti-insulin using fluorescein isothiocyanate labeled insulin (FITC-insulin). Linear calibration curves over 2 orders of magnitude are obtained with a detection limit of 0.2 nM. The competitive assay utilizes FITC-insulin and the antibody

Fab fragment to quantitate for unlabeled insulin in a standard or sample. Linear calibration curves over 1 order of magnitude are obtained with detection limits of 3 nanomolar for insulin with this type of assay.

Using the competitive assay, single islets of Langerhans are analyzed for insulin content and glucose stimulated insulin release. The results correspond well with those found in the literature. Static incubations are utilized to demonstrate the time resolved release of insulin over a 20 minute period. The dependence of insulin secretion on  $\text{Ca}^{+2}$  content is also observed. These applications demonstrate the capability of analyzing in a microenvironment for a low level amount of protein in a complex biological matrix. The assay is also used to investigate antibody antigen binding interactions. The binding constants of FITC-insulin and insulin for the Fab fragment of an anti-insulin are determined using a Scatchard analysis. This provides a rapid efficient method for analysis with only minute amounts of sample being required.

## CHAPTER 1 INTRODUCTION

Determination of trace levels of compounds in a complex biological matrix has been a challenge to analytical chemists for years. Recently, there has been an interest in incorporating immunoaffinity interactions into capillary electrophoresis (CE) based methods to perform such analyses. By using the selectivity of immunoaffinity interactions and the sensitivity and efficiency of capillary zone electrophoresis with laser induced fluorescence detection (CZE-LIF), a rapid immunoassay has been developed which is capable of microscale analysis on biological samples.

### Immunoassays

Immunoassays are among the most sensitive and selective means for quantitation of proteins and peptides and have therefore become increasingly popular for a wide variety of clinical and biochemical analyses. Quantification of a material depends on the determination of a labeled binder's distribution between its "bound" and "free" phases when combined with the analyte. If these phases are of the same state, the assay is termed homogenous. A heterogeneous assay consists of at least one phase in a solid state and is the format most readily used.

Immunoassays can be classified as noncompetitive or competitive. In a noncompetitive assay, an excess of labeled antibody is used to determine sample antigen. A competitive assay involves the use of a competition in binding created between antibody

and labeled antigen to detect the unlabeled antigen in the sample. In a competitive binding immunoassay, a limiting amount of antibody is mixed with sample and a fixed amount of labeled analyte. As the concentration of analyte (unlabeled) in the sample increases, less of the antibody binding sites are available for the labeled analyte. After incubation, analyte and label which are bound to the antibody are separated from that which remains free in solution. The amount of analyte is then indirectly determined by measuring the relative amount of label in the bound and /or free fractions.

All immunoassays rely on labeled antigens, antibodies or secondary reagents for detection. These labels are most commonly radioisotopes, fluorophores or enzymes (1).  $^{125}\text{I}$  and  $^3\text{H}$  are the most common radioactive tracers and they provide convenient and highly sensitive endpoints for immunoassays. Radioimmunoassays (RIAs) often have detection limits at the picomolar level. However, with the environmental hazard created by the use of these tracers, there has been a move towards developing alternative labeling procedures.

One such 'non-isotopic' alternative has been the use of fluorometric compounds. Another more commonly used tracer is the enzyme label. The product of the enzyme label is detected using spectrophotometric means. The most common type of enzyme assay is the enzyme linked immunosorbent assay (ELISA) in which antigen or antibody is coated onto the wall of a microtiter plate where it binds with the corresponding antibody or antigen in the sample. The complex is quantitated by the addition of an enzyme labeled specific antibody with the concentration being determined colorimetrically. The most attractive feature of ELISA is that enzyme

coupled to the antigen/antibody complex provides a type of chemical amplification by accumulating product during enzyme-substrate incubation. The sensitivity of these procedures is comparable to that of RIA and has the added conveniences of being able to do multiple samples with some steps being automatable.

The primary drawback of common immunoassay formats is that they tend to be slow, manually intensive procedures. This stems from the manner in which they are normally performed. Typical procedures generally require incubation periods of several hours and many washing steps. Analysis times can range from several hours to days. When high throughput is necessary, immunoassays are performed in batches in 96 well microtiter plates (typically 250  $\mu$ L volumes); however, this is not desirable when rapid feedback is necessary or for totally automated procedures. Therefore, recent immunoanalytical research has been directed toward developing rapid, automated immunoassays.

One development has been the introduction of commercial instrumentation in the past 5 years for semi or complete automation of some immunoassay formats. The main limitations to these systems are the limited number of assays which can be performed with such systems.

One type of assay for which commercial automated instruments have been designed is the fluorescence polarization immunoassay (FPIA). Fluorescence polarization is a measure of the time averaged rotational motion of fluorescent molecules. These assays are based on the concept that there will be an increase in fluorescence polarization upon the binding of a fluorescently labeled low molecular weight antigen to an antibody.

This change in polarization is due to a difference in the large hydrodynamic volume of the antigen/antibody complex. These assays are designed as homogenous competitive immunoassays that measure changes in polarization in the presence of competing analyte antigen. These assays have the advantages of being simple to operate, require fewer steps than ELISAs or RIAs and can be easily automated. Their major drawback has been a limitation to low molecular weight compounds (1-10 kilodaltons, kD) because the change in polarization seen in binding of antigen to large molecules is much less than with small molecules hence reducing the sensitivity of the FPIA. However, due to the emergence of several methods for identifying antigen mimicking peptides for almost any monoclonal antibody, FPIAs may be designed for almost any assay system (2).

An example of using FPIA in the detection of a larger molecular weight compound was in the nM level detection of human chorionic gonadotrophin (hCG), a protein of 38 kD (2). The procedure involved the screening of 221 synthetic peptides against a monoclonal anti-hCG by the above mentioned techniques. The one which gave the highest binding was then tagged with tetramethylrhodamine and used in a competitive assay. The detection limit of the assay was limited by the affinity of the antibody for both hCG and the tracer peptide. This assay demonstrated the usefulness of FPIA for larger molecular weight proteins and is thought to expand the usefulness of this type assay.

Another type of assay for which commercial instruments have been designed is a time-resolved fluorescence immunoassay. This type of assay is based on the lifetime of fluorescence after single consecutive excitations and allows for separation between short and long decay emission components by delaying detection. By utilizing this principle it is

possible to enhance the sensitivity of an assay by reducing background signal often caused by bio-organic molecules which have very short emissions. Lanthanide chelates, particularly europium, have been used as labels primarily due to the longititivity of their fluorescent emissions (3). One assay of this type utilized terbium chelates derivatized with a phosphate ester of 5-fluorosalicylate (4). This derivatization allowed for enzyme amplification of the signal. Detection limits of 2.5 fM were achieved for  $\alpha$ -fetoprotein using this ultrasensitive procedure.

Latex immunoassays, which are an amplified method of immunoagglutination, have become a popular type of assay due to their simplicity and the fact that no bound/free separation step is required (3). These assays are homogenous and utilize antibody bound latex particles. Quantitation is based on detection of agglutinated IgG-latex particles after their exposure to the antigen of interest. Detection is often performed by turbidimetry, nephelometry or automated particle counting. One disadvantage of this type of immunoassay is that in the lower concentration range of antigen a long incubation time is often required. For this reason acceleration techniques for latex immunoagglutination are being investigated to make this type assay more rapid.

One recent development in this area has been in the microfabrication of a 0.4  $\mu$ L multiwell reactor for performing latex immunoassays (5). An AC field was applied across this reactor which reduced reaction times normally requiring 20-30 minutes to 30-60 sec. The reduction of reaction time was thought to be due to an increase in collisions and a decrease in volume. A detection limit on the pM level was attained for human  $\alpha$ -

fetoprotein as a model system. This system was designed as part of a project to develop a fully automated flow injection analysis (FIA) technique for sensitive latex immunoassays.

FIA have also been adapted to many immunoassay formats. They typically employ an immunoreactor column that is packed with antibody derivatized silica beads and utilize electrochemical or optical detection. Another type of detection developed for FIA is the use of liposomes to entrap fluorophors (6). Because one liposome can entrap multiple fluorophors, a signal amplification was achieved without the necessary incubation step as in ELISAs. Nanomolar detection limits were achieved with this format which could process up to 4 samples in an hour and had the potential for using multiple columns to increase sample throughput.

Several groups have investigated immunoassay formats based on high performance immunoaffinity chromatography (HPIC) to improve speed and automation (7-11). In HPIC, a high performance column containing immobilized antibodies is used for the rapid separation and determination of a given sample component. These immunoassays can be performed in a few minutes to one hour with detection limits comparable to conventional assay formats.

In addition, several capillary based enzyme linked immunoassays have been developed which reduce the time needed for detection by decreasing the diffusional path length of the substrate. One such assay utilized electrochemical detection with 70  $\mu$ L micro-hematocrit tubes as an incubation bed for quantitation of 2,800 molecules and was completed in 25 minutes (12). Although not automated, this format may be amenable to automation. Another capillary assay utilized 100  $\mu$ m capillaries in an LC type

arrangement (13). A stop flow format with this system was found to provide detection limits on the zeptomole level in 10 minutes. Conventional ELISAs on this detection level would take 12-24 hours for incubations. CE is another technique that may be useful in performing rapid, automated immunoassays as developed in this research.

### CZE

Capillary electrophoresis is a highly efficient separation technique which is based on the differences in migration of analytes in a high electric field applied across a narrow bore capillary (10-75  $\mu\text{m}$  i.d.). In contrast to conventional electrophoresis, much higher fields can be applied and therefore faster separations can be obtained due to the heat dissipation provided by the high surface to volume ratios within the capillaries. There are several modes of CE with the most common being capillary gel electrophoresis, isoelectric focusing, isotachophoresis and capillary zone electrophoresis.

In CZE, a potential is applied across a small buffer filled capillary placed between two buffer reservoirs (see Figure 1-1). Analytes, introduced into the capillary either by electromigration or gravity, migrate differentially through the capillary in discrete zones based on their charge to mass ratios. Due to the presence of electroosmotic flow (eof) in a bare capillary, analytes migrate toward the cathode and can be detected. The eof is formed because an electrical double layer is present at the capillary surface. This flow has a flat profile because it originates near the walls of the capillary because the diffuse double layer is very small. The double layer is created due to an attraction of cations from the buffer to the acidic silanol groups on the capillary surface. Upon application of an electric

field, these positive counterions migrate in the direction of the cathode carrying the buffer and its contents along the length of the capillary.

The velocity of the EOF or electroosmosis ( $\mu_{eo}$ ,  $\text{cm}^2/\text{V s}$ ) affects the migration time ( $t_m$ , s) of analytes. The migration time is also dependent on the voltage (V) applied across the capillary and can be expressed as follows (14):

$$t_m = \frac{L^2}{(\mu_{ep} + \mu_{eo}) V} \quad \text{Equation 1-1}$$

where L is the length of the capillary and  $\mu_{ep}$  is the electrophoretic mobility of the solute. As seen from Equation 1-1, the amount of time an analyte remains in the capillary is minimized by using short columns with high electric fields. These conditions will also serve to minimize any molecular diffusion of the analyte which is a major cause of zone broadening in CZE.

One important feature of CZE is the possibility for highly efficient separations. Theoretical plate counts approaching 1 million have been reported for some protein separations (15). Such high efficiencies are possible due to the absence of band broadening effects caused by having a stationary phase and the flat flow profile which is achieved (14). The separation efficiency can be measured as the number of theoretical plates (N) obtained which can be expressed as follows (14):

$$N = \frac{(\mu_{ep} + \mu_{eo}) V}{2 D} \quad \text{Equation 1-2}$$

where D ( $\text{cm}^2/\text{s}$ ) is the diffusion coefficient of the analyte. The equation implies that the highest efficiencies can be achieved at the highest electric field strengths. This is true as

long as heating in the capillary is not a factor and all other conditions such as injection size are optimized.

Having high efficiencies in CE is important in obtaining good resolution between two analytes. The expression for resolution ( $R_s$ ) showing its dependence on  $N$  is given in Equation 1-3 (14).

$$R_s = \left( \frac{N}{16} \right)^{1/2} \frac{\mu_1 - \mu_2}{\mu_{ave}} \quad \text{Equation 1-3}$$

where  $\mu_1$  and  $\mu_2$  are the  $\mu_{ep}$  of the two analytes and  $\mu_{ave}$  is their average.

Resolution is an important aspect of the immunoaffinity interactions utilized in this work. These separations are based on a change in the electrophoretic pattern as a result of biospecific complexation. The principle of the method is represented in Table 1-1 and uses an approximation for the electrophoretic mobility ( $\mu$ ) of the species as being equal to the charge ( $z$ ) divided by a fraction of the mass ( $m$ ) (16). This schematic shows that the capability of separating the antigen/antibody complex ( $A \cdot Ab$ ) from the free antigen ( $A$ ) or antibody ( $Ab$ ) relies on differences in the charge to mass ratios of the species.

Table 1-1. Schematic of immunoaffinity interactions in CE.

	<b>A</b>	<b>+</b>	<b>Ab</b>	$\leftrightarrow$	<b>A•Ab</b>
<b>Mass</b>	$m$		$M$		$M + m$
<b>Net Charge</b>	$\pm z$		$Z$		$Z \pm z$
<b>Mobility</b> $\mu$	$\frac{z}{m^{2/3}}$		$\frac{Z}{M^{2/3}}$		$\frac{Z \pm z}{(M + m)^{2/3}}$

Affinity interactions have only recently, within the past 5 years, been utilized in CE. They have been used primarily in the development of methods to determine thermodynamic and kinetic parameters of binding using Scatchard analyses (16-24) (discussed in more detail in Chapter 5). Other work has been directed towards using capillary gel electrophoresis to develop base specific separations of oligodeoxynucleotides (25-28). In this type separation, the ligand, which includes bases complementary to those in the oligonucleotide sample solute, are incorporated into the gel matrix. They can interact by forming base paired complexes to the oligonucleotides and are then separated based on a difference in mobilities.

The ability to separate antibody/antigen complexes by CZE was first demonstrated by detection of the formation of singly and doubly bound complexes for human growth hormone (hGH) with anti-hGH (29). In this work, results were compared to those obtained by conventional HPLC and isoelectric focusing, but no assays were performed.

Work presented in this dissertation was the first report of an immunoassay by CZE (30). At about the same time, other groups reported quantitative assays based on affinity type interactions. One example was a microscale agglutination immunoassay which utilized CE with laser-based particle counting detection (31). The assay was based on the agglutination of antibody coated particles in the presence of an antigen. The particles were electrophoretically migrated past a continuously irradiating laser beam. The light scattering events were counted for the agglutinated particles while the unreacted ones were electronically eliminated. This assay was extraordinarily sensitive, a detection limit

of 620 molecules for glucose-6-phosphate dehydrogenase was achieved, allowing enzyme determination in single erythrocytes.

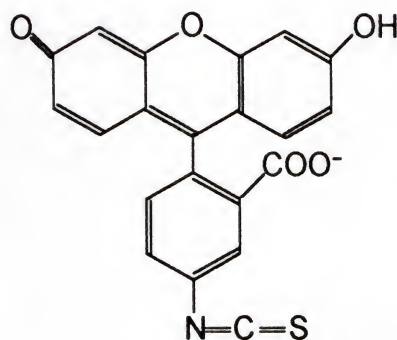
In other work, the amount of hGH was determined with a 5 pM detection limit utilizing fluorescence detection and capillary isoelectric focusing (IEF) for separation (32). The technique used was termed affinity probe capillary electrophoresis because the Fab' fragment of an antibody used to complex the antigen was labeled with a fluorescent dye for detection. Good separation was achieved with low detection limits owing to the use of the IEF mode of CE in combination with laser induced fluorescence detection. In IEF a preconcentration effect is obtained due to the use of the entire length of the capillary for sample introduction. Analytes are then concentrated into a narrow band at their pI. The system is then mobilized to pass by the on-line fluorescence detector. Fluorescence detection is a very sensitive detection mode and is easily adapted to CE.

#### Fluorescence Detection

Fluorescence is a short lived luminescence procedure ( $<10^{-8}$  s) brought about by excitation of a molecule through absorption of a photon. It is a radiational emission between states with the same spin quantum number (33). A molecule in its ground electronic state ( $S_0$ ) can absorb radiation and be promoted to any one of several vibrational excited states ( $S_1$ ) as shown schematically in Figure 1-2. The excess vibrational energy is immediately lost in solution whereby the molecule undergoes vibrational relaxation to the lowest level of the excited state. The excited molecule can then return to its ground state by one of several mechanistic steps. Fluorescence always involves a transition from the lowest vibrational level of an excited electronic state to one

of the vibrational levels of the ground state whereupon it again immediately relaxes to the lowest state. A consequence of these vibrational relaxations is that the fluorescence emission band is always displaced to lower energy i.e. longer wavelengths than the excitation radiation.

The most intense and useful fluorescence is found in compounds that contain aromatic functional groups with low energy  $\pi-\pi^*$  transition levels. Because many molecules do not contain such functional groups, derivatization with a fluorophore is commonly performed. One such fluorophore used in this work is fluorescein isothiocyanate (FITC) which is commonly used to label amine groups. Characteristic of this compound are excitation and emission maxima of 495 and 520, respectively. This makes it highly amenable to excitation with one of several inexpensive, low power lasers such as the 442 nm line of a He-Cd laser or the 488 nm line of an Ar<sup>+</sup>-ion laser. The structure for the molecule is as depicted below.



FITC

Due to the high sensitivities attainable with fluorescence, it has emerged as a very popular means of detection for CE. Requirements for attaining good fluorescence detection with CE include 1) a stable light source, since fluctuations in the residual

background signal determine the limit of detection (LOD), 2) a sturdy but adjustable mounting device for the capillary, and 3) low stray light levels, which include room light plus scattering and fluorescence from the capillary walls. Several configurations and designs have been adapted for use with CE giving extremely sensitive detection. A simple, on-column laser induced fluorescence detection system was reported to give detection limits of 3 pM for a solution of fluorescein (34). Features of this system included the use of the 488 nm line of an Ar<sup>+</sup> laser as the excitation source, off-angle detection and the mounting of the capillary at 20° with respect to the laser beam to minimize scatter from the capillary walls. Another system utilized a sheath flow cuvette chamber as a detection cell to enhance signal and reduce background scatter from the capillary surface. Detection limits of 1-5 pM, or 2-6 zeptomoles injected, were reported for FITC derivatized amino acids (35). In another scheme, a charge-coupled device with time delayed integration was used to detect FITC amino acids in the 20-80 zeptomole range (36).

Other systems have been designed to take advantage of advancements in laser technology. Diode lasers have been used to detect amino acids labeled with a succinimidyl ester at the subattomole level (37). The availability of lasers that operate in the deep UV have made excitation of natural fluorescence possible. Detection limits in the low nM (38) and upper pM (39) range have been reported for species containing tryptophan or tyrosine.

The system used in this work is an epillumination design utilizing a microscope to house the optical system (see Figure 1-3). With this system, a collinear arrangement is used for excitation and to collect the emission radiation. A beam from a laser is directed

into the back of the microscope where it passes through a bandpass filter and is reflected by a dichroic mirror into a microscope lens which focusses the beam onto the separation capillary. The reflected light is then collected by this same lens where it passes through the dichroic because it is of a longer wavelength. It then passes through a series of filters including another bandpass, a longpass and a spatial filter to remove background and scatter from the capillary. The light is then focused onto a photomultiplier tube located at the top of the microscope.

Advantages of using such an arrangement include ease of alignment as the capillary can be viewed through the microscope eyepieces and manipulated into the focused laser beam by adjustment of the XYZ displacement device of the microscope. There is a reduction in background due to a decrease in Raman scattering effects which predominate in perpendicular directions. It also simplifies use of high numerical aperture lenses which enhance fluorescence collection. With a similar arrangement, detection of picomolar amounts of fluorescein labeled amino acids have been reported (40).

Detection for CZE-LIF in the zeptomole range with concentrations on the picomolar level have been attained mostly for derivatized amino acids. However, at such levels the analysis of real samples is fraught with difficulties. These difficulties are due in part to the need for covalent derivatization of the analyte of interest which can be nonquantitative due to the presence of other species that may be labeled. Therefore, an excessive burden is placed on the separation system as well as the detector to remove interferences from other compounds or excess reagents. The use of fluorescently labeled immunochemicals as highly selective tagging reagents could help ameliorate this problem

as has been demonstrated by the importance of immunoassay methods in the analysis of complex samples. The immunoassays developed in this work detect insulin using an anti-insulin and fluorescein isothiocyanate labeled insulin as the immunochemicals. The selection of insulin as a model compound for these assays was based primarily on the usefulness for the applications of interest, to be discussed in Chapter 4.

### Insulin

Studies of insulin are of importance particularly to the medical field because of its role in diabetes. Insulin is a protein composed of two polypeptide chains connected by two interchain disulfide bridges (see Figure 1-4) (41). The shorter chain, called the A chain due to its acidic nature, is composed of 21 amino acids; two of which are involved in an intrachain disulfide bond. The second chain, or B chain, consists of 29-31 amino acids dependent on the species with 30 being the most common number. The variants in the structure from species to species go beyond this difference in number with several amino acids often being changed; however, many regions are highly conserved. It is important to note regions of invariance include the location of the three disulfide bonds, the A chain amino-terminus and regions in both chains near the carboxyl terminal. These regions are believed to be important in the tertiary structure of the compound and play an important role in its function (41).

The differences in the structural features of the insulins used in this work are represented in Table 1-2. All residues are the same as those for human insulin as in Figure 1-4 except those indicated (42). With most amino acids being conserved in these species, they should function primarily the same in the assay as designed. A difference could occur

if there was a structural difference in the epitope that would interfere with binding the antibody. It is of interest to note that the rat is the only mammal known to produce 2 forms of insulin; this is not uncommon to other species such as fishes, however. Also of interest in these variations as well as in other species is that many are located in or near the region known as the A chain loop, A8, A9 & A10, in the 3-D structure of the molecule. This region has been found to be a common epitope for many anti-insulins (43).

Table 1-2. Variants in Insulin Structure.

Species	A4	A8	A9	A10	B3	B9	B29	B30
Human	Glu	Thr	Ser	Ilu	Asn	Ser	Lys	Thr
Bovine	-	Ala	-	Val	-	-	-	Ala
Rat 1	Asp	-	-	-	Lys	Pro	-	Ser
Rat 2	Asp	-	-	-	Lys	-	Met	Ser

- indicates an unchanged residue

As mentioned above, the insulins used in this work are human, rat and bovine. The human insulin is a pharmaceutical preparation used to create standard competitive assay curves that are used to detect rat insulin released from single islets of Langerhans. The bovine insulin was labeled with fluorescein isothiocyanate to be used as the fluorescent tracer. Isothiocyanates are known to react with amines to form thioureas as indicated by the reaction in Figure 1-5 (44). The FITC-insulin used in this work was commercially available (Sigma, St. Louis, MO).

### Antibody.

The anti-insulin used is a monoclonal antibody. Antibodies are large proteins produced in the body in response to foreign molecules (45). They are a large family of glycoproteins that share structural and functional features. Antibodies are composed of one or more Y shaped units. Each of these units is composed of four polypeptide chains,

two each of identical polypeptide chains called the light and heavy chain. Antibodies are divided into five classes bases on the number of Y-units and the type of heavy chain they contain. The type used in this work is the IgG class.

IgG molecules weigh about 155 kD and are bivalent with three protein domains (see Figure 1-6). Two of these domains form the arms of the Y-shape and contain the antigen binding sites. These branches are known as the Fab fragments. The third domain, called the Fc fragment, forms the base of the Y and is important in other aspects of the immune response including binding to certain cells in the body. The Fc portion also contains many of the carbohydrate moieties of the molecule which consists of a variable amount of glycosilations or acidic sugar groups. The region between the Fab and Fc fragments is known as the hinge.

The two heavy chain polypeptides of this class are identical and weigh about 55 kD. They each associate with one of the two light chains through the amino terminal region to form the antigen binding site. Each of these light chains is also identical and weighs about 25 kD. The carboxy terminal regions of the heavy chains fold together to make the Fc region. These chains are held together by interchain disulfide bonds and noncovalent interactions. Each light chain is connected by one interchain disulfide bond to the heavy chain. The heavy chains of an IgG are held together near the hinge region by three such disulfide bonds.

Each chain type consists of variable and constant regions about 110 amino acids in length which combine to form the antigen binding site. The light chain consists of one region of each type. The heavy chains contain one variable and three constant regions.

The differences in this heavy chain determine the four subclasses of IgG. These are known as IgG<sub>1</sub>, IgG<sub>2a</sub>, IgG<sub>2b</sub> and IgG<sub>3</sub>. The subclasses used in this work were of the types IgG<sub>2a</sub> and IgG<sub>1</sub> due to their resistance to secondary digestions in certain enzyme reactions used (discussed later).

As mentioned above, all antibodies used in this work were of the IgG<sub>2a</sub> and IgG<sub>1</sub> types and were obtained as part of monoclonal preparations. Antibodies raised in this manner are produced as descendants of one hybridoma cell line and are therefore identical. The importance of using antibodies prepared in this manner is due to their specificity for a certain antigen and their homogeneity. Having a homogenous supply of antibody is important in obtaining an efficient and reproducible CZE separation that will yield consistent quantitation when complexed with insulin in the assay.

#### Statement of Research

This research describes efforts aimed at combining the selectivity of immunoassay methods with the speed, automation and sensitivity of CZE-LIF. Two types of CZE-based immunoassays, one noncompetitive and the other competitive, are developed in Chapters 2 and 3. Two applications which benefit from such an analysis are described in Chapters 4 and 5.

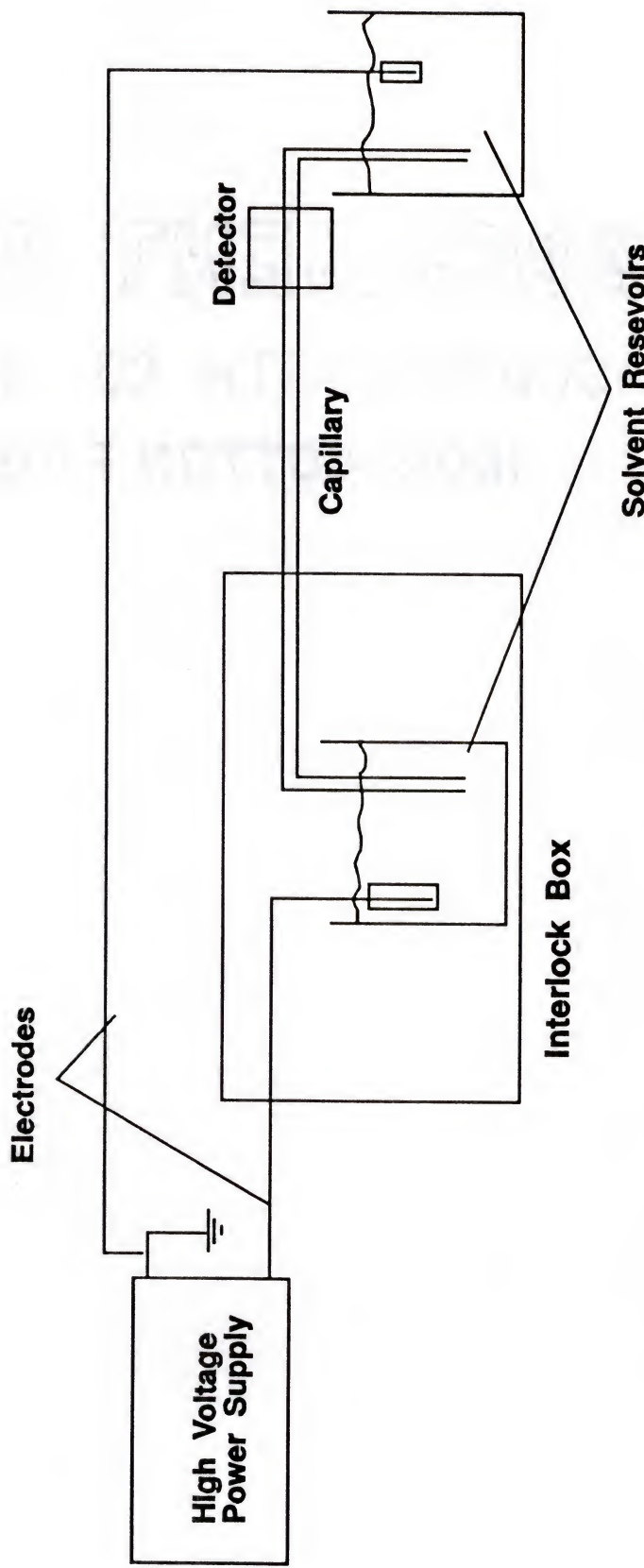


Figure 1-1. Schematic of a capillary electrophoresis system.

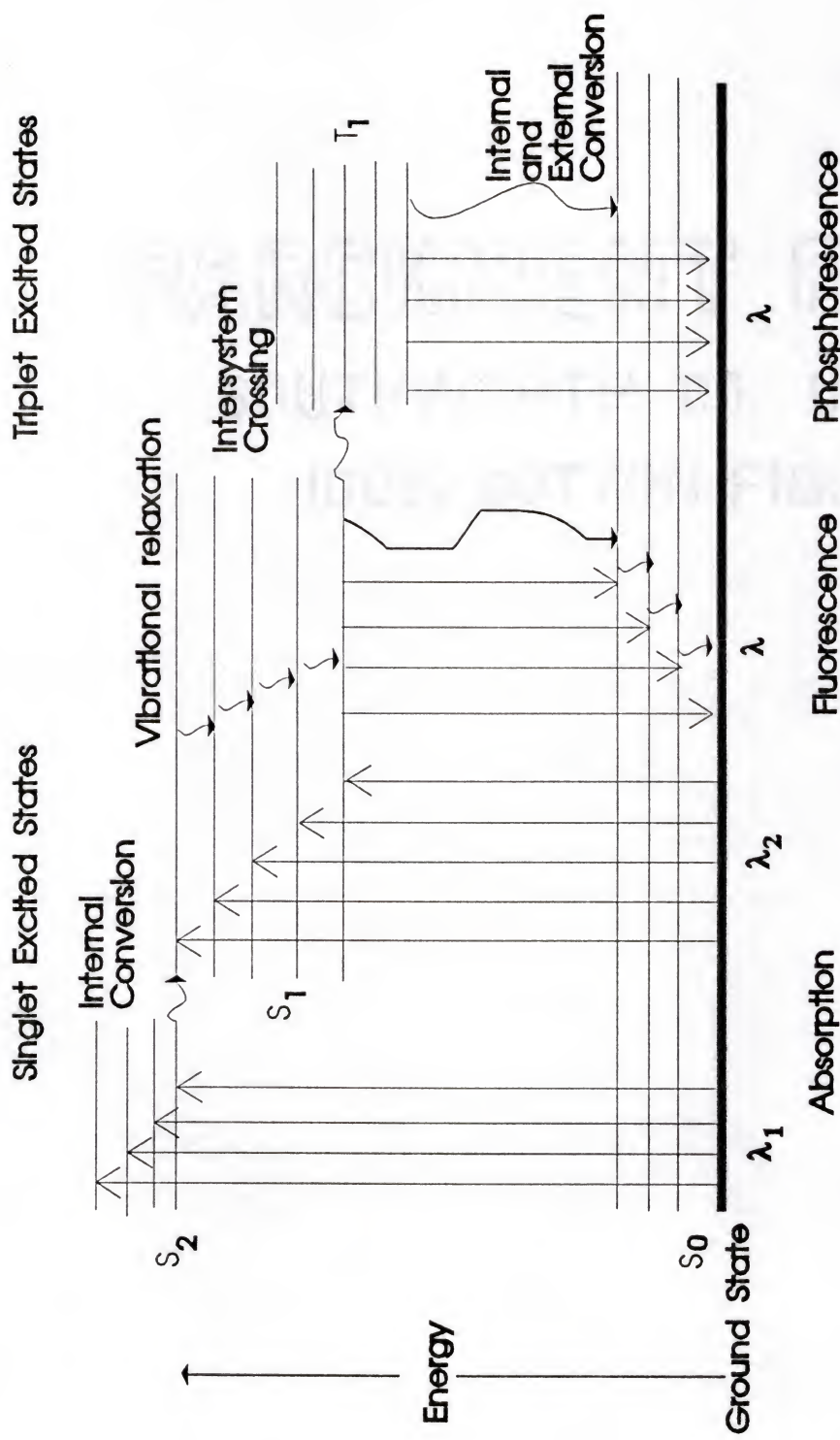


Figure 1-2. Partial energy diagram for a photoluminescent system.

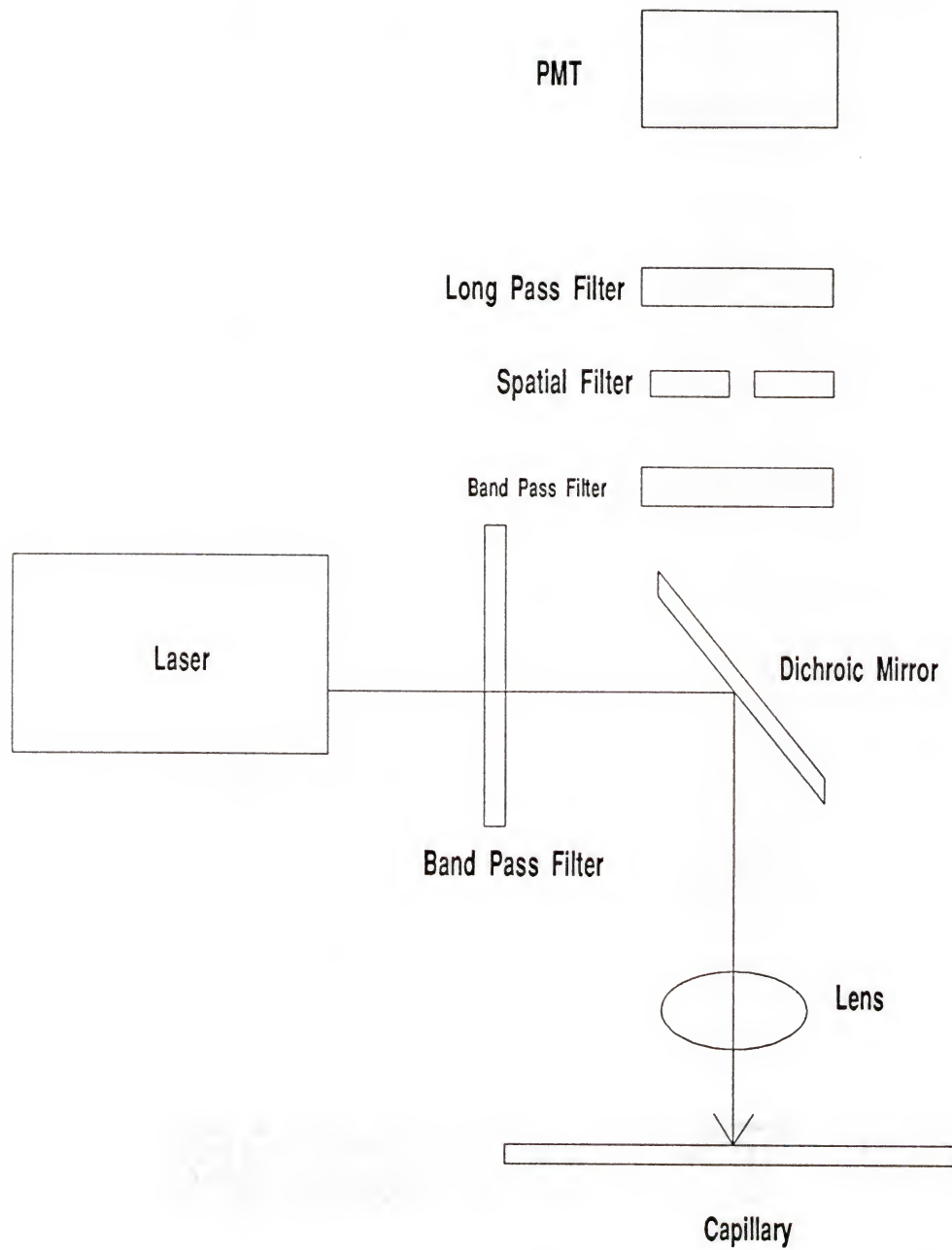


Figure 1-3. Schematic of epillumination detection apparatus.

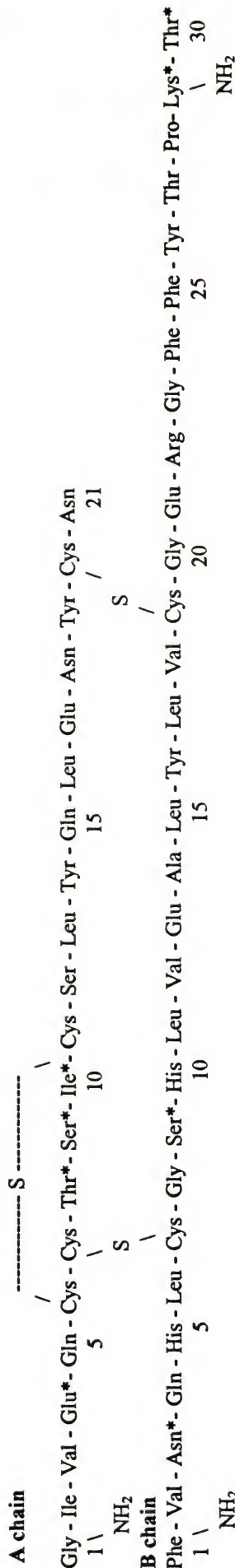


Figure 1-4. Amino acid sequence for human insulin. Inter- and Intra- chain disulfides are as indicated. An amino acid labeled with an asterick (\*) indicates a location for variation among the species used in this work. Locations of amines available for fluorescent labeling are indicated.

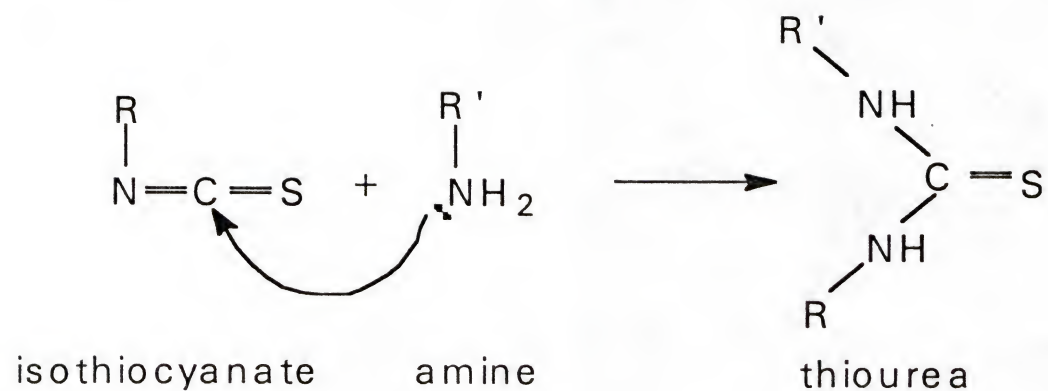


Figure 1-5. Mechanism for FITC labeling.

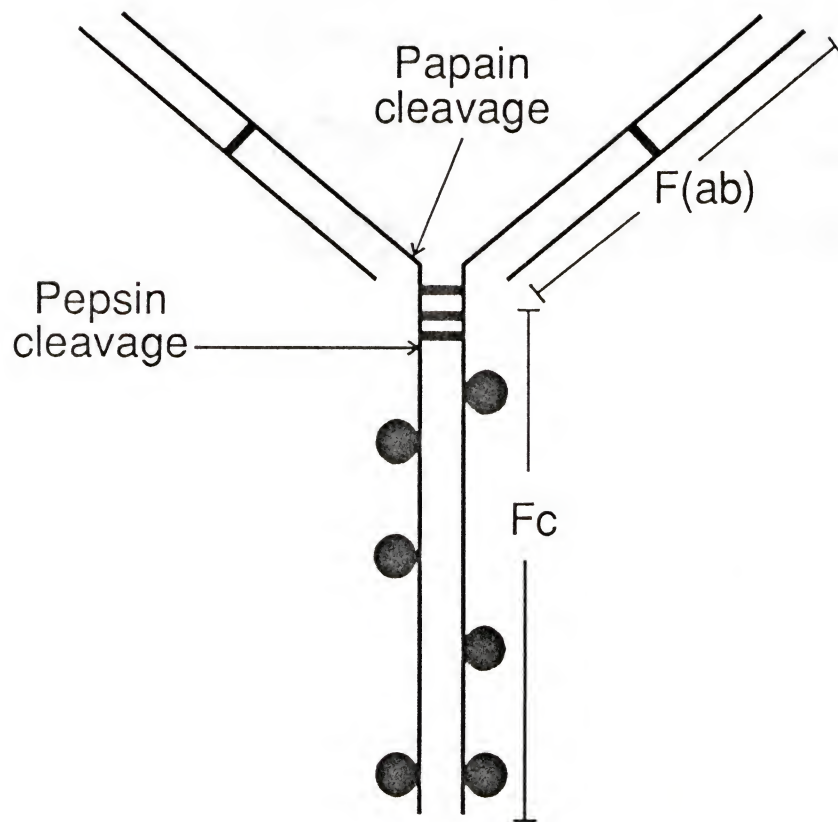


Figure 1-6. Structure of an antibody showing enzymatic cleavage sites pertinent to this research.

## CHAPTER 2 NONCOMPETITIVE ASSAY

### Introduction

The noncompetitive assay was developed based on the following reasoning. If it is desired to determine the amount of antigen in a sample, then a known amount of fluorescently labeled antibody specific for that antigen could be added to the sample. The labeled antibody should form a complex specifically with the antigen of interest. If there is an excess of the fluorescently labeled antibody, then the formation of the complex should be quantitative in the mixture. A capillary electrophoresis separation of the mixture should reveal two zones by fluorescence detection, one corresponding to the excess free labeled antibody and the other corresponding to the complex. If the complex is stable on the time scale of the separation, then it should be possible to quantify the amount of antigen in the mixture based on the amount of complex formed and/or the decrease in the amount of free fluorescently labeled antibody. In theory, the reverse arrangement could be used and antibody quantitated using labeled antigen. In this case, a separation by CZE would yield a zone for the complex and one for the excess labeled antigen.

Examining the complex formation in more detail, the binding reaction between the antibody (A) and the antigen (B) can be looked at in mathematical terms (32). The reaction can be written as



The dissociation constant ( $K_d$ ) can be defined as

$$K_d = \frac{[A][B]}{[AB]}$$

where  $[A]$ ,  $[B]$  and  $[AB]$  are concentrations of the antibody, antigen and complex, respectively.

Using the law of mass action, this can be rewritten as

$$K_d = \frac{([A]_0 - [AB])([B]_0 - [AB])}{[AB]}$$

where  $[A]_0$  and  $[B]_0$  are the total concentrations of A and B respectively. If the approximation that  $[B]_0 \ll [A]_0$  is used, then the theoretical linearity of the response can be predicted by rewriting the law of mass action as

$$K_d = \frac{[A]_0 ([B]_0 - [AB])}{[AB]}$$

Rearranging this equation the complexation ratio of the antigen with the antibody can be written as

$$\frac{[AB]}{[B]_0} = \frac{[A]_0}{K_d + [A]_0}$$

This equation indicates the response of complex formation should be linear as long as the amount of antibody is greater than the amount of antigen and that these amounts remain constant. The above theory also predicts the linearity can be extended in the high concentration range by increasing the original concentration of added antibody.

The separation of the complex from the labeled fragment will disturb the binding equilibrium state and as a result dissociation of the complex will occur throughout the separation process. Thus, it is possible that the amount of complex detected may in fact

be less than that found in the actual assay mixture. The rate of loss will be dependent on two factors, the dissociation rate of the complex and the rate of separation. Therefore, separations need be performed as fast as possible with antibodies with high binding constants.

To determine if an antibody will be suitable for this separation, one can look at the dissociation kinetics of the reaction. Because they are first order, i.e.  $d[AB]/dt = k_{-1}[AB]$ , the half life of the complex can be written as  $t_{1/2} = \ln 2 / k_{-1}$ . Therefore in order to detect at least half of the complex formed and using a run time of 15 minutes, it would be necessary for  $k_{-1}$  to be smaller than  $0.8 \times 10^{-3} \text{ s}^{-1}$ . This value is in the range for antibodies with  $K_b = 1 \times 10^9 \text{ L/mol}$  (46).

This chapter will discuss the development of the noncompetitive assay via initial experiments using whole antibody and UV detection through the best conditions obtained using Fab fragments and laser induced fluorescence detection. In order to demonstrate the noncompetitive assay, fluorescein isothiocyanate labeled insulin (FITC-insulin) was used to quantitate unlabeled anti-insulin or Fab fragment. This arrangement was used because the labeled insulin was commercially available and a labeling scheme for the antibody would be difficult and needed to be developed. Initial experiments were performed with the whole antibody using UV detection. The use of UV detection allowed for the development of suitable separation conditions for the antibody, insulin, and complex(es) as all species could be detected. Once the separation conditions were established, fluorescence detection was used to quantitate anti-insulin Fab fragments. Later work

involved the labeling of the antibody to be used in a noncompetitive immunoassay to detect antigen in a sample.

### Experimental

Chemicals. The whole antibody used was a monoclonal IgG<sub>1</sub> anti-insulin with a reported specificity for human, porcine and bovine insulin with a constant of  $1 \times 10^9$  L/mol. It was purchased as a 1 mg/mL solution (Catalog #CR2024M, Cortex Biochem, Inc., San Leandro, CA). Fab fragments were prepared with a commercially available kit as described in Appendix A from a mouse monoclonal IgG<sub>2a</sub>. The antibody (HL111) was produced from a hybridoma line originally developed by Schroer et al.(43). The cells were obtained from the American Type Culture Collection (ATCC HB 124, Rockville, MD). Schroer et al have reported that the antibody has a binding constant of  $5 \times 10^7$  L/mol for insulin (43). It cross reacts with insulin from human, beef, pork, rabbit, rat and chicken. The antibody was obtained at concentrations of 15-50 mg/ml in phosphate buffered saline following a protein G affinity chromatography purification of mouse ascites fluid from the University of Florida Hybridoma Laboratory. For Fab' labeling, an IgG<sub>1</sub> anti-insulin clone number AE9D6 was used (HL901). It was reported to be specific for the A chain loop of human insulin with an affinity of  $3 \times 10^8$  L/mol (43). It was also prepared by the University of Florida Hybridoma Laboratory and obtained as a solution of 15 mg/ml in a pH 7 phosphate buffered saline solution.

The insulin used was a pharmaceutical preparation of human insulin in a solution of 100 units/ml ( $7 \times 10^{-4}$  M) containing phenol as a stabilizer (Novolin R, Novo Nordisk Pharmaceuticals, Princeton, NJ). The FITC labeled insulin was obtained from Sigma

Chemical Co. (St. Louis, MO) and was reported to have 1.5 mol FITC/ mol of bovine insulin. Mouse IgG used in interference studies was also obtained from Sigma. For the labeling experiments, the pepsin, mercaptoethylamine, ammonium sulfate, and EDTA's were all from Sigma. The iodoacetamide fluorescein (IAF) was obtained from Molecular Probes (Eugene, OR). Chemicals used to make the buffer solutions were obtained from Fisher.

CZE. UV separations were performed in 50  $\mu\text{m}$  inner diameter (i.d.), 350  $\mu\text{m}$  outer diameter (o.d.) fused silica capillaries coated externally with polyimide (Polymicro Technology, Phoenix, AZ). Capillary lengths were 60-80 cm with inlet to detector lengths of 20 cm. A detector window was made by burning a small section of the polyimide with a match in the desired region. The charred outside coating could then be gently removed by wiping with a methanol wetted kimwipe. The interior of the capillaries were pretreated with 10 min rinses of 0.1 M NaOH, DI  $\text{H}_2\text{O}$  and migration buffer at the beginning of each day. Voltage was applied across the capillary using a Bertan 230 high-voltage power supply (Hicksville, NY). The high voltage end of the capillary was housed in an interlock box to prevent accidental electrical discharges to the operator. Separations were performed by applying a negative voltage and injecting samples at the grounded end of the capillary. Electrokinetic injections were made by inserting the end of the capillary into the sample for 10 s and applying 10 kV. Detection was accomplished on-line using a Spectra 100 UV-Vis detector equipped with a capillary flow cell (Spectra-Physics, San Jose, CA). Wavelength measurements were made at 210 nm with a sensitivity of 0.005 AUFS and a 1 s rise time. The output of the detector was interfaced to an IBM-compatible computer

(25mhz, 386 from Gateway 2000, Sioux City, SD) using a data acquisition board (AT-MIO-16f-5, National Instruments, Austin, TX). The data were collected at a rate of 10 Hz. The board also controlled the voltage supply as well as maintained the potential across the interlock system. It was controlled using locally written software. This software was also used for data analysis, i.e., calculating peak migration times, areas, heights, and plate numbers using a statistical moments format.

For fluorescence work, the fused silica capillaries were 25  $\mu\text{m}$  i.d., 150  $\mu\text{m}$  o.d. and 25-30 cm in length. Effective length to the detector window was 12-15 cm. The detection windows were made in this thinner bore capillary by placing a small piece of glass capillary over the desired region. The capillary was then filled with a drop of concentrated  $\text{H}_2\text{SO}_4$  and heated by means of a heat gun to dissolve the polymer coating. The window was cleaned by gently wiping with a methanol wetted kimwipe. This technique proved to be less stringent than the match burning and led to less capillary breakage when trying to remove the charred polymer on these thinner capillaries.

Capillaries were pretreated with rinses of 1 M NaOH, DI  $\text{H}_2\text{O}$ , and migration buffer. The time of these rinses varied greatly and are discussed in more detail in Appendix B. Separations were performed as before with the exception that hydrodynamic injections were used instead of electrokinetic. These were made by inserting the inlet of the separation capillary into the sample vial and raising the vial 9 cm for 5 s. For some experiments, voltage was applied across the capillaries using a Spellman CZE 1000R high voltage power supply (Plainview, NY) due to an incompatability found between the Bertan source and the computer interface.

Detection was accomplished using an epillumination fluorescence microscope equipped with appropriate lenses and filters (Axioskop, Carl Zeiss, INC, Hanover, MD) similar to that described elsewhere (40). For some experiments a 14 mW, 442 nm line from a He-Cd laser (Liconix, Santa Clara, CA) was used as the exciting light. When this laser was used as the source, a 442 nm interference filter (20 nm bandwidth) was used. Other experiments utilized a 488 nm interference filter for the 488 nm line of an air-cooled Ar<sup>+</sup> laser set to a power of 10 mW (Spectra Physics Model 161B, Mountain View, CA). The light was reflected into the back of a 40x, 0.75 NA Zeiss neofluar lens by a dichroic mirror with a 510 nm transition. The light was focused into the center of the CZE capillary at a section which had a 1 cm section of polyimide removed. The capillary was mounted on the stage of the microscope using a carrier design similar to that described elsewhere (40).

The capillary carrier was a piece of plexiglass which was painted black and about the size of a microscope slide. A 1 cm hole was drilled in the center to allow passage of excess laser light. The capillary was aligned across the carrier by means of a small groove carved into its surface. Two smaller pieces of plexiglass were placed over the capillary at either end of the carrier and held it in place by means of screws. Sometimes it was necessary to also apply electrical tape to the capillary to keep it from shifting out of alignment of the laser upon application of the voltage. The ends of the capillary were then placed into buffer reservoirs located at both sides of the microscope stage.

The laser beam was aligned and focused with the capillary by adjusting the stage position and focus of the microscope while viewing the capillary through the microscope

eyepieces. Optimization and alignment procedures are discussed in detail in Appendix C. Emitted radiation was collected by the same lens and passed through the dichroic mirror, a 510 nm bandpass filter and a 520 nm long pass filter. The emitted light was measured using a commercially available photometer system (DCP-2, CRG Electronics, Houston, TX). This instrument was custom fit to the phototube of the microscope. In the DCP-2, emitted light passing the longpass filter was spatially filtered using a rectangular, adjustable diaphragm set at a 1 mm thickness and 2 mm width, and focused onto a photomultiplier tube (R928, Hamamatsu, Bridgewater, NJ). The PMT was operated with a voltage setting of 750 V. Current amplification was adjusted to maintain the signal on scale. The output of the current to voltage converter was interfaced to the computer system described earlier. The data were collected at 20 Hz and low pass filtered with a cut-off frequency of 10 Hz.

For some experiments, a Beckman P/ACE System 2200 (Beckman Instruments, Fullerton, CA) equipped with an Ar<sup>+</sup> laser and fluorescence detection system was used. With this system, separations took place in 37 cm long, 50  $\mu$ m i.d. capillaries placed into the LIF cartridge. A potential of 29 kV was applied across the capillary with the effective separation length being approximately 30 cm. Injections were performed by high pressure at the cathode for 2.5 s. The capillary was rinsed for 2 min with 0.02 M TAPS pH 9 electrophoretic buffer between each run.

Sample preparation. For the whole antibody studies, solutions were prepared by diluting the desired analyte in the migration buffer. The samples were diluted to 3 ml volumes in glass vials and injected immediately.

For the fluorescence assays, solutions of FITC-insulin and Fab were prepared using a pH 7.5, 0.05 M sodium phosphate buffer as the solvent. FITC-solutions were prepared by dissolving solid FITC-insulin in the buffer. The Fab solutions were prepared by diluting the sample as it was collected from the Protein A column (see Appendix A).

To perform non-competitive assays for Fab, an aliquot of the FITC-insulin stock solution was added to the Fab solution. The solution was then adjusted to a final volume of 3 mL by adding 0.05 M sodium phosphate buffer pH 7.5 with 0.025 M  $K_2SO_4$ . The concentration and volume of Fab added were varied to obtain the concentration of Fab desired in the final sample volume. The samples were incubated at  $22^0C$  in borosilicate glass V-vials from Wheaton (Fisher). (Plastic microvials were tried but, they occasionally gave irreproducible results.) Incubation times were between 5 and 10 min unless otherwise noted. When mouse IgG was added to the samples, it was added from a 1.5 mg/mL solution to the FITC-insulin solution to give the desired concentration in the final incubation volume.

Calculations. For quantitative studies and construction of calibration curves, normalized peak areas were calculated as follows. The area of individual peaks was calculated using a statistical moments program written in-house. For each electropherogram, the sum of the areas of all of the peaks due to complex or free FITC-insulin was calculated. The total area was then normalized to the largest total area obtained in the series of separations for the calibration. This normalization was performed to account for variations in the injection volume. The fact that the same

concentration of FITC-insulin was added to all of the samples allows this normalization to be performed.

The detection limit for the non-competitive assay was calculated by determining the concentration of anti-insulin Fab which would give a signal twice the peak-to-peak noise. The signal in this case was the height of the tallest complex peak.

### Results and Discussion

Electrophoresis of antibody and insulin. In selecting the conditions for separation, the main consideration taken into account was the potential for the antibody and/or the insulin to adsorb to the capillary surface. Such adsorption is well documented for separations involving peptides and proteins in CZE and leads to considerable peak broadening and asymmetry. This adsorption problem makes it difficult to obtain the high efficiencies theoretically possible by CE which will be necessary to adequately resolve the insulin/antibody complex from the uncomplexed species. An overview of the adsorption problem in CZE and related information to condition selection are provided in Appendix B.

Several buffer systems were used to develop a suitable separation for the insulin and antibody based on these adsorption considerations (see Table 2-1). The 0.05 M sodium phosphate/ 0.1 M potassium sulfate pH 7.5 buffer was finally selected as it gave the best peak shapes and greatest number of theoretical plates for the species of interest. Because this buffer contained a high amount of salt, a large amount of heat was generated in the capillary upon application of the voltage. This heat generation can lead to the

broadening of peaks. The electric field strength used was 200 V/cm to avoid problems due to heating. Separation times were on the order of 18 min.

Table 2-1. Antibody buffer systems.

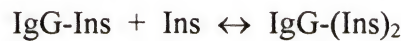
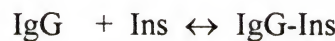
BUFFER	COMMENTS
Fluorad 350 $\mu$ g/ml in 0.05 M sodium phosphate pH 7	poor insulin peak shape
Polybren coating with 0.05 M sodium phosphate pH 7	poor insulin peak shape
0.1 M Tris pH 7.5	no antibody peak, noisy baseline
0.05 M sodium phosphate pH 7.5	antibody peak tailed
0.05 M sodium phosphate pH 7.5 + 0.1 M KCl	noisy baseline
0.05 M sodium phosphate pH 7.5 + 0.1 M $K_2SO_4$	insulin and antibody good shapes
0.05 M sodium phosphate pH 7.5 + 0.05 M $K_2SO_4$	antibody tailed

Figure 2-1 is a series of electropherograms showing the separation of insulin (peak 2), antibody (peak 1) and a mixture of the two. The mixture contained a 100-fold molar excess of the insulin and shows the formation of a new peak (peak 3) which is well resolved from the antibody. This peak is assumed to be due to the formation of the complex between the insulin and antibody. The complex was expected to migrate in this region because its mobility should be more similar to the large MW antibody than the smaller insulin. By the results of this experiment, it does appear as if complex formation between the insulin and antibody occurs and is stable on the time scale of the separation.

Several mixtures of the insulin and antibody were then prepared and run under the same conditions to monitor the dependence of complex formation on the amount of insulin present in the sample. The results from this experiment are depicted in the electropherograms A-D in Figure 2-2. As the amount of insulin was increased, the antibody (peak 1) began to form a shoulder peak (peak 2). An equimolar ratio showed no

presence of the antibody but did show the shoulder peak and the formation of another new peak (peak 3). Finally, a large excess of insulin showed only the latest eluting peak (peak 3) and the excess insulin peak (peak 4). The two new peaks detected are believed to be due to the formation of the singly bound (peak 2) and doubly bound (peak 3) form of the complex between insulin and the antibody.

Because antibodies are bivalent, it is expected that upon mixing the equilibrium achieved will involve the formation of two types of complexes. One complex will be formed for the antibody with only one antigen bound and the other for the doubly bound version. The equilibrium can be represented as follows:



The results here showed the complex formation was at least semi-quantitative as the varied amounts of insulin caused peaks to be formed in a predictable pattern. The 1:1 molar ratio indicated that all the insulin and antibody are bound due to the absence of peaks in those regions. The two new peaks formed were in expected proportions as it was expected that more of the antibody would be involved in single binding before beginning to form double complexes as the antibody became depleted.

With these results, the noncompetitive assay was attempted using the whole antibody and FITC-insulin with the fluorescence detection scheme. The electropherograms in Figure 2-3 are mixtures of FITC-insulin and whole antibody. The separations between the FITC-insulin peaks (labeled 1, 2 and 3) and the complex (C) are seen. The different FITC-insulin zones represent insulin tagged at different locations.

This is believed to be due to the availability of two possible tagging sites on the insulin, therefore two singly labeled and one doubly labeled forms are obtained. It would be preferable to use a single form of the FITC-insulin; however, for these initial studies the FITC-insulin was used without further purification. A calibration curve prepared under these conditions was both nonlinear and irreproducible. These results were attributed to dissociation of complex during the run. The raised baseline trailing to the end of the FITC-insulin zones supports this conclusion. It was thought that faster run times would improve quantitation by allowing less dissociation, therefore, the use of Fab fragments in the assay became of interest.

The Fab fragment of the antibody was more appealing to use in the noncompetitive assay for several reasons. The first reason was due to the simplification of the mathematical model. Fab fragments bind antigens with a 1:1 ratio as opposed to the 2:1 ratio found with antibodies. The second reason was the elimination of the Fc portion of the antibody. As mentioned in the section on antibodies, these Fc fragments contain glycosylations which tend to adsorb to the capillary surface. By removing them from the antibody, the amount of salt in the migration buffer could be reduced thereby allowing higher electric field strengths to be used in the separation. This is beneficial not only to the improvement in efficiency and a savings of time but to the possible reduction of losses due to complex dissociation during the separation. Peak shape may also be enhanced because the molecular weight distribution is more uniform. The MW can vary because the size and amounts of the glycosylations can vary from antibody to antibody even in a monoclonal preparation. This heterogeneity in mass can cause a variation in size and/or pI

of the antibody and therefore effect its migration causing multiple or broad peaks. A final reason for using Fab is that a labeling scheme to fluorescently tag the antibody for a noncompetitive assay is more easily performed with related fragments (to be discussed later).

Fab separation conditions. Suitable separation conditions for the Fab fragments were developed using the experimental conditions for the whole antibody with UV detection. The salt concentration of the buffer found most suitable for the antibody separation was used and then reduced until the peak shapes of the Fab fragment and insulin were no longer suitable. The migration buffer selected was 0.05 M sodium phosphate/ 0.025 M potassium sulfate at pH 7.5. When the 25  $\mu$ m i.d. capillaries were used, an electric field strength of 500 V/cm was applied which gave currents of about 55  $\mu$ A. Run times of 3 minutes or less could be achieved under these conditions.

The use of high electric field strengths and short run times was necessary in order to obtain well-formed complex peaks as illustrated in Figure 2-4. The 3 peaks present in all the electropherograms (labeled 3,4,6) were FITC-insulin forms. The other peaks (labeled 1,2,5) were due to formation of complex upon addition of Fab. All of the separations shown in Figure 2-4 were performed on the same capillary using the same sample injected. The only difference between the runs was the electric field used. As the electric field strength was increased, the migration times decreased and the peaks associated with complex formation became more well-developed. For example, peak 5 at 167 V/cm appeared only as a bump on the baseline. At 333 V/cm, this peak was further developed and at 500 V/cm a well-formed peak was discernible. A similar trend was seen

for peaks 1 and 2; however, at 167 V/cm the band only appeared as an increase in the baseline.

A possible interpretation of these results is that the complex is not stable on the time scale of the slower separations. Therefore, during the course of the slower runs, the complex dissociates giving no peak or poorly formed peaks for the complex. At higher electric field strengths, the separation time is shorter and the complex is stable during the course of the run giving well-formed zones.

This interpretation implies fast dissociation of the antibody/insulin complex as discussed in the theory section. This dissociation may partially result from the relatively low binding constant of the antibody. In addition, the use of high electric field strengths may promote the dissociation of the complex. This is because as soon as the complex is dissociated, the two components are rapidly moved apart by the electric field. In addition, they are moved into a region containing lower concentration of the complex partner, therefore decreasing the possibility of complex reformation. It is suspected that a complex with slower kinetics of dissociation, such as is found with antibodies with higher affinity constants, would not require such fast separation times since the half-life of the complex would be longer.

Another consideration in the separation conditions was the amount of time the samples needed to be incubated before an equilibrium in the binding would be achieved. As can be seen by Figure 2-5, association was achieved and maintained as rapidly as the samples were mixed and injected. In addition, if the samples were allowed to incubate overnight, they gave identical results, within experimental error, to what had been

obtained with 5 to 10 min incubations. Therefore, no incubation period was required before the samples were injected onto the system. These findings were in contrast to RIA and ELISA procedures which require hours and sometimes days before results can be attained.

These results imply a fast formation of complex in solution. This rapidity is partially due to the fact that both reactants are in solution and no reactants are surface bound as in most immunoassays. These fast kinetics are not uncommon for a homogenous solution system as that being used here (32, 46). It is frequently observed that in solution antigen-antibody binding can occur at diffusion-limited rates (47). ELISA and RIA systems are a heterogeneous solution-solid phase arrangement which can adversely affect the kinetics of complex formation because the binding of antibodies to a surface restricts their motion (48).

The assay. Figure 2-6 shows a pair of electropherograms illustrating the concept of the non-competitive assay. For this assay, FITC-insulin was used as the fluorescently-labeled antigen and monoclonal anti-insulin Fab fragments were used as the analyte. The upper figure shows data from a solution containing 100 nM FITC-insulin. Electropherograms of the FITC-insulin revealed three zones (labeled 2, 3 and 5).

The lower portion of Figure 2-6 shows the same insulin solution with 50 nM anti-insulin Fab added. With Fab present in the sample solution, the height of the FITC-insulin peaks decrease and two new peaks (labeled 1 and 4) appear in the electropherograms. The new peaks are apparently due to the formation of complex with the variants of FITC-insulin. Presumably, the peak in front of each free FITC-insulin peak is associated with

Fab complexing with that variant of FITC-insulin. In other words, peak 1 is the complex with FITC-insulin in peak 2 and peak 4 is the complex with FITC-insulin in peak 5. It was expected that the complex would migrate before the FITC-insulin, since studies with UV absorbance detection showed that the Fab has a more positive electrophoretic mobility than the FITC-insulin and would migrate at approximately 55 s under these conditions. The complex with the smallest FITC-insulin (labeled peak 3) was occasionally observed, as in Figure 2-4, however it was usually unresolved from peak 2.

Figure 2-7 illustrates a calibration curve for the measurement of Fab by the non-competitive assay using 100 nM FITC-insulin as a fluorescent tag. Each point is the average normalized area of three runs. The average relative standard deviation (RSD) of the normalized area for the complex peaks was 3.7% and for the free FITC-insulin peaks was 4.4%. The curves show that quantification can be performed by both the decrease of free FITC-insulin peaks or the increase in complex peaks. The use of either peak for quantification is possible because fluorimetry experiments show that there is no quenching of the fluorescence upon complexing of the Fab with the FITC-insulin. The curves also show the expected non-linearity at high concentrations of Fab due to saturation of the FITC-insulin. As mentioned in the theory, it should be possible to extend the linear dynamic range (LDR) beyond the two orders of magnitude illustrated here by using higher concentrations of FITC-insulin which would allow higher concentrations of Fab to be measured without saturation. Improvements in the detection limit, discussed below, would also improve the LDR.

The detection limit, calculated as described in the Experimental Section, for this assay was about 2 nM. Using an injection volume of 0.1 nL, this concentration detection limit corresponds to a mass detection limit of 200 zeptomoles. The injection volume was computed two ways. The first was a calculation involving the Hagen-Pouiselle equation for fluid flux in a capillary based on the conditions of raising a 25  $\mu$ m i.d. capillary for 9 cm for 5 s (49). The equation is as follows:

$$Q = \frac{\pi d_c^4}{128\eta} \rho g$$

where  $Q$  is the volume flowing in a second,  $d_c$  is the capillary diameter (cm),  $\eta$  is the viscosity of the buffer (approximately 0.01g/cm s),  $\rho$  is the density of the buffer (approximately 1 g/mL) and  $g$  is diffusion due to gravity 980 cm<sup>2</sup>/s.  $Q$  is then multiplied by the time of injection and a correction factor for the height the capillary is raised (i.e. 9 cm / 30 cm).

The injection volume was also measured and found to be approximately 42 pL. This measurement was made by placing the capillary end into a fluorescent sample which was raised 9 cm. The sample could then flow by gravity to the detector window. By calculating the volume of the capillary and dividing by the amount of time it took the sample to reach the detector, the flow rate was determined. This rate was then multiplied by the injection time and the volume was calculated. The calculation was performed as follows:

$$\text{Capillary Volume} = \pi r^2 h = \pi (13.5 \times 10^{-4} \text{cm})^2 \cdot 14.5 \text{ cm} = 8.3 \times 10^{-5} \text{ mL}$$

$$\text{Flow} = 8.3 \times 10^{-5} \text{ mL} / 10000 \text{ s} = 8.3 \times 10^{-9} \text{ mL/s}$$

$$\text{Injection Volume} = 5 \text{ s} \times 8.3 \times 10^{-9} \text{ mL/s} = 42 \text{ pL}$$

where the capillary used was 27  $\mu\text{m}$  in i.d. with 14.5 cm to the detector. The amount of time it took the sample to reach the detector window was 2.8 h. The injection time was 5 s.

The direct measurement of the injection volume would be the more accurate of the two ways of determining the detection volume; however, it has been noted that it is possible to acquire an injection in CE by placing the end of the capillary into a sample vial. This injection is due to a droplet of the sample forming on the tip of the capillary. Therefore, mass detection limits have been calculated by using the Hagen-Pouiselle equation to prevent the underestimation of injection volume.

Interference study. An important advantage of utilizing antibody-antigen interactions is specificity. In order to examine possible interferences due to non-specific interaction of the insulin with another antibody, mouse IgG was added in a large molar excess to the sample to study its effects on complex formation between FITC-insulin and anti-insulin. Mouse IgG was added because it would be the most likely interferent since it is similar in structure and function to Fab but is not specific for insulin. The addition of 10  $\mu\text{M}$  mouse IgG to a solution containing 25 nM FITC-insulin produced no detectable complex peaks and no effect on the FITC-insulin zone shapes or migration times. Thus, no non-specific adsorption of the FITC-insulin to IgG was observed. In addition, the presence of 0.5  $\mu\text{M}$  mouse IgG (the only concentration tested) in sample solutions did not effect the slope or intercept calibration curves for anti-insulin Fab over the range shown in

Figure 2-7. A comparison of results of data obtained with and without the IgG is shown in Table 2-2.

Table 2-2. Interference study data.

[Fab] nM	Complex/ Free Fitc-Ins no IgG	Complex/ Free Fitc-Ins 500 nM Mouse IgG
100	0.44	0.42
50	0.20	0.22
25	0.11	0.11
10	0.030	0.027
5	0.017	0.014

Improving the LOD. To lower the limit of detection, several improvements were investigated. First was the use of a laser which provided more efficient excitation of fluorescein. The 442 nm line of the He-Cd laser is well removed from the 490 nm absorbance maximum of fluorescein. Fluorescence spectra of the FITC-insulin in the migration buffer show that a ten-fold gain in signal could be obtained by using 490 nm instead of 442 nm excitation.

The detection limit was also improved by using a purified form of FITC-insulin which yields only one zone by electrophoresis. The fact that the fluorescent signal was divided among the three different FITC-insulin zones increased the detection limit by about two-fold.

Also, antibody with a higher binding constant and longer half-life could improve the detection limit in two ways. First, more of the Fab would be complexed at a given concentration. Secondly, a longer half-life would allow longer separation columns to be used and thus larger injection volumes. These conditions could be used to improve the concentration detection limit by about 7-fold, assuming an injection volume of 1 nL

instead of 0.14 nL, without affecting the mass detection limit. In fact, detection limits of 50 pM were obtained for FITC-arginine using a 90 cm long by 25  $\mu$ m i.d. column and approximately a 1 nL injection volume. (As discussed earlier, using longer analysis times was unsuccessful with the present antibody because of an apparent dissociation of the complex during longer separations.) Thus significant improvements in detection limit were possible with relatively simple changes in the method.

A noncompetitive assay was then performed with some of these improved conditions. One improvement was the use an Ar<sup>+</sup> laser which emits light at 488 nm. The second improvement was to use purified FITC-insulin in the assay. (Purification was performed as described in Appendix D.)

Examples of electropherograms for the noncompetitive assay obtained using these conditions are shown in Figure 2-8. Using the purified FITC-insulin, one peak is obtained for the labeled insulin (peak2) and one complex peak is formed between the FITC-insulin and the Fab. A calibration curve was constructed using 10 nM of the purified FITC-insulin mixed with concentrations of Fab ranging from 0.5-20 nM. A limit of detection of 0.15 nM was obtained which was an improvement of over one order of magnitude from the previously used conditions.

Though the detection of antibody may be of use in clinical studies, the goal of this work was to detect antigen and not antibody. Therefore, further work was directed toward developing a labeling scheme for the antibody so that it could be used to quantitate unlabeled antigen, as originally outlined for the noncompetitive assay. Indeed this has

already been demonstrated using IEF and rhodamine labeled anti human growth hormone as discussed in Chapter 1 (32).

#### Labeling of Fab'

In reversing the assay to quantitate for unlabeled insulin, there are two main considerations to be taken into account: 1) the separation of the Fab from the Fab-insulin complex and 2) the labeling of the antibody of Fab fragment.

The separation of the Fab from its insulin complex will be more difficult because there is no longer the addition of a negative charge upon complex formation associated with the FITC label on the insulin. This means the mobility difference will only be effected by the molecular weight change upon complexing with the insulin. To determine if this separation would be possible, UV experiments were performed to visualize all species involved. Figure 2-9 is a series of electropherograms illustrating the results. The complex peak formed does appear to be resolved from the free Fab. However, experiments performed with smaller ratios of insulin to Fab fragments never showed the presence of two totally resolved peaks for the Fab and Fab-insulin complex. Instead results were inconclusive. However, it is presumed that the peaks will be better resolved by using smaller capillaries and higher electric field strengths as can be done with the fluorescence system. This presumption is supported by the fact that in CZE higher electric field strengths lead to faster, more efficient separations (14).

The second consideration for this assay was the labeling scheme for the antibody fragment. Such a scheme has been developed based on the labeling of the anti-hGH Fab' with tetramethylrhodamine iodoacetamide performed by Shimura and Karger (32). The

idea is to fluorescently label free thiol groups of the Fab' fragment of the antibody. These groups are well removed from the antibody binding region and hence will not cause steric hindrance in binding with the insulin. The whole antibody is not used because these groups exist only upon reduction of the F(ab')<sub>2</sub> fragment of the molecule.

The general labeling scheme is depicted in Figure 2-10. The first step is to enzymatically cleave the antibody with pepsin to form the F(ab')<sub>2</sub> fragments. This digestion proceeds most efficiently with the IgG<sub>1</sub> subclass to cleave the antibody just below the three disulfide bonds found in the antibody's Fc portion (50). The F(ab')<sub>2</sub> fragments can be reduced with a mild reducing reagent such as mercaptoethylamine or dithiothreitol to obtain 2 Fab' fragments. These Fab' fragments are like Fab fragments except that they contain either 3 free thiol groups or 1 free and 1 bridged group along a part of the Fc fragment still remaining. The thiol groups are to be the site of the remaining tagging chemistry.

It was thought by the findings of Karger however, that it was first necessary to produce only monothiol Fab' forms for labeling so that a preferential tagging site was obtained (32). The problem was that multiple tags on the same fragment could cause internal quenching of the fluorescence due to the close proximity of the thiols in the molecule. To obtain such single thiol forms, a controlled oxidation was carried out using 1  $\mu$ M Cu<sup>+2</sup> added to the sample in the form of copper sulfate for 1 h. This reaction was stopped by addition of 1M Na•EDTA. The antibody fragment was then labeled with the fluorophore.

The labeling was accomplished by reaction of the free thiol with a fluorescent iodoacetamide. The reaction is a nucleophilic substitution of an alkyl halide and proceeds as follows (51):



where  $\text{Fab}'-\text{S}^-$  represents the free thiol on the antibody fragment and  $\text{ICH}(\text{FL})\text{COO}^-$  is representative of the fluorescent iodoacetamide.

Attempts at such a labeling scheme were carried out as follows. The antibody used was the HL111 IgG<sub>1</sub>. This particular class of antibody was used for several reasons. First, the pepsin reaction is known to be more efficient for this class because it is not subject to secondary cleavage to form smaller fragments such as Fab (50). Secondly, the location and number of the disulfide bridges is most suited for labeling with this subclass.

To prepare  $\text{F}(\text{ab}')_2$  fragments, 500  $\mu\text{L}$  of the antibody preparation was mixed with 500  $\mu\text{L}$  of 0.02 M sodium acetate buffer pH 3.5 containing 50  $\mu\text{g}$  of pepsin (Sigma). The solution was mixed and left to react for 6 h at 37°C. 50  $\mu\text{L}$  of 3 M Tris buffer pH 8.8 were then added to neutralize and stop the reaction.

The fragments were then precipitated by adding approximately 500  $\mu\text{L}$  of a saturated ammonium sulfate solution to 500  $\mu\text{L}$  aliquots of the reaction solution in a micro-centrifuge tube (Fisher). The precipitation was accomplished by slow addition of the saturated solution at 4°C followed by centrifugation at 12000 rpm for about 5 min (Microfuge System, Fisher). It was found that the precipitation steps were most successful when carried out in a 4°C cold room as the solutions were kept cold at all times. This precipitation procedure is commonly used in biochemistry and is described in

detail in the Antibody Laboratory Manual (45). The saturated solution was prepared by dissolving about 17 g of ammonium sulfate in 100 mL of H<sub>2</sub>O and was stored in the refrigerator. Precipitation is reported to occur at a content of about 50% (NH<sub>4</sub>)<sub>2</sub>SO<sub>4</sub>.

The supernatant was removed with a Pasteur pipette and discarded. The antibody fragments were then reconstituted in 500  $\mu$ L of 0.1 M sodium phosphate solution pH 7 containing 10 mM of the reducing agent mercaptoethylamine and 5 mM EDTA. The reduction of F(ab')<sub>2</sub> to Fab' was allowed to proceed for 30 min at room temperature. The Fab' fragments were recovered using the above described ammonium sulfate precipitation. The precipitate was rinsed 2 times with the saturated (NH<sub>4</sub>)<sub>2</sub>SO<sub>4</sub> solution to remove all traces of EDTA. The controlled oxidation was then carried out by dissolving the Fab' fragments in 100  $\mu$ L of 0.1 M phosphate buffer pH 7 and adding 1  $\mu$ L of a 1 mM CuSO<sub>4</sub> solution. After 1 h, the reaction was stopped by addition of 4  $\mu$ L of 0.1 M Na•EDTA in the phosphate buffer.

The reaction steps were monitored using traditional electrophoretic techniques with silver staining on a PhastGel electrophoresis system (Pharmacia Biotech, Piscataway, NJ). The methods used were as described in the Pharmacia technical notes. SDS-Page analysis was performed as a molecular weight indicator on the pepsin and reduction reactions to determine the presence of whole antibody, F(ab')<sub>2</sub> and Fab'. Results showed bands at about 110 and 25 kD, as compared to standards, which would be indicative of F(ab')<sub>2</sub> and Fc fragments, respectively. The reduced mixture showed bands at 48 and 25 kD indicating Fab' and Fc fragments.

Fluorescent labeling of the Fab' was accomplished by adding 100  $\mu$ L of 1 mM iodoacetamido fluorescein (IAF) dissolved in phosphate buffer pH 7. The reaction was conducted for 30 min in the dark at 37°C.

Initial purification was carried out by size exclusion HPLC by injecting 100  $\mu$ L of solution onto a Synchropak GPC 100 (250 x 4.6 mm). The mobile phase was 0.1 M sodium phosphate buffer pH 7.5 with a flow rate of 1 mL/ min. UV detection was performed at 210 nm. Fractions of 1 mL were collected using an Isco Retriever 5000. Fractions at 2 and 3 minutes were found to contain a fluorescent peak other than those found in the IAF blank fractions by CZE using the Beckman system. Upon addition of insulin, this broad peak migrating at about 2 minutes appeared to shift to a later time. This shift indicated the presence of labeled antibody fragment. A Phastgel IEF of these fractions also indicated insulin binding because fractions containing a mixture of excess insulin to Fab' shifted to a more acidic pH than the Fab' sample. This shift would be expected because the pI of insulin is about 5.5 and the pI of the Fab' was above 6.5. This separation based on pI shows that a separation using capillary IEF should be possible if adequate resolution is not achieved using the free solution format.

These preliminary results indicate that some fluorescently labeled Fab' was made that could bind insulin. Further purification is needed to determine the number of products made, to remove excess IAF and any unlabeled fragments for use in a noncompetitive assay. One possibility for purification is to use conventional slab gel IEF for separation and then to extract the bands from the gel. These fractions could then be used for the CE separation by free solution or IEF.

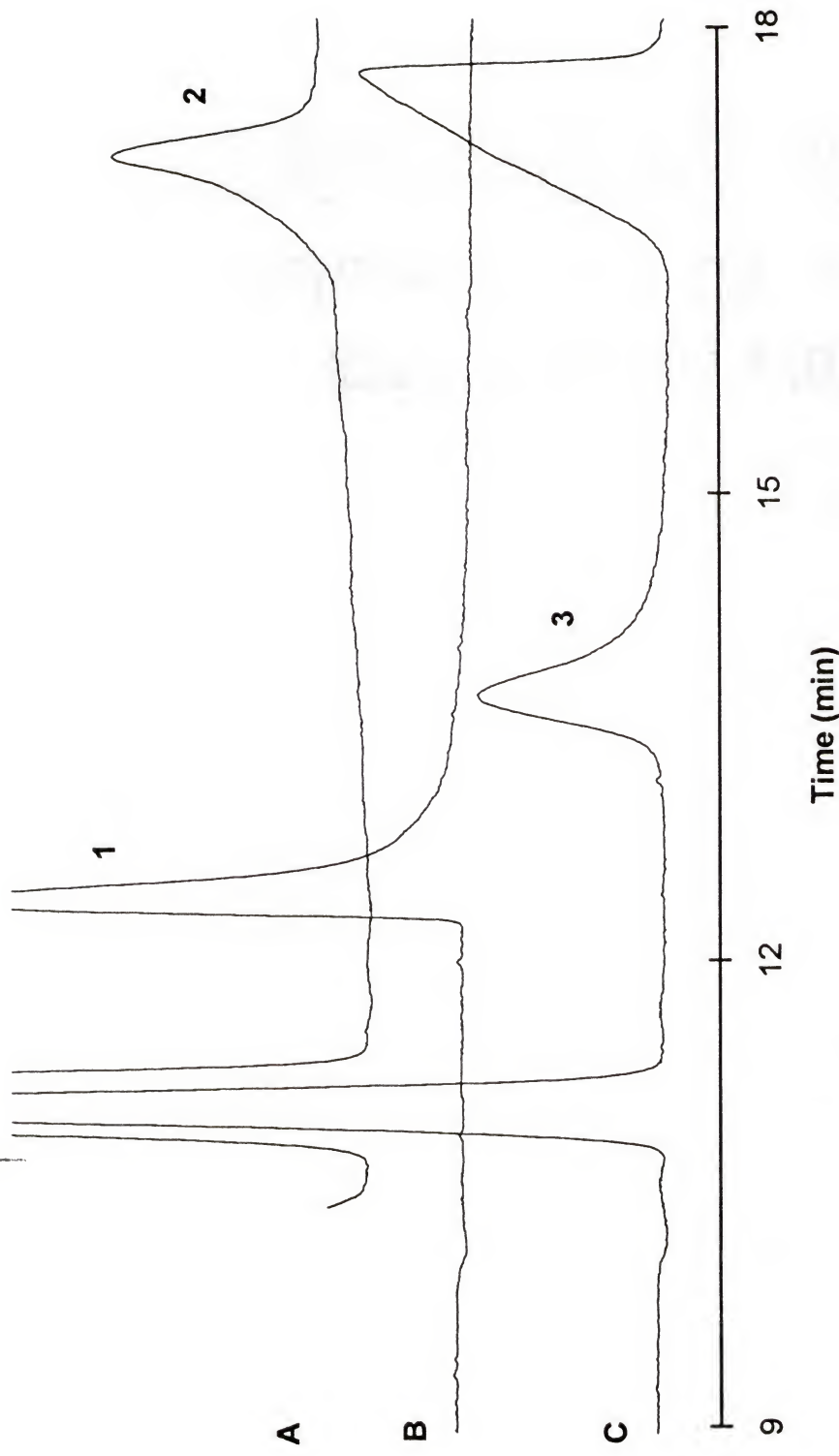


Figure 2-1. Electropherogram A is an injection of 700  $\mu$ M human insulin (peak 2). B is an injection of 7  $\mu$ M antibody (peak 1). Electropherogram C is a mixture of 1:100 moles of antibody to insulin which shows the complex peak 3. The peak not labeled is due to phenol present in the insulin preparation. Conditions are as described in text.

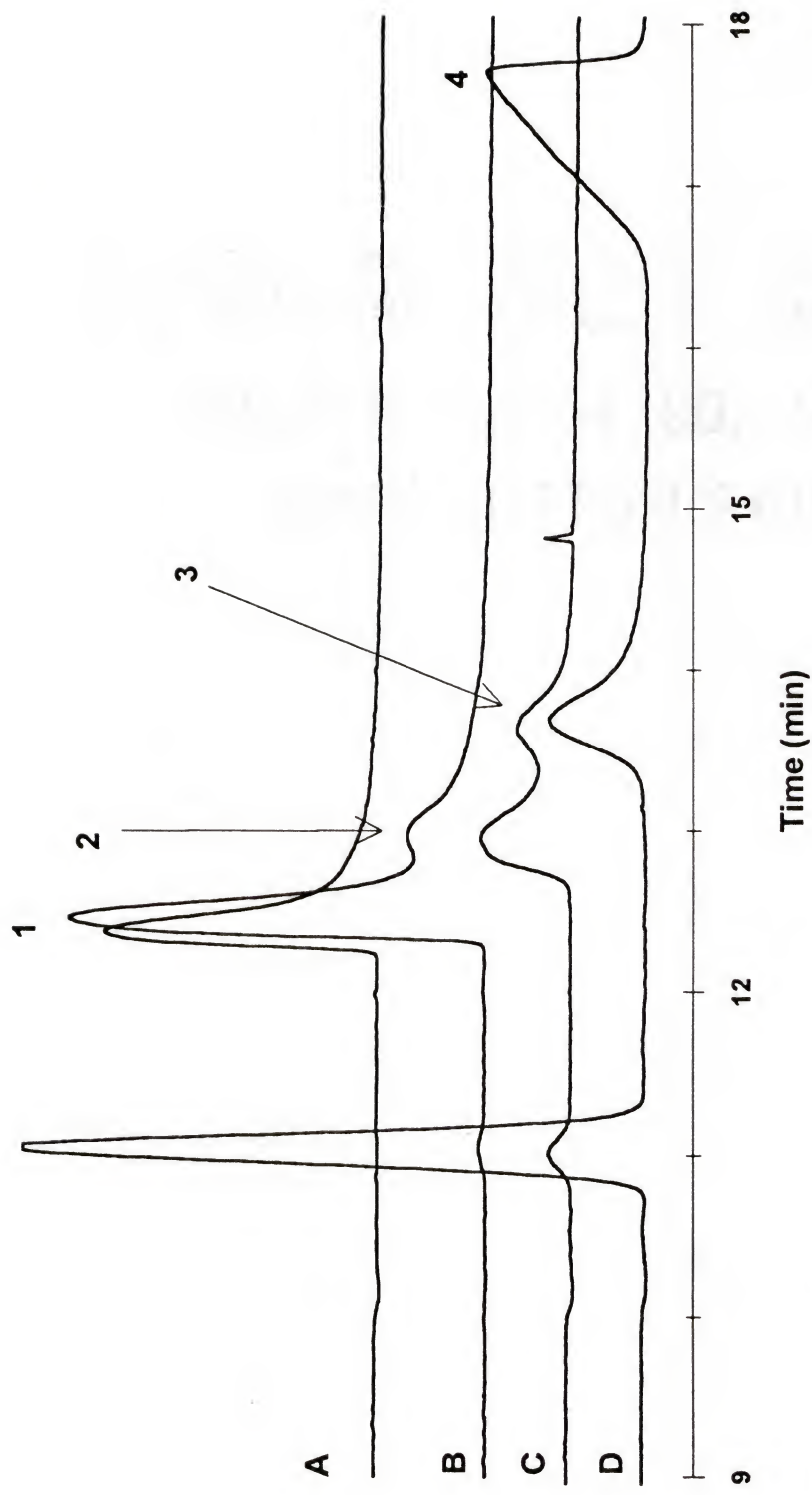


Figure 2-2: Electropherograms A, B, C and D are molar mixtures of insulin to antibody in the ratios of 0:1, 1:6, 1:1, and 50:1, respectively. Conditions and labels are as described in the text. The peak not labeled is due to phenol present in the insulin preparation.

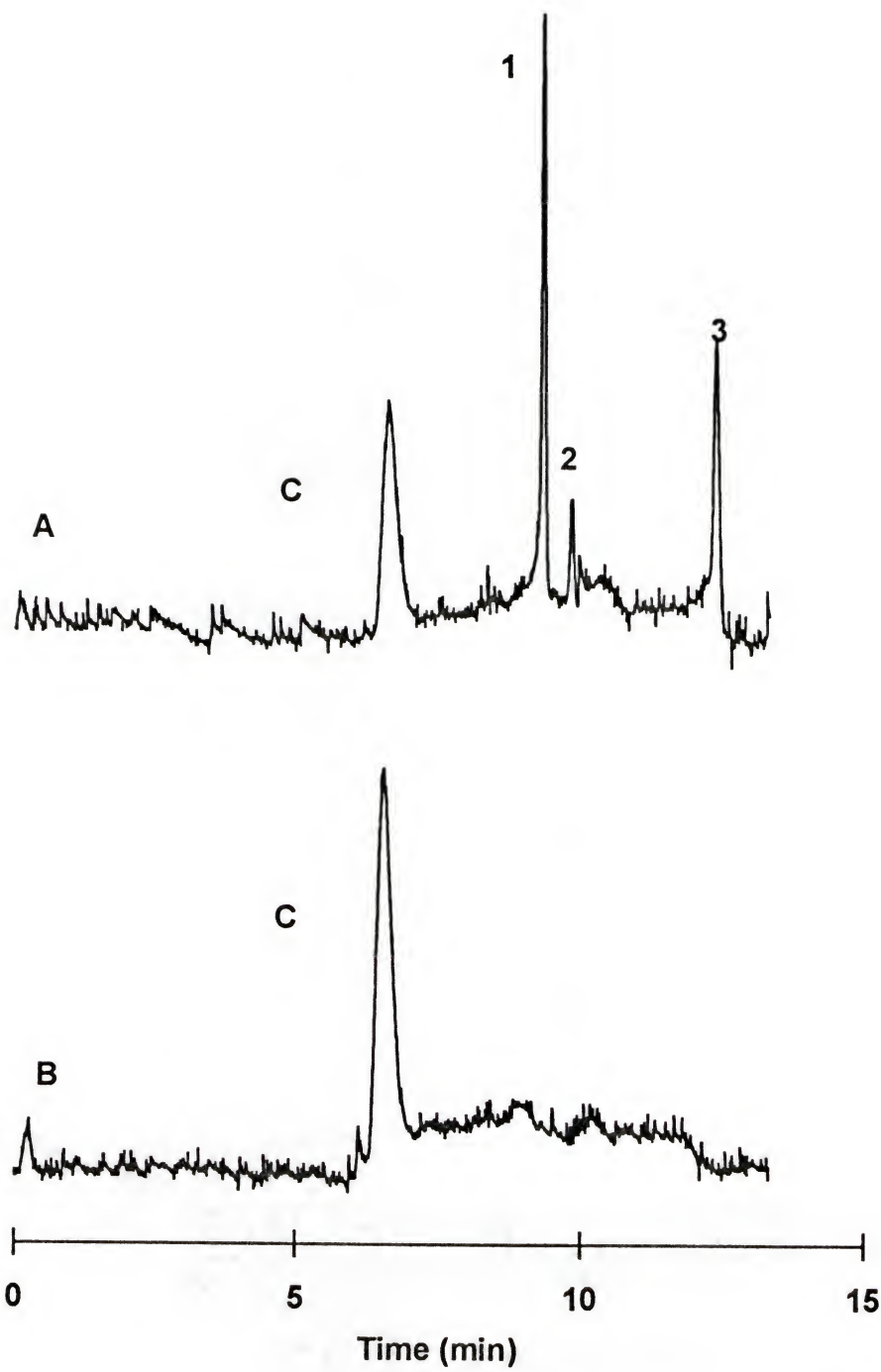


Figure 2-3. Electropherograms A and B are of mixtures of 2.5  $\mu$ M and 5  $\mu$ M Fab with 5  $\mu$ M FITC-insulin, respectively. Peaks 1,2 and 3 are FITC-insulin forms. C is FITC-insulin/Fab complex. Conditions: 25  $\mu$ m i.d. capillary, 30 cm long, 15 cm to detector window, -10 kV, 0.05 M phosphate/ 0.1 M sulfate pH 7.5 buffer.

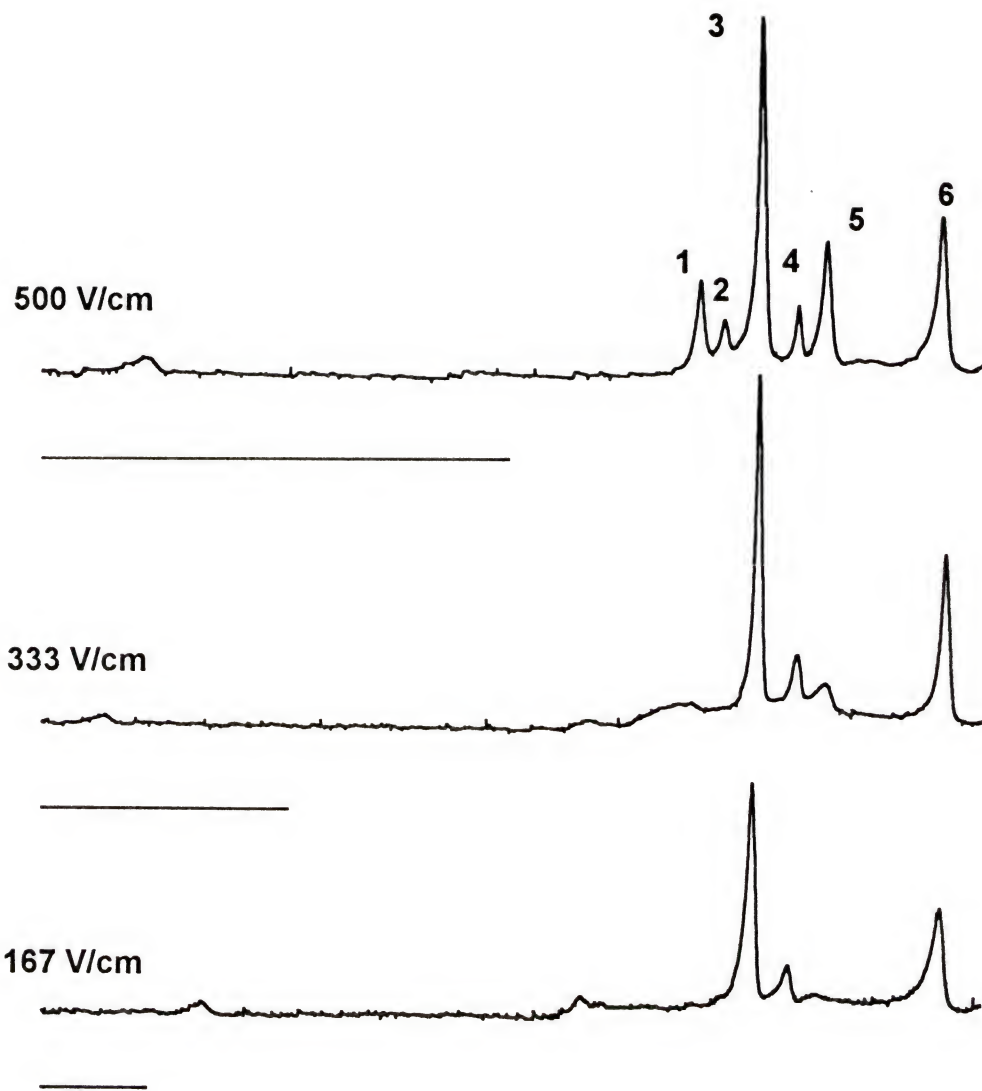


Figure 2-4. Electropherograms at different electric field strengths of mixtures containing  $1.5 \mu\text{M}$  FITC-insulin and  $0.75 \mu\text{M}$  Fab. Each trace starts at the beginning of the separation. The bar under each electropherogram is 1.0 minute long. Peaks 3, 4, and 6 are FITC-insulin. Peaks 1, 2, and 5 are due to the formation of complex of Fab with FITC-insulin in peaks 3, 4, and 6 respectively.

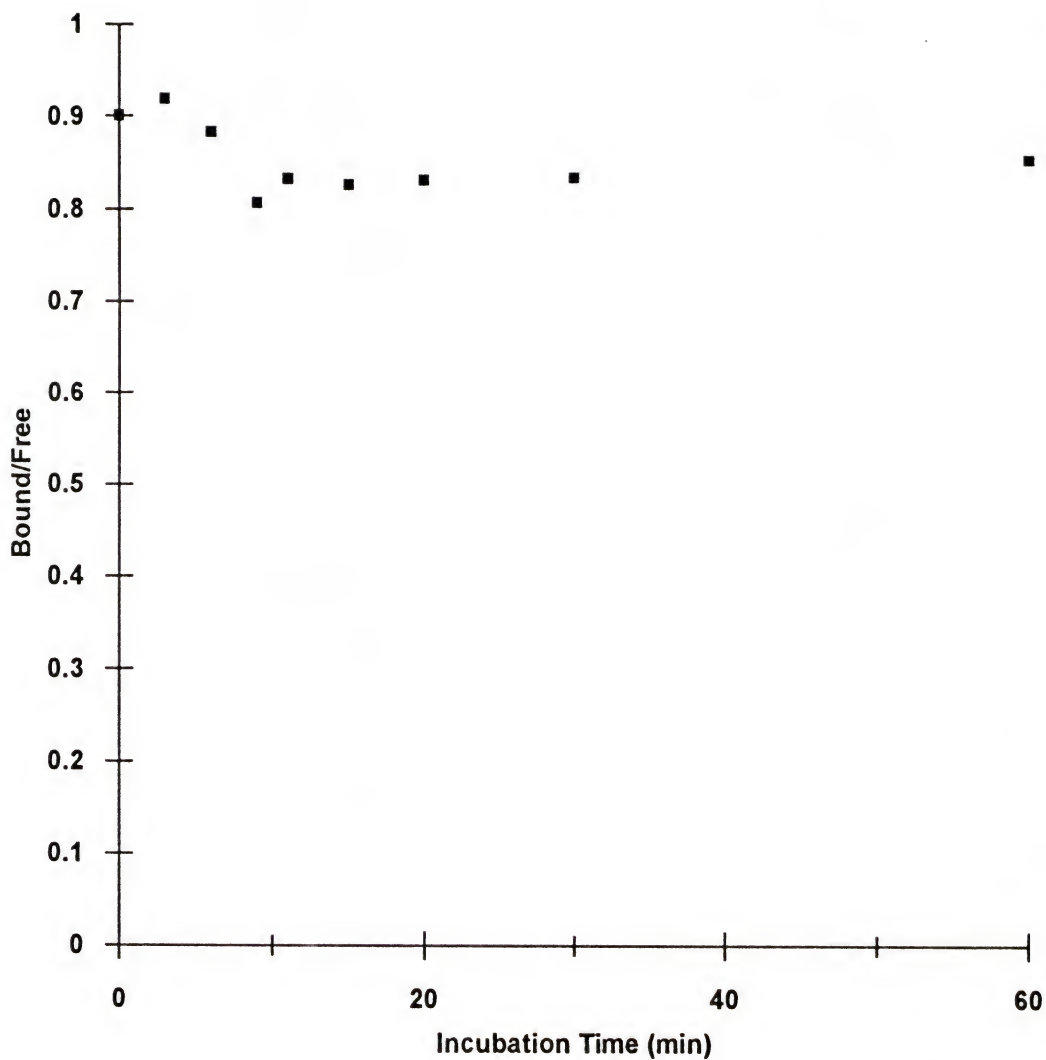


Figure 2-5. Plot of bound area/free area for FITC-insulin versus the time from mixing to injection.

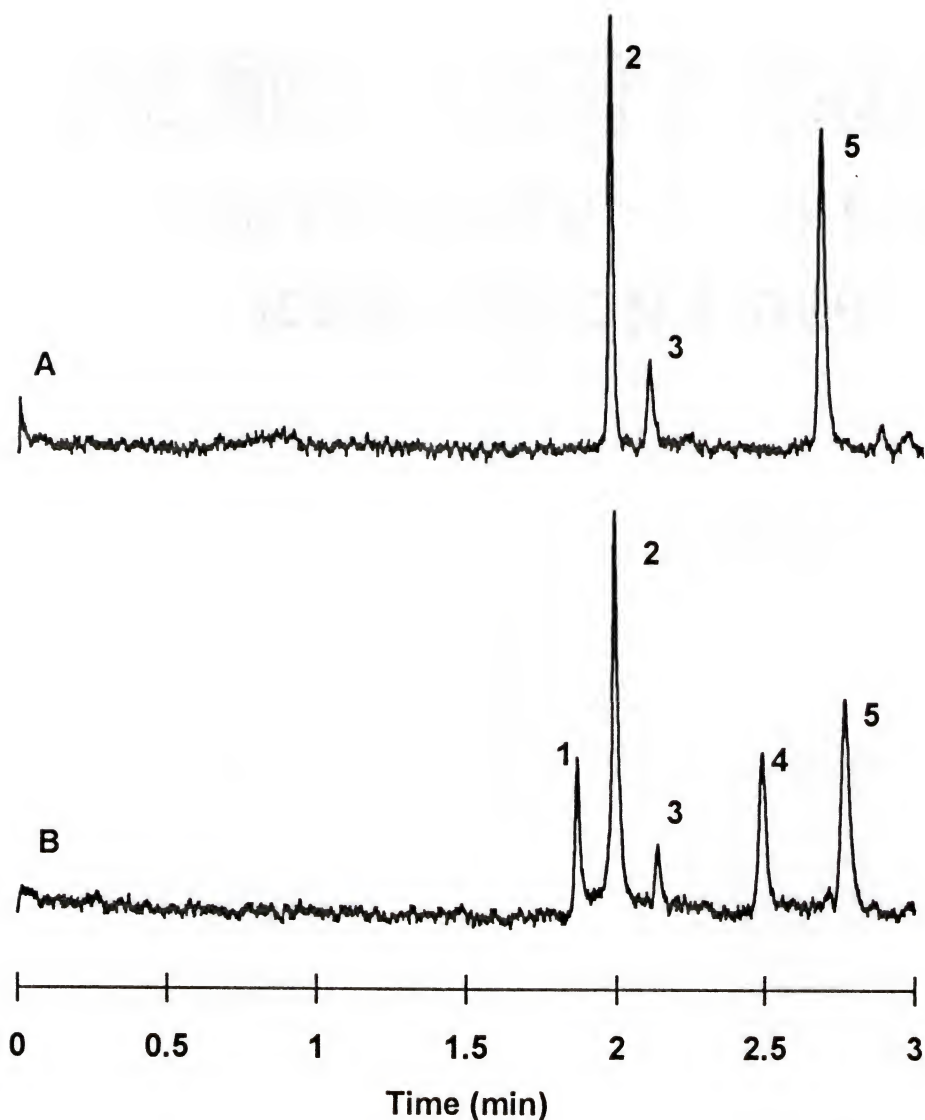


Figure 2-6. Electropherogram A is of 100 nM FITC-insulin under conditions described in the experimental section. Electropherogram B is of 100 nM FITC-insulin and 50 nM Fab. Peaks 2,3, and 5 are FITC-insulin. Peaks 1 and 4 are due to the formation of complex of Fab with FITC-insulin in peaks 2 and 5 respectively.

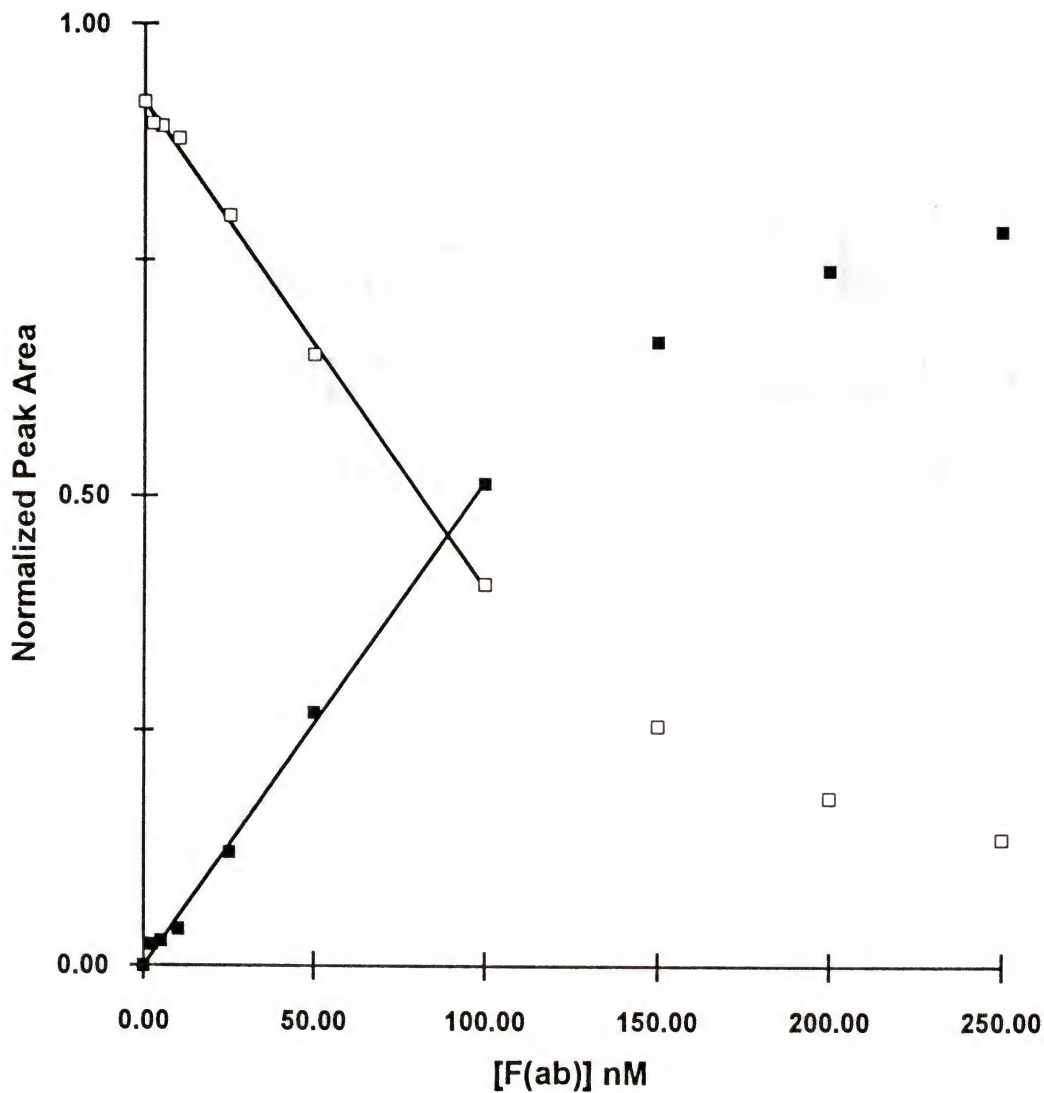


Figure 2-7. Calibration curve for determination of F(ab) by the non-competitive assay. Normalized peak areas calculated as described in the text. The solid squares are peak areas for F(ab)-FITC-insulin complex and the hollow squares are peak areas for FITC-insulin. The error bars (one standard deviation) are within the points. The lines drawn represent the linear least squares fit through the points indicated and had a correlation coefficient of 0.997.

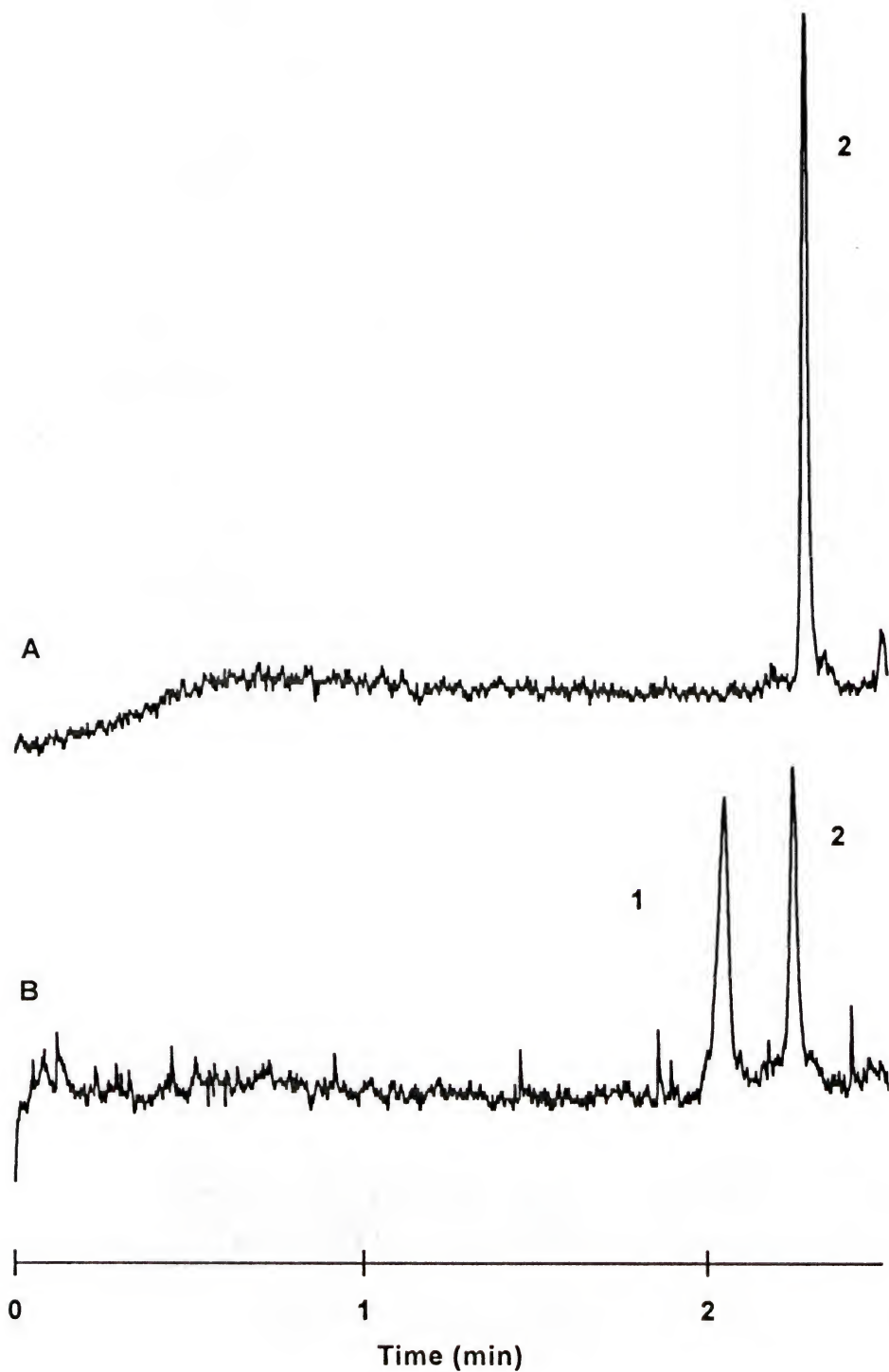


Figure 2-8. Electropherogram A is an injection of 20 nM FITC-insulin purified fraction 3 (peak 2). Electropherogram B is a 1:1 M mixture of Fab and FITC-insulin 3. Conditions are as described in text.

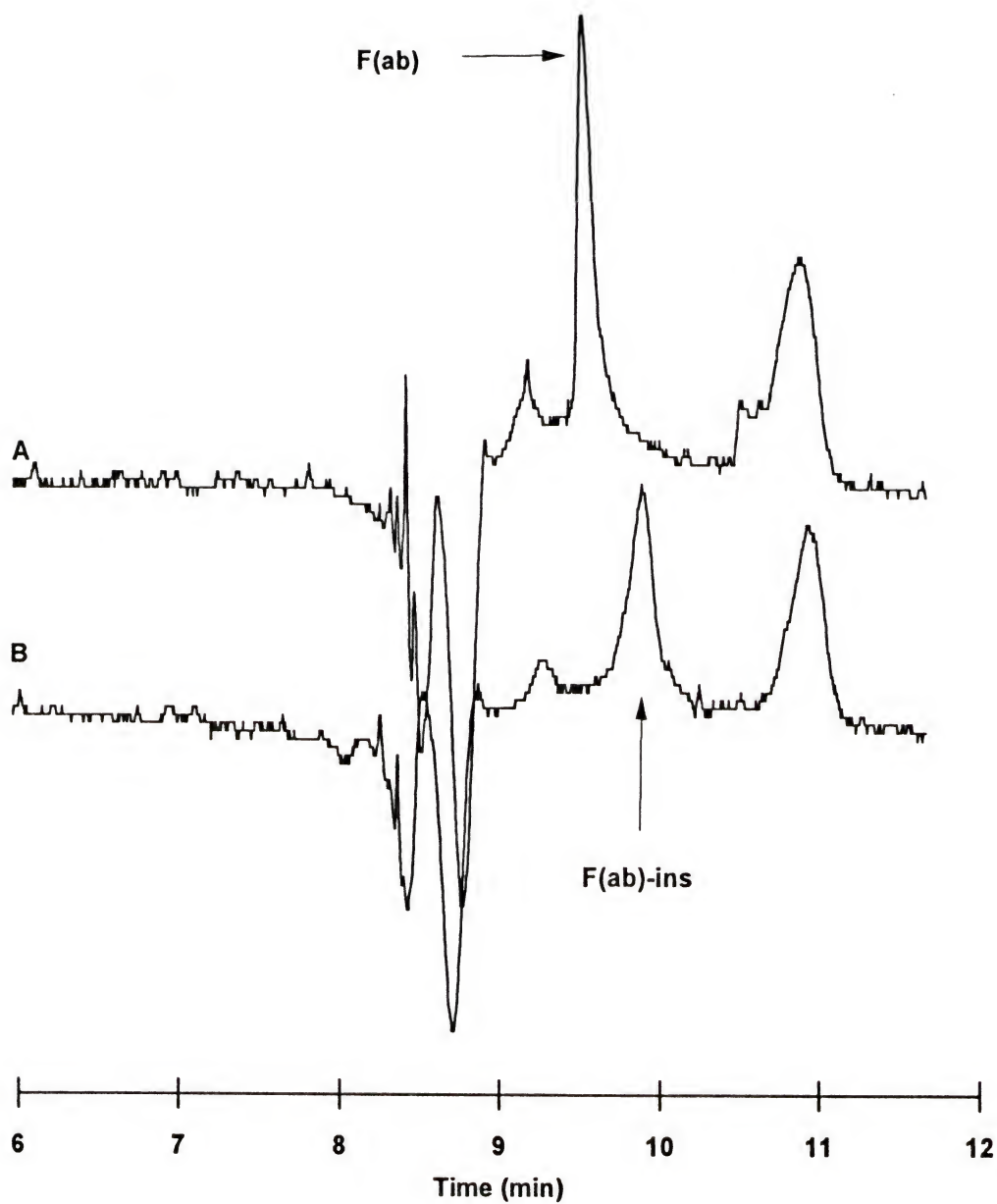


Figure 2-9. Electropherograms of  $2.5 \mu\text{M}$  Fab (A) and a 1:1 M ratio of Fab and Insulin (B) done with UV detection. The dips and unlabeled peak are due to the Fab buffer. Conditions are as in the antibody UV section.

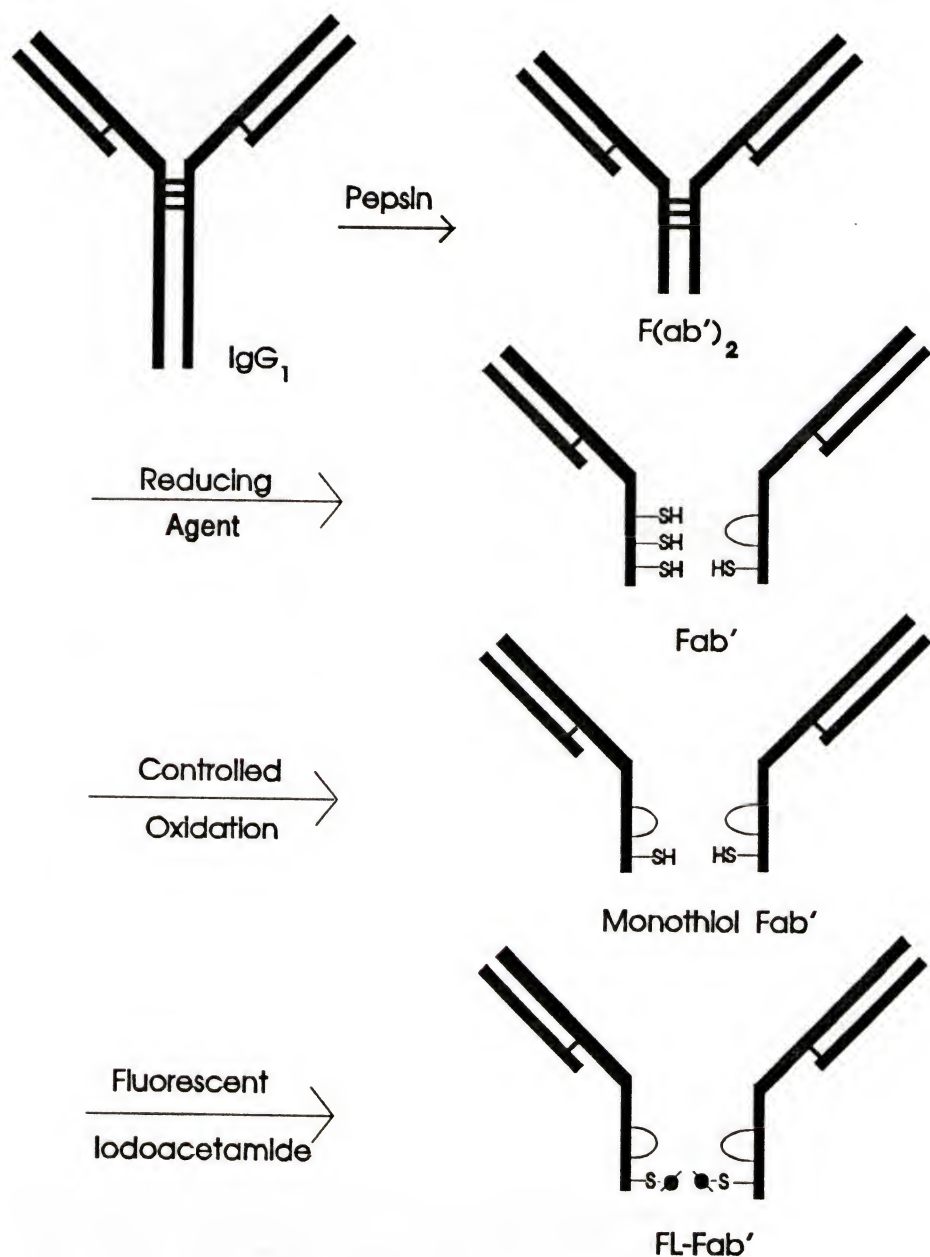


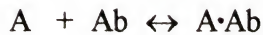
Figure 2-10. Fab' labeling scheme as described in the text.

## CHAPTER 3 COMPETITIVE ASSAY

### Introduction

The principle of competitive assay is that if fluorescently-labeled antigen and a limiting concentration of antibody, or fragment of antibody, are added to a sample solution, then labeled antigen and sample antigen will compete to form complex with the antibody. A separation by CZE with fluorescence detection will yield two zones, one due to the complex between fluorescently-labeled antigen and antibody and the other due to free fluorescently-labeled antigen. Antigen in the sample will increase the amount of free fluorescently-labeled antigen as the unlabeled sample antigen binds with some of the antibody. This releases some of the fluorescent antigen from the complex, therefore decreasing the amount of complex formed between the fluorescently-labeled antigen and antibody. Thus, it should be possible to quantify antigen based on comparison of the two zones with standards.

Quantitative aspects of this assay can be viewed in terms of a mathematical model developed for protein binding assays (52). With this type of assay, the equilibrium between the fluorescent antigen ( $A^*$ ), the sample antigen (A) and the antibody (Ab) can be described by the following relationships:



where  $A^*\cdot Ab$  and  $A\cdot Ab$  are the complexes formed between the antibody and the labeled and unlabeled antigens, respectively. Differential equations to describe the dynamics of these relationships can be written and solved to obtain a quadratic relationship between the concentration of the bound over free labeled antigen ( $B^*/F^*$ ) and the total amount of unlabeled antigen ( $A_{total}$ ) in a sample. Equation 1 describes the relationship with the assumption that the labeled and unlabeled antigen have identical properties and participate in the binding identically.

$$\left(\frac{B^*}{F^*}\right)^2 + \frac{B^*}{F^*} (A^*_{total}K_{eq} - Ab_{total}K_{eq} + A_{total}K_{eq} + 1) - Ab_{total}K_{eq} = 0 \quad \text{Equation 1}$$

$A^*_{total}$  is the original amount of fluorescent antigen added to the sample,  $Ab_{total}$  is the amount of antibody (or antibody fragment) added and  $K_{eq}$  is the equilibrium or binding constant of the antibody. This equation allows the  $B^*/F^*$  to be predicted for a given antigen concentration range.

Figure 3-1 shows theoretical plots for antibodies with binding constants of  $5 \times 10^7$  L/mol (C) and  $5 \times 10^8$  L/mol (A) and a concentration of 100 nM for both labeled antigen and antibody. The expected sigmoidal shape is obtained for a plot of  $B^*/F^*$  vs. log unlabeled antigen concentration and has a limited linear range which can be used to quantitate unknown samples. The plots demonstrate the effects on the expected calibration curve when using antibodies of different binding constants or by varying the concentrations of antibody and labeled antigen in the assay.

Comparing plots A and C shows that an increase in the binding strength of the antibody serves to improve the assay by increasing the bound/ free ratio. This increases

the assay sensitivity which is seen as an increase in the slope of the plot. Also, the lower linear region of the plot is extended which in turn lowers the limit of detection. The effects of changing concentrations of the labeled antigen and antibody are shown in plots B-E. For a given binding constant, a decrease in concentration of the equimolar ratio of labeled antigen to antibody causes a slight decrease in the binding ratio (plots C & D). A decrease in the amount of labeled antigen added relative to the antibody concentration causes a decrease in the slope. A slight increase in the slope is seen when the labeled antigen is in excess; however, there is not a significant improvement in the LDR which would improve the limit of detection. Therefore, the best improvement in terms of sensitivity and LOD would be found with an increase in the binding constant of the antibody. An increase in the binding constant of the antibody would also decrease dissociation of the complex during the CZE separation as discussed in Chapter 2.

This chapter describes development of the competitive assay. Capillaries coated with a neutral hydrophilic polymer were used to improve reproducibility and reliability of the CZE separations. LOD's limited by the antibody binding capacity were attained and are of the magnitude necessary for future applications (discussed in Chapters 4 & 5).

### Experimental

Chemicals. Fab fragments were prepared as described in Appendix A from the HL111 monoclonal mouse anti-insulin IgG<sub>2a</sub> ( $K_b = 5 \times 10^7$  L/mol) described in the noncompetitive assay experimental section. Two higher binding antibodies were also used. One was the HL901 IgG<sub>1</sub> with an affinity of  $3 \times 10^8$  L/mol described in Chapter 2 (43). A third antibody used was obtained from BiosPacific (Catalog/Clone #

A61250228P, Emeryville, CA). It was a monoclonal IgG<sub>1</sub> with an affinity constant of 8.1 X 10<sup>8</sup> L/mol and was reported to cross react with rat, mouse, human, bovine and porcine insulins. The entire 1 mg/ml fraction obtained in pH 7.4 PBS was used to prepare the Fab fragments. Human insulin used in the competitive assays was diluted from a pharmaceutical preparation (Novolin R, Novo Nordisk Pharmaceuticals, Princeton, NJ) which also contained phenol as a stabilizer. The biological buffers and capillary coating chemicals were all obtained from Sigma. All other chemicals were obtained as described previously.

CZE. All CZE conditions were as previously described for the noncompetitive assay except, when coated capillaries were used, a positive voltage was applied and injections were made from the grounded end. Hydrodynamic injections were performed as before with the 25  $\mu$ m i.d. capillaries. For 50  $\mu$ m i.d. capillaries, injections were performed by raising the vial 2.5 cm for 2.5 s which gave injection volumes of approximately 0.30 nL obtained by calculation with the Hagen-Pouiselle equation. Preliminary work was done using the He-Cd laser as the excitation source. Later work used the Ar<sup>+</sup> laser. Modified capillaries were prepared using 50  $\mu$ m i.d., 350  $\mu$ m o.d. capillaries by a procedure described below. When these capillaries were used, columns were pressure rinsed with the electrophoretic buffer for 1 min between runs. Data were collected and analyzed as before.

For some experiments, the Beckman P/ACE System 2200 was used. With this system, separations took place in a 27 cm long, 50  $\mu$ m i.d. acrylamide coated capillary placed into the LIF cartridge. A potential of 29 kV was applied across the capillary with

the effective separation length being approximately 6 cm. Injections were performed electrokinetically at the negative end of the capillary for 2.5 s at 2.5 kV. The capillary was rinsed for 2 min with the 0.02 M tricine pH 8 electrophoretic buffer between each run.

Modification of capillaries. Capillaries were coated with a monolayer of a linear polyacrylamide using a method similar to that developed by Hjerten (53). Capillaries were first treated by flowing under He pressure for 1 h with 1M NaOH. This was followed by a 5 min rinse with H<sub>2</sub>O. Next, 40 µL of  $\gamma$ -methacryloxypropyltrimethoxysilane was dissolved while stirring (about 15 minutes) in 10 mL of H<sub>2</sub>O adjusted to pH 3.5 with acetic acid. The capillary was filled under He pressure and left standing for 1 h. This procedure was performed twice. Excess silane was removed from the capillary by a water rinse. A 4% w/w solution of acrylamide, containing 1 µL/mL N,N,N',N'-tetramethylethylenediamine (TEMED) and 1 mg/mL ammonium persulfate, was deareated and passed through the capillary under He pressure. The solution was left standing in the capillary and removed after 60 min with H<sub>2</sub>O. The coated capillary was then dried under a stream of He. For best results, the capillaries were filled with electrophoresis buffer and left overnight.

Sample preparation. FITC-insulin and Fab solutions were prepared using a pH 7.5, 0.05 M sodium phosphate buffer as the solvent. The human insulin was prepared by diluting the pharmaceutical preparation of 100 units/mL ( $7.16 \times 10^{-4}$  M) with buffer.

To perform competitive assays for human insulin, FITC-insulin and Fab were mixed to give a final concentration of 100 nM each. The volume and concentration of human insulin added was varied to obtain the desired concentration in the final sample

solution. The solution volume was adjusted to 3 mL by adding pH 7.5 0.05 M sodium phosphate buffer with 0.025 M  $K_2SO_4$ . Samples were incubated as described for the non-competitive assay. When coated capillaries were used, an internal standard (IS) was added to the solutions to give a final concentration of 50 nM.

The IS used was FITC-labeled glutamic acid. This was prepared by dissolving 1 mg/mL glutamic acid in 0.2 M sodium bicarbonate pH 9. A 1 mL aliquot of this solution was mixed with 1 mL of 200  $\mu$ M FITC dissolved in this same buffer. The solution was left to react overnight at room temperature in the dark. Suitable dilutions were made with the electrophoretic buffer. The IS was made fresh every 3-4 days and stored in the refrigerator.

One important consideration for the sample preparation in the competitive assay was the mixing order of the reagents. It was determined experimentally that the results were not effected by mixing the labeled and unlabeled insulins and then adding the Fab or by mixing the labeled insulin and the Fab and then adding the unlabeled insulin. A change was not observed in the equilibration time or amount of complex formed. This result was critical for future use in applications so that unlabeled insulin could be determined by the addition of the FITC-insulin and Fab to the sample.

Calculations. For construction of calibration curves with the uncoated capillaries, peak areas were calculated as before. For quantitation on the coated capillaries, peak areas of an internal standard and FITC-insulin were calculated using the statistical moments program. The area of the FITC-insulin was normalized by dividing it by the IS area to account for any variability in injection volumes. A plot of normalized peak area vs.

concentration of human insulin was then prepared. The detection limit for the competitive assay was calculated by dividing the standard deviation of the blanks by the slope of the calibration plot (33).

### Results and Discussion

The assay. For the competitive assay described here, insulin was the analyte, FITC-insulin was used as the fluorescently-labeled antigen, and these solutes were in competition to complex with Fab from anti-insulin. A typical electropherogram demonstrating this type of assay using unpurified insulin is found in Figure 3-2. The blank sample (B) contains a 1:1 mixture of FITC-insulin and Fab. Upon addition of unlabeled human insulin (A), a decrease is seen in the size of the complex peak, while a corresponding increase is seen in the free FITC-insulin peak. These changes are due to the displacement of some of the labeled FITC-insulin from the complex by the unlabeled insulin.

A potential advantage of the CZE-based competitive assay demonstrated by this figure, not explored in this work, is that multiple antigens could be measured at one time. This is illustrated by the observation that the three FITC-insulin zones could easily have been three different antigens. Related to this idea is that the CZE-based assay could be useful for evaluating cross-reactivity of a single antibody or Fab with different antigens.

A typical calibration curve for the competitive assay is shown in Figure 3-3. The points represent the average normalized peak area, calculated as described in the Experimental Section, of three runs. The average RSD was 6.3% for the complex peaks and was 2.9% for the free FITC-insulin peaks. The plot demonstrates that

increasing insulin in the sample solution caused the expected increase in the area of zones due to free FITC-insulin and the expected decrease in the area of zones due to FITC-insulin/Fab complex. The curve exhibits non-linearity at higher concentrations of insulin indicating saturation of the Fab with insulin. The LOD of the competitive assay was 3 nM or 420 zmol injected, which is similar to that for the non-competitive assay under the conditions employed here (using the  $5 \times 10^7$  L/mol antibody and the He-Cd laser). In order to improve the detection limit of this assay, it first became necessary to investigate better separation conditions as it was difficult to obtain capillaries which gave reproducible peak areas. The problem appeared to be protein adsorption to the capillary surface since electropherograms yielded broad, tailed peaks. This was thought to be primarily due to the quality of the capillary as successive cleanings occasionally improved peak shape.

Improving the assay. Two approaches to circumvent the adsorption problem were investigated. The first approach was to change the composition of the buffer. (See Table 3-1.) The best results in terms of reproducibility were obtained for high salt concentrations of pH 7 0.05 M sodium phosphate/ 0.2 M Na<sub>2</sub>SO<sub>4</sub>. However, this required the use of smaller i.d. capillaries (10  $\mu$ m) to better dissipate the heat generated which did not allow the LOD to be improved due to the smaller capillary diameter.

Table 3-1. Electrophoresis buffers.

Buffer	Comments
0.05 M sodium phosphate pH 7.5 + 0.05 M K <sub>2</sub> SO <sub>4</sub>	poor reproducibility
0.05 M sodium phosphate pH 7.5 + 0.05 M K <sub>2</sub> SO <sub>4</sub> + acetonitrile	N<1000
0.05 M sodium phosphate pH 7 + 0.1 M K <sub>2</sub> SO <sub>4</sub>	reproducibility better (RSD 10%)
0.05 M sodium phosphate pH 7 + 0.2 M K <sub>2</sub> SO <sub>4</sub>	best reproducibility, high current
0.05 M sodium phosphate pH 7 + 1M Glycine	excessive current
0.05 M sodium borate pH 9	poor complex formation
0.1 M sodium borate pH 9	excessive current
0.85 M CHES pH 7.8 +0.05 M NaAC	insulin N > 100,000 complex does not form
0.01 M Tricine pH 8 + 0.025 M K <sub>2</sub> SO <sub>4</sub>	good efficiencies for insulin&complex poor resolution

The second approach to reduce the adsorption was to use coated capillaries.

Several types of coatings were investigated (see Table 3-2). The linear acrylamide coating was selected because it gave the most consistent results and several groups have found that adsorption was greatly reduced with similar type coatings (54, 55). They could also be prepared in-house by a relatively simple procedure.

Table 3-2. Capillary coatings.

Column & Manufacturer	Coating Type	Comments
DB-Wax J&W Scientific	Polyethlyene Glycol	long run times poor peak shapes
DB-1 J&W Scientific	Dimethylpolysiloxane	insulin poor peak shape
BioCap LPA Bio-Rad	Linear polyacrylamide	insulin poor peak shape
eCAP Neutral Beckman	neutral polymer (proprietary)	good results after conditioning for 1-2 days in electrophoretic buffer
Hjerten <sup>(53)</sup>	linear polyacrylamide	FITC-insulin N>80000
Towns & Regnier <sup>(56)</sup>	ODS/Brij 35 surfactant	FITC-insulin not detected

The procedure used to coat the capillaries (as described in the experimental) was originally developed by Hjerten (53) and modified for several other applications (55, 57). The method is based on a bifunctional compound, in this case  $\gamma$ -methacryloxypropyltrimethoxysilane, in which one group reacts with the surface and the other with a monomer taking part in a polymerization process. One or two of the trimethoxy groups of this compound react with the surface silanol group, whereas the acryl group reacts with the acryl monomers of acrylamide. This forms a thin, neutral monomolecular layer of non-crosslinked polyacrylamide on the capillary surface which greatly reduces the electroosmotic flow in the capillary. The mechanism for this procedure is shown in Figure 3-4.

The coating of these capillaries was not always successful. The procedure outlined in the experimental section gave the highest rate of success. The best results were obtained upon using fresh reagents, therefore, when the failure rate increased all new chemicals were ordered. The ease of coating decreased with capillary i.d., i.e. 50  $\mu\text{m}$  worked better than 25  $\mu\text{m}$  which were better than 10  $\mu\text{m}$  i.d. This problem seemed to be related to the cleaning of the surfaces as the larger the i.d. the less stringent of a base rinse was necessary to activate the surface for uncoated work. Therefore, it was essential that the capillary surface be thoroughly cleaned before the coating was applied. The best way to do this was rinse with 1M NaOH. For best results, the columns were stored in fresh electrophoretic buffer for at least one day before use. Columns could be made in advance and stored in this buffer making sure to change it every couple of days to prevent bacterial

growth. Most columns lasted several days of use if they were rinsed between runs. A mild acid rinse sometimes successfully regenerated deteriorating column performance.

Once the columns were prepared, several tricine buffers were tried to determine the best electrophoretic conditions. The tricine buffer was used on the basis of a recommendation from Beckman Instruments Co. for similar capillaries and the fact that good results had been obtained previously on the uncoated capillaries. A 0.02 M tricine buffer pH 8 gave the best plate counts and peak shapes. An electric field strength of 1000 V/cm was used giving a current of approximately 5  $\mu$ A. These conditions were then used for all subsequent coated capillary work. An advantage of using these capillaries was that a commercial automated instrument could be used. This instrument could not be used under previous conditions because it was found that the complex formation was not satisfactory in the 25  $\mu$ m i.d. capillaries when used with that system due to the configuration of the capillary in the cartridge.

Figure 3-5 shows a pair of electropherograms illustrating the differences in the separation of the unpurified FITC-insulin on both a bare and acrylamide coated capillary. As can be seen from the figure, the order of the separation was reversed upon coating. This reversal in migration is due to the greatly reduced EOF which allows for the charge of an injected species to dominate its migration in the coated capillary. FITC-insulin injected in the uncoated capillary migrates toward the cathode because it is carried by the EOF, therefore the doubly labeled form which has two negative charges migrates slowest. Upon coating however, this flow is greatly reduced because the silanol groups are blocked; therefore it is not strong enough to overcome the electrophoretic mobility ( $\mu_{ep}$ )

of the negatively charged FITC-insulin. The voltage is thus reversed so the sample migrates toward the cathode by an electrostatic attraction and the doubly labeled form elutes first.

An electropherogram obtained for a mixture of purified FITC-insulin and Fab on an acrylamide coated capillary is shown in Figure 3-6. Note that two complex peaks are observed suggesting more than one form of the Fab is present. Indeed, using UV absorption detection two zones were observed for Fab as shown in Figure 3-6 ( $t_{\text{mig}} = 8$  and 13 min). The multiple zones are thought to be due to a microheterogeneity in the Fab or to a variability in the cleavage sites of papain on the whole antibody. It is assumed that these zones were not observed in the uncoated capillaries due to poor resolution because lower electric field strengths were used. It could also have been due to adsorption of one of the peaks. An electropherogram for an injection of a mixture of the Fab and FITC-insulin on a 10  $\mu\text{m}$  capillary is shown in Figure 3-7 which supports these findings. With the smaller i.d. capillary, a greater electric field strength could be used due to better heat dissipation and a poorly resolved doublet is observed for the complex peak (peak 1).

In the competitive assay, it was possible to quantitate insulin based on either the complex peaks or the free FITC-insulin peaks. The most consistent results were obtained by quantitating the free FITC-insulin peak relative to an internal standard. This also permitted assays to be performed more rapidly because FITC-insulin migrated significantly faster than complex. It was necessary only to let the FITC-insulin peak elute then rinse the capillary with buffer between runs to remove the complex. Examples of electropherograms used for assay of insulin on the coated capillaries are shown in Figure

3-8. The blank (solid line) contains 50 nM IS (peak 1), 100 nM Fab, and 100 nM FITC-insulin (peak 2). The figure illustrates that addition of 10 nM insulin (dashed line) to the sample causes an increase in free FITC-insulin which can be used to quantitate insulin in the sample.

It is thought that the inconsistencies in quantification using the complex peaks are due to adsorption of Fab onto the capillary surface complex or to dissociation during the separation. The dissociation occurs to a greater extent with modified capillaries because the electroosmotic flow is greatly reduced, therefore the Fab and Fab/FITC-insulin complex migrate slowly. Long migration times increase the likelihood of the complex dissociating during the run and preventing its detection as discussed previously. Small peaks and baseline shifts that are detected after free FITC-insulin migrates through the column are apparently due to FITC-insulin that has dissociated from the complex and migrated through the capillary. Although these inconsistencies in the complex peak are not desirable, it does not prevent quantitation based on free FITC-insulin.

Figure 3-9 illustrates a competitive calibration plot constructed on the coated capillaries using the purified FITC-insulin and the  $\text{Ar}^+$  laser. Each data point represents the average of three consecutive runs. The average RSD was 3.4% with an  $R^2$  value of 0.997. The detection limit for this competitive assay under the improved conditions was still 3 nM even though similar conditions had produced a 10 fold improvement in the noncompetitive assay LOD. It was determined theoretically that the LOD of this type of assay is limited by the binding capacity of the antibody being used.

Improvements in the LOD can be attained by utilizing an antibody with a higher affinity for insulin. This was mentioned in the introduction and is demonstrated here by Figure 3-10 which compares theoretical results to actual data for the bound/ free ratio of FITC-insulin as a function of insulin in the sample. To obtain the bound/ free ratios for this plot, it was necessary to use data from separation conditions described previously when both the FITC-insulin / Fab complex and free FITC-insulin were reproducible. The theoretical curves are based on Equation 1 using Fab and FITC-insulin concentrations of 100 nM and the concentration of unlabeled insulin varied from 1 to 100 nM. The data agree well with the theoretical plot of an antibody with  $K_b = 5 \times 10^7$  L/mol (solid line) suggesting that these CE-based assays follow expected behavior for immunoassays. The detection limit predicted from this theoretical plot, assuming an RSD of 3 %, is 5 nM, which is in good agreement with the value of 3 nM that was obtained experimentally. Also shown in the figure (dashed line) is a plot with the binding constant of the antibody increased to  $5 \times 10^8$  L/mol. The increase in sensitivity afforded by the lower dissociation constant would lead to a detection limit of approximately 0.3 nM in this case, assuming that the standard deviation for the blank remained the same.

Two new antibodies were obtained to try and improve the LOD. The first antibody had a reported binding constant of  $3 \times 10^8$  L/mol. The electropherograms in Figure 3-11 show the results of mixing equal ratio's of the Fab fragments of the two antibodies with FITC-insulin. As can be seen by the figure, much less of the higher binding new antibody Fab actually complexed with the insulin (peak 2) as indicated by a smaller complex peak (peak 1) in comparison to the old antibody. It was assumed that

this disturbing result was due to steric hindrance of the binding of insulin to the antibody based on the location of the fluorescent labels on the insulin.

The most common epitopes on insulin tend to be near amino acids A1 and B29 (43). These two locations are near each other in the 3-D structure of insulin and both contain amino groups that are believed to be labeled by FITC. The epitope for the higher binding antibody is known to be in this region and therefore the label would disturb the binding of insulin to the antibody. Therefore, for further improvements to be made in the assay detection limit, an antibody with higher binding and with an epitope outside of this region must be obtained.

The second antibody obtained had a reported binding constant of  $8.1 \times 10^8$  L/mol for rat insulin and an unknown epitope. This antibody did bind the insulin but unfortunately its affinity for the FITC-insulin was not much better than the previously used  $5 \times 10^7$  L/mol antibody. These results were seen through a comparison of electropherograms of equimolar mixtures of the two Fabs with FITC-insulin which showed complex and FITC-insulin peaks of the same area and heights. It can only be assumed that the FITC tag must in some way interfere with the binding or that it cross reacts with the labeled bovine insulin, with a lesser affinity than rat insulin.

Mathematically, an assay of this type in which labeled antigen ( $A^*$ ) has a different binding constant than the unlabeled antigen (A) can be described by the following equation which simplifies to Equation 1 under the conditions that  $K^* = K$  (58):

$$\left(\frac{B^*}{F^*}\right)^2 + \frac{B^*}{F^*} (A^*K^* - Ab\ K^* + 1) - Ab\ K^* + \frac{\frac{B^*}{F^*} A\ K \left(\frac{B^*}{F^*} + 1\right)}{\frac{K}{K^*} \frac{B^*}{F^*} + 1} = 0 \quad \text{Equation 2}$$

where the variables are defined as in Equation 1 with  $K^* = K_b$  of  $A^*$  and  $K = K_b$  of  $A$ .

An assay performed under the conditions that  $K^* < K$  give results less favorable than if  $K^* = K$ . An example of results of this type are illustrated in Figure 3-12 in which the  $B^*/F^*$  ratio is plotted versus unlabeled antigen concentration ( $[A]$ ). As can be seen from the figure, the sensitivity of the assay is greatly decreased due to a decrease in the slope caused by a lesser degree of binding. Therefore, this antibody could not be used to improve the detection limit. For further improvements, a different antibody with a high binding constant needs to be obtained or a different labeling scheme used for the insulin employed.

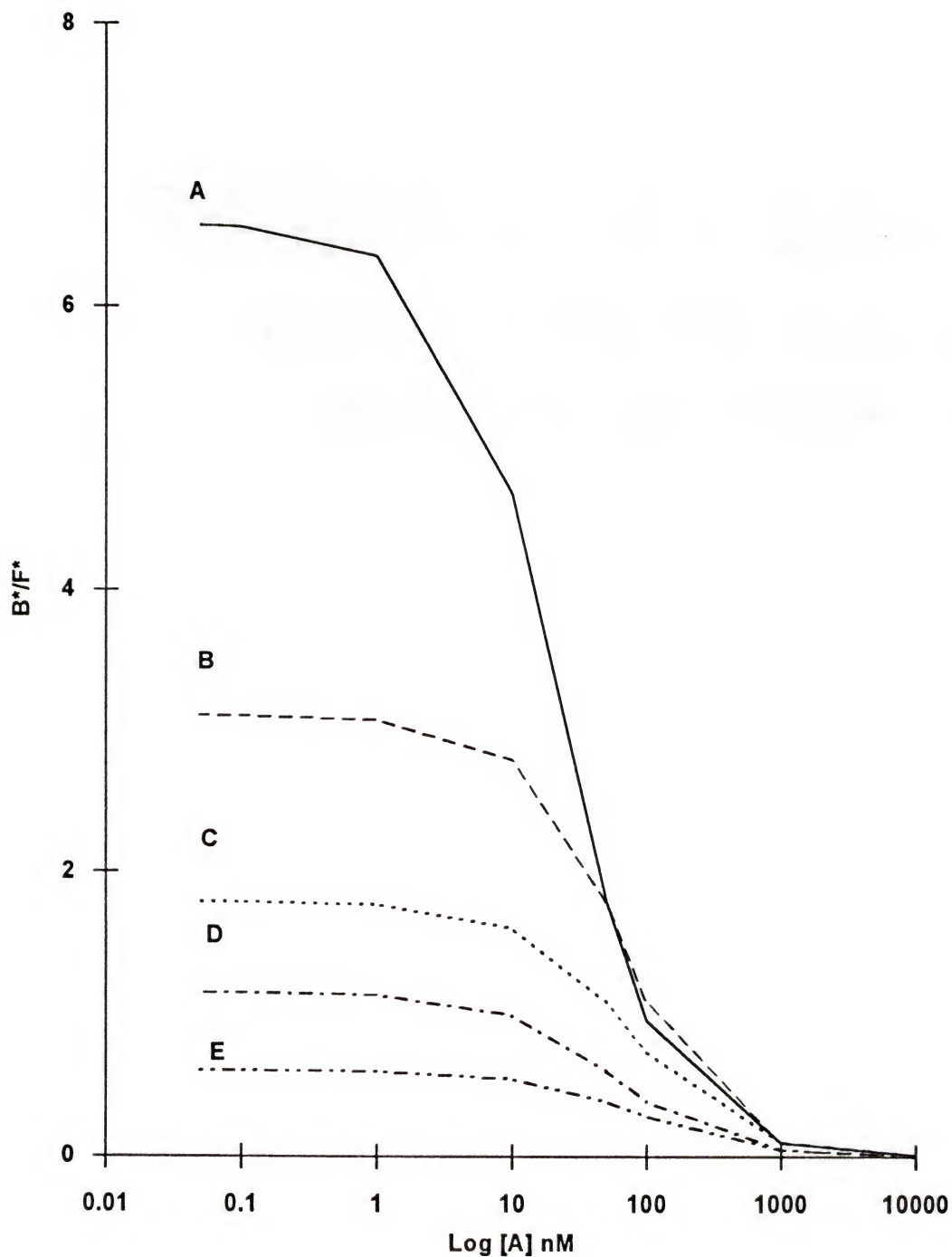


Figure 3-1. Theoretical plots for the competitive assay. Conditions used to generate plots are as follows: Curve A-  $K_b = 5 \times 10^8$ ,  $[A^*]_{\text{total}} = 100 \text{ nM}$ ,  $[Ab^*]_{\text{total}} = 100 \text{ nM}$ ; Curve B-  $K_b = 5 \times 10^7$ ,  $[A^*]_{\text{total}} = 100 \text{ nM}$ ,  $[Ab^*]_{\text{total}} = 50 \text{ nM}$ ; Curve C-  $K_b = 5 \times 10^7$ ,  $[A^*]_{\text{total}} = 100 \text{ nM}$ ,  $[Ab^*]_{\text{total}} = 100 \text{ nM}$ ; Curve D-  $K_b = 5 \times 10^7$ ,  $[A^*]_{\text{total}} = 50 \text{ nM}$ ,  $[Ab^*]_{\text{total}} = 50 \text{ nM}$ ; Curve E-  $K_b = 5 \times 10^7$ ,  $[A^*]_{\text{total}} = 50 \text{ nM}$ ,  $[Ab^*]_{\text{total}} = 100 \text{ nM}$ .

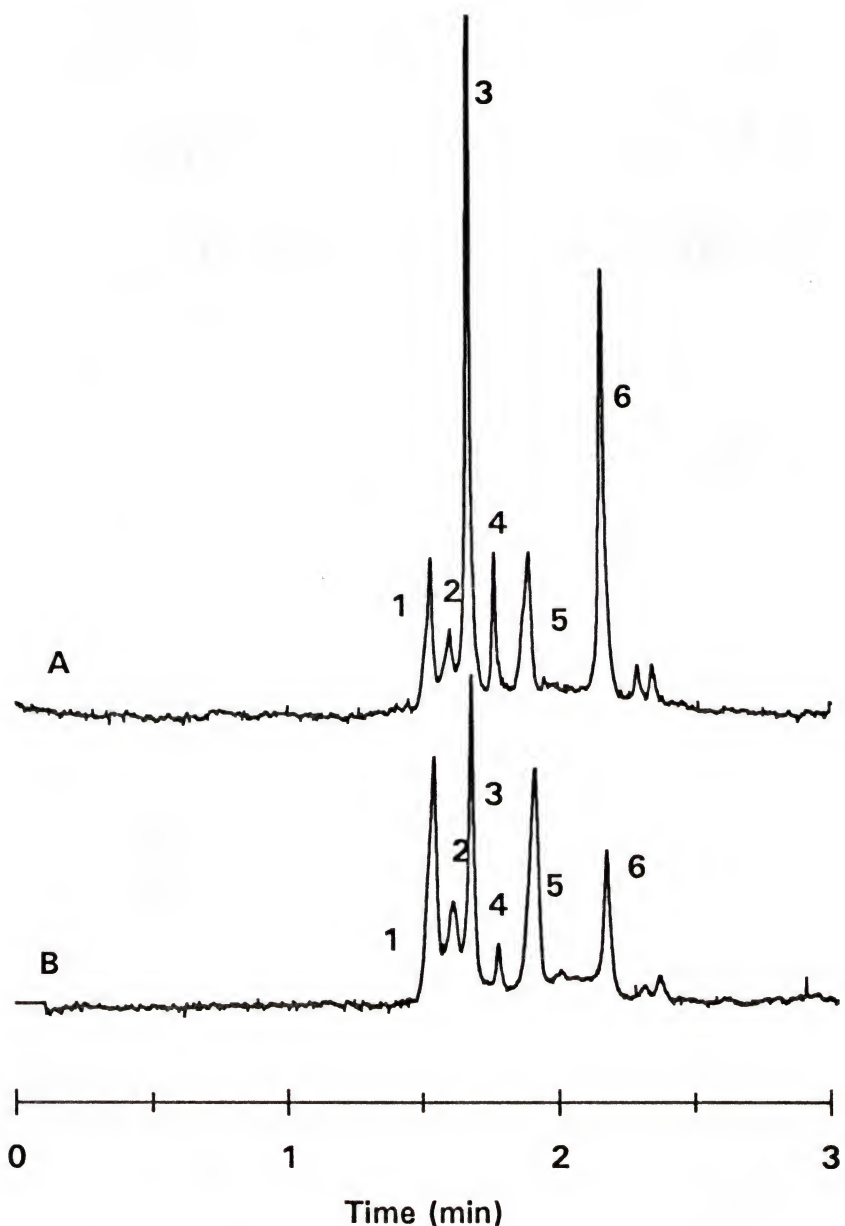


Figure 3-2. Electropherograms demonstrating the competitive assay. B is the blank sample of a 1:1 M ratio of Fab:FITC-insulin. A shows the increase in FITC-insulin (peaks 3, 4 and 6) and decrease in complex peaks (1, 2 and 5) upon addition of unlabeled insulin.

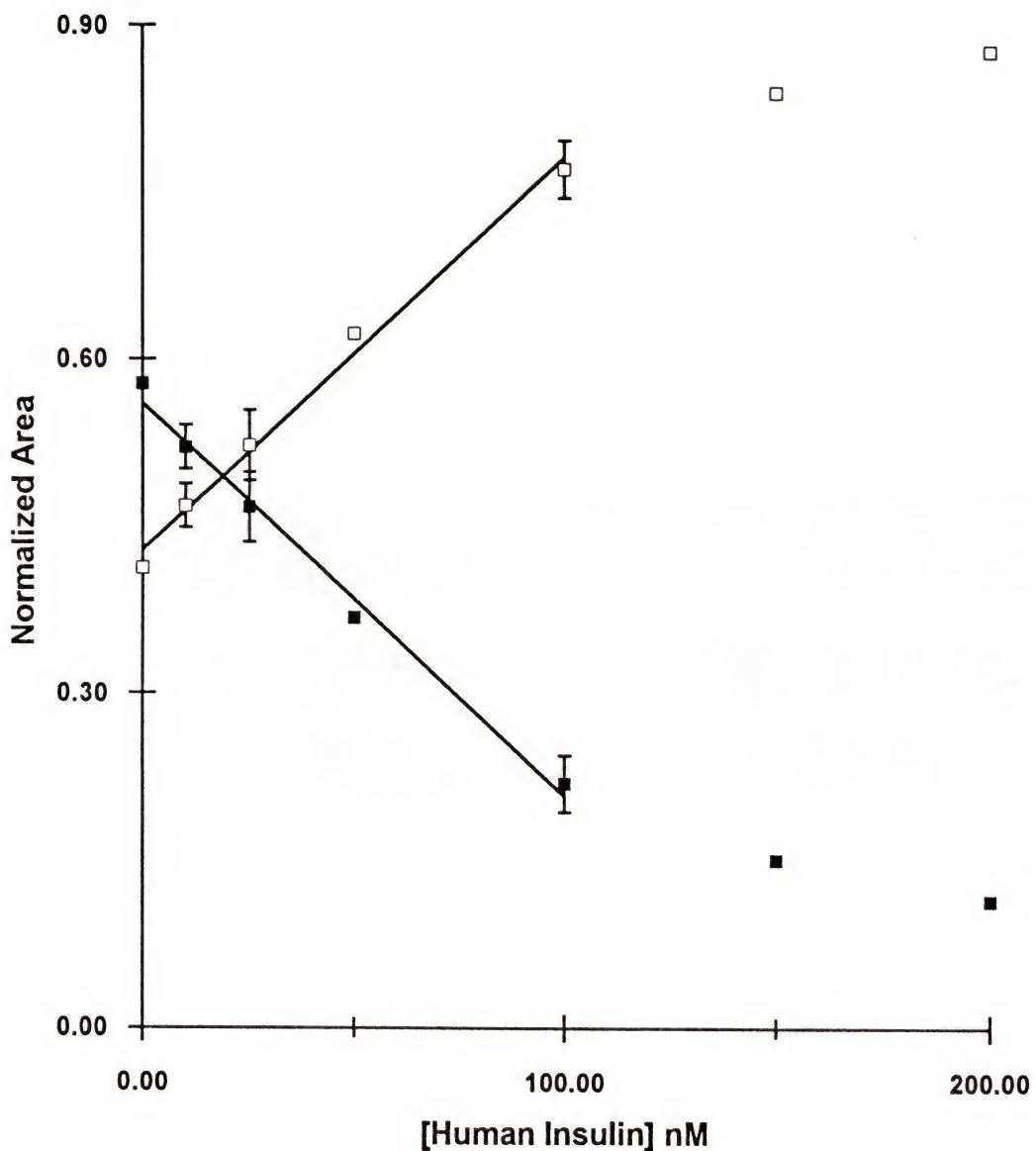


Figure 3-3. Calibration curve for the determination of insulin by the competitive assay using 100 nM each of FITC-insulin and Fab. Normalized peak areas calculated as described in the text. The solid squares are peak areas for Fab-FITC-insulin complex and the hollow squares are peak areas for FITC-insulin. The lines drawn represent the linear least squares fit through the points indicated and had a correlation coefficient of 0.992. The error bars (one standard deviation) are within the points where they are not shown. The He-Cd laser was used as the excitation source.

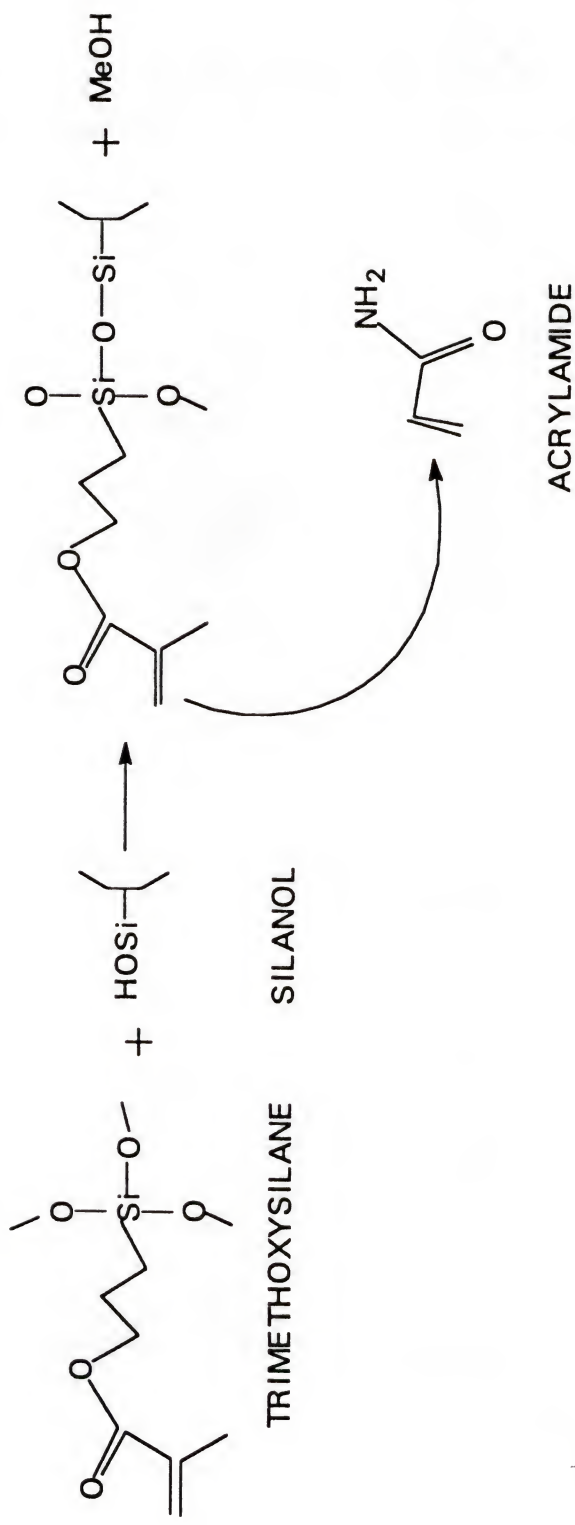


Figure 3-4. Mechanism for acrylamide coating of capillaries.

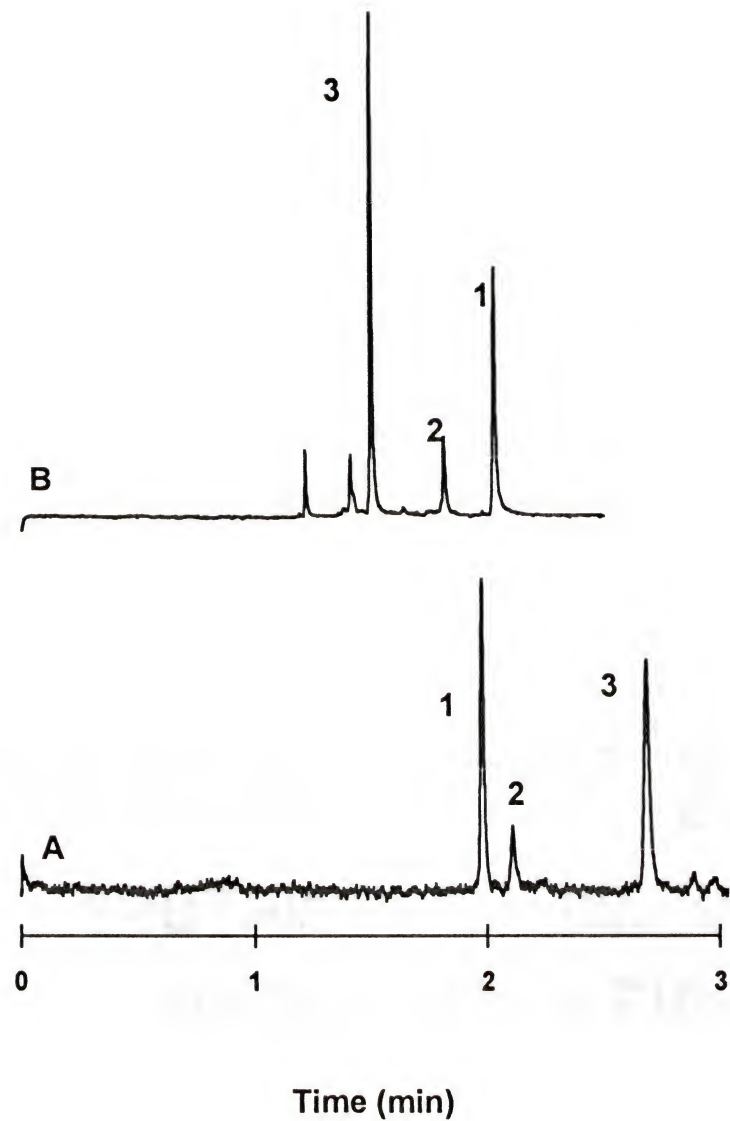
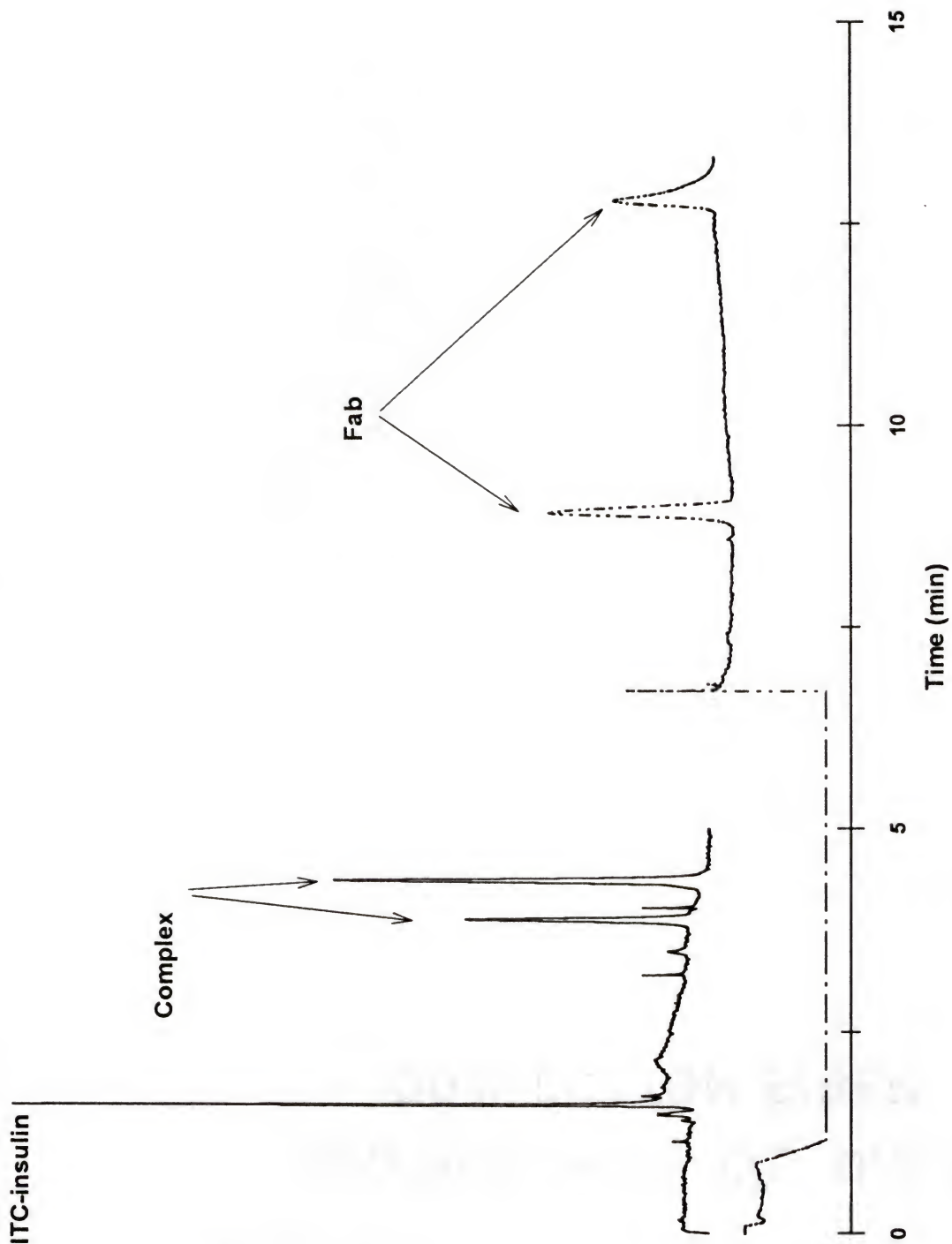


Figure 3-5. Electropherograms of FITC-Insulin on bare (A) and acrylamide coated (B) capillaries. Peaks 1 & 2 are singly labeled forms and peak 3 is the doubly labeled form. Conditions are as described in the text.



**Figure 3-6. Solid Line.** Electropherogram obtained using LIF for a mixture of FITC-insulin and Fab in a 1:1 ratio. **Dashed Line.** Electropherogram obtained using UV absorbance detection of purified Fab. The dip in the UV trace is due to buffers present in the purified Fab.

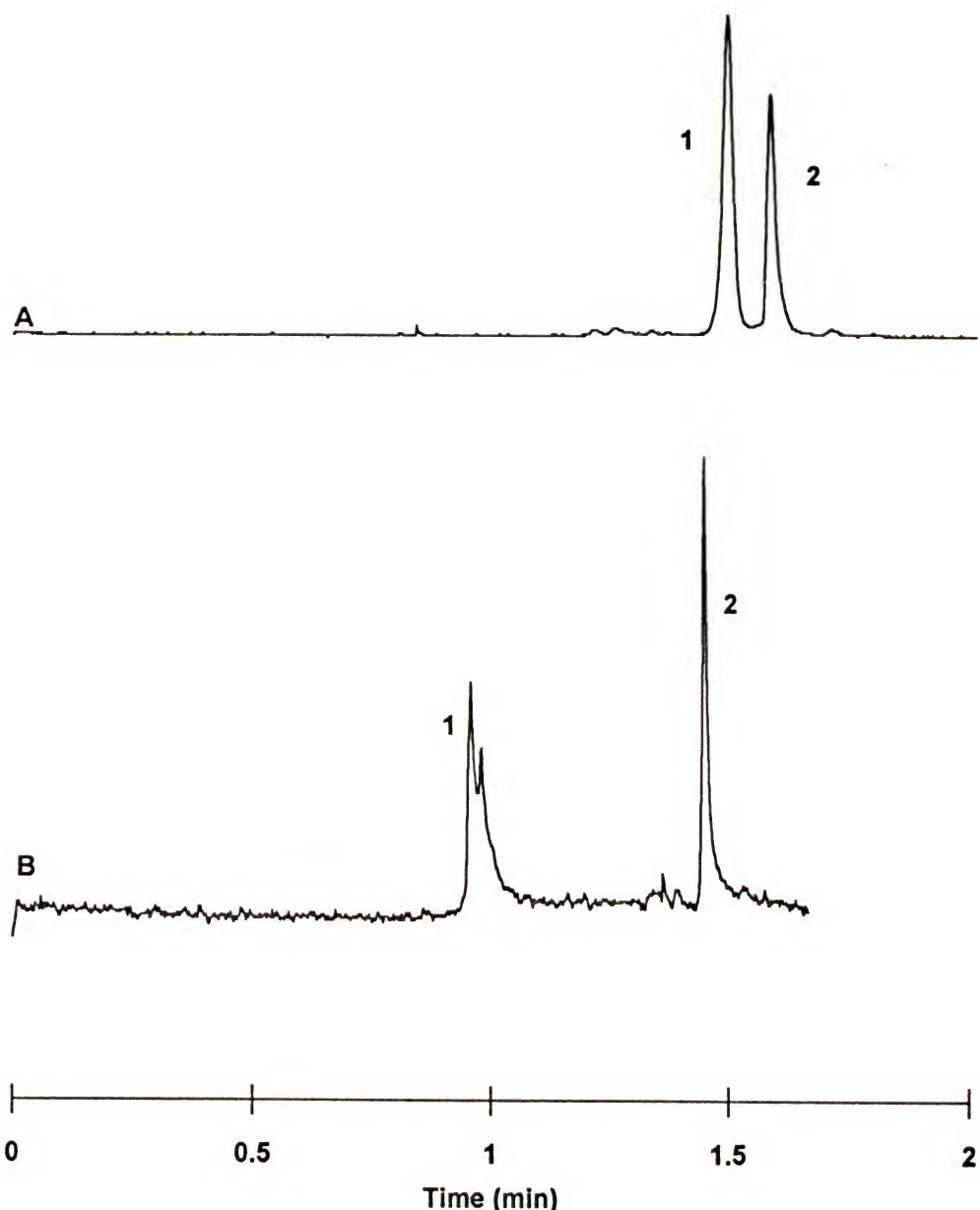


Figure 3-7. Electropherograms of mixtures of purified FITC-insulin (peak 2) and Fab showing the differences in complex formation (peak 1) with an electric field strength of 500 V/cm on a 25  $\mu$ m i.d. capillary (A) and 800 V/cm on a 10  $\mu$ m i.d. capillary (B).

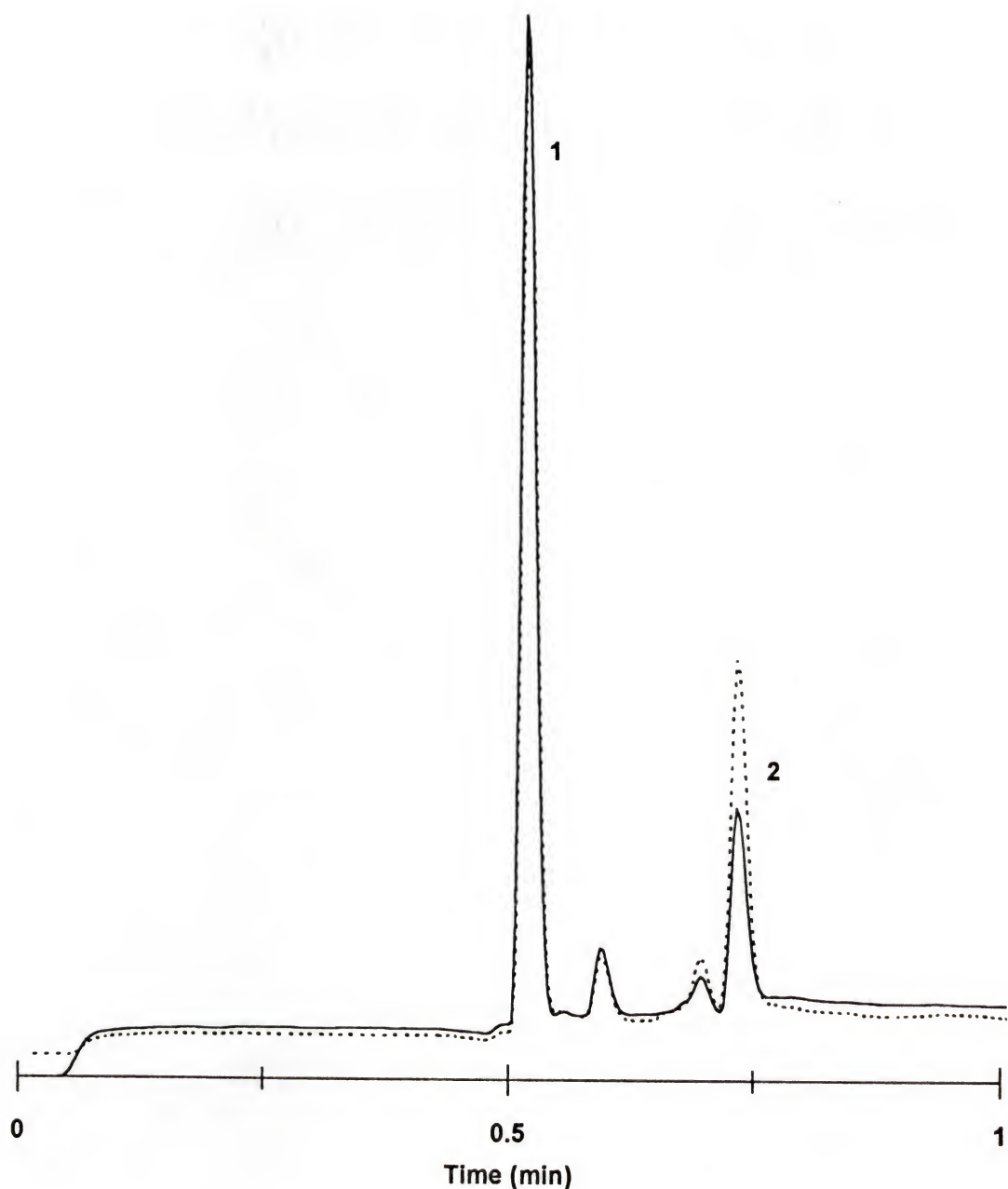


Figure 3-8. Overlay of electropherograms illustrating detection of 10 nM insulin by competitive assay using 100 nM purified FITC-insulin (peak 2) and Fab. Electropherograms of the blank (solid) and 10 nM insulin (dashed) were performed consecutively using procedures described in the Experimental Section. Peak 1 is the internal standard. Unlabeled peaks are due to impurities in IS and FITC-insulin.

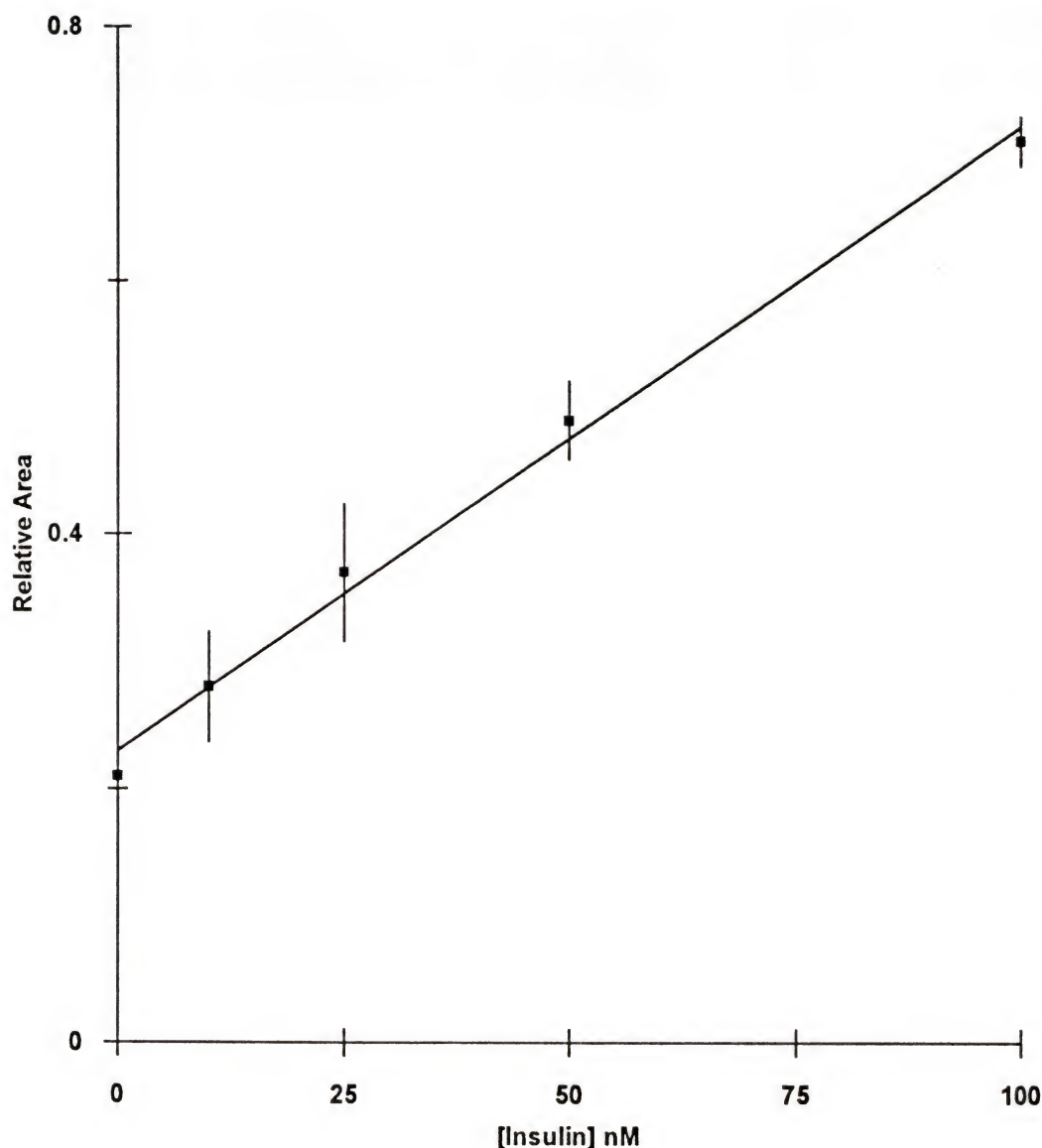


Figure 3-9. Calibration curve for the determination of insulin by a competitive assay using 100 nM each FITC-insulin and Fab on coated capillaries. The line drawn represents the linear least squares fit through the points. Each point represents the average of 3 runs per sample and error bars are 1 standard deviation.

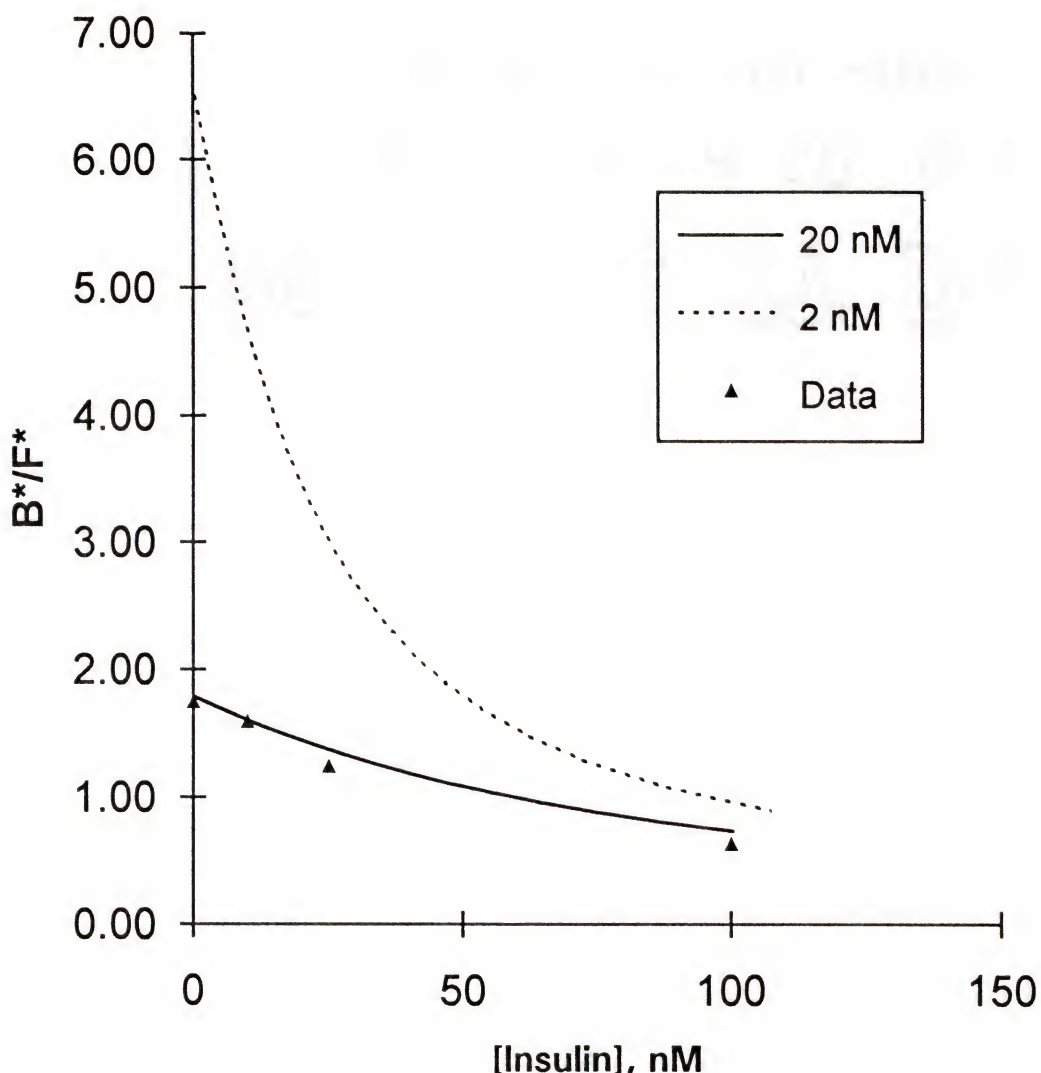


Figure 3-10. Theoretical (lines) and actual data for ratio of bound FITC-insulin to free FITC-insulin ( $B^*/F^*$ ) as a function of unlabeled insulin concentration. Theoretical lines calculated using equation 1 and a binding constant for the antibody of  $5 \times 10^7$  (solid) and  $5 \times 10^8$  (dashed).

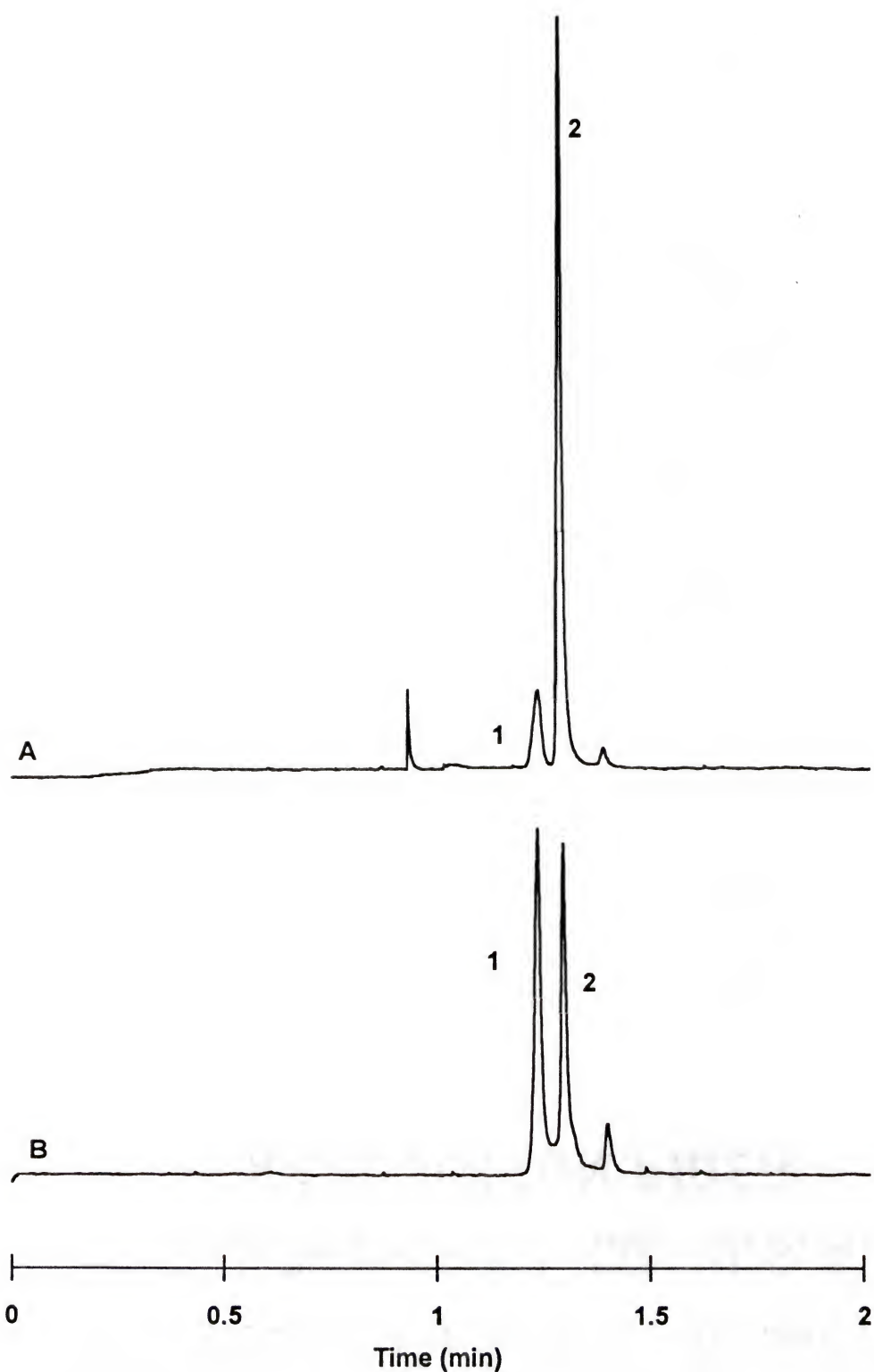


Figure 3-11. Electropherograms of injections of 1:1 M ratios of the two different Fab fragments with the purified FITC-insulin (peak 2). The upper electropherogram (A) is from the  $3 \times 10^8$  antibody and the lower (B) is from the  $5 \times 10^7$  antibody. Peak 1 is the complex.

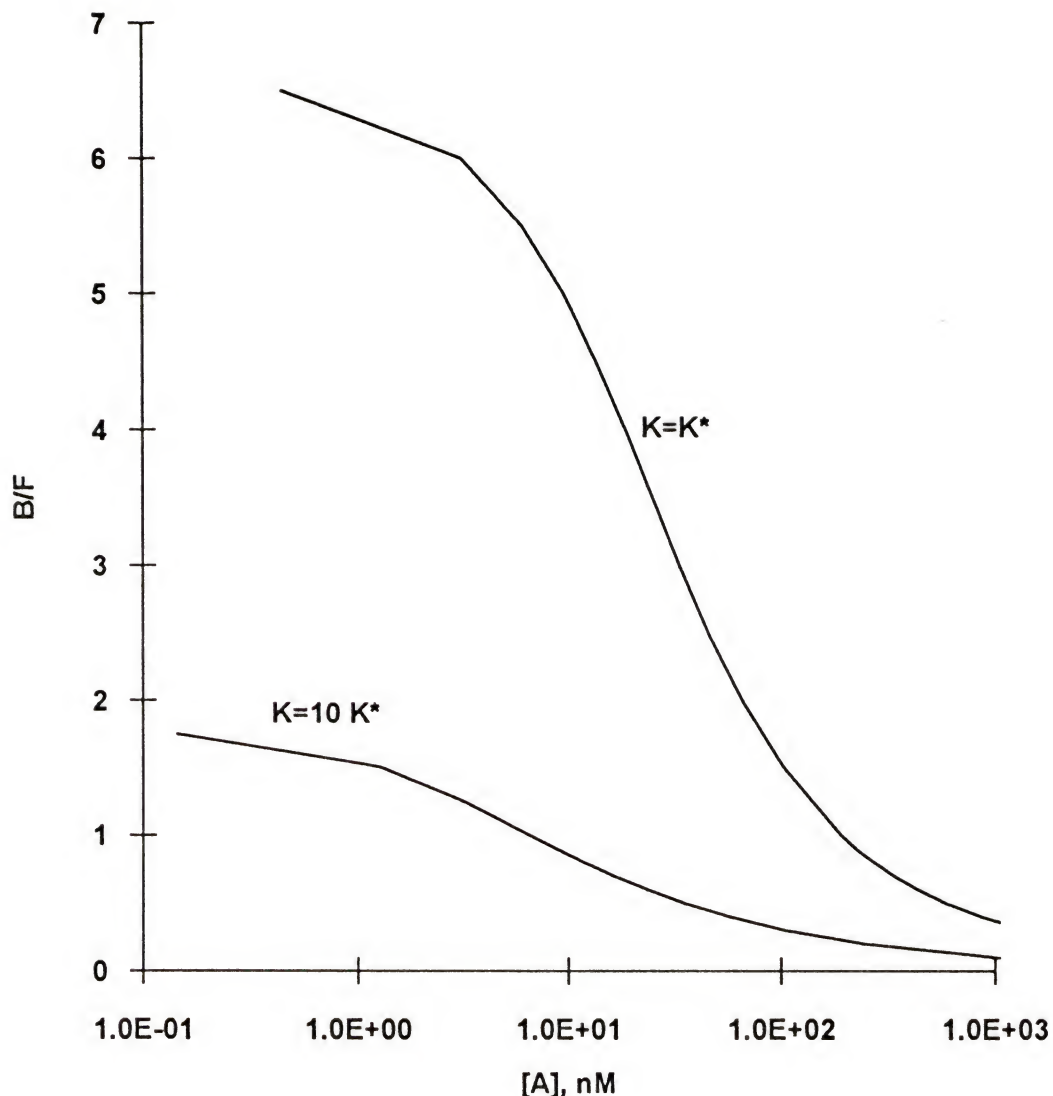


Figure 3-12. Plots generated using equation 2 for labeled antigen and unlabeled antigen having different  $K_b$ 's. Conditions used:  $K^* = 5 \times 10^8 M^{-1}$ ,  $[A^*] = 100 nM$ ,  $[Ab] = 100 nM$ .

## CHAPTER 4

### APPLICATION I

#### INSULIN MEASUREMENTS AT SINGLE ISLETS OF LANGERHANS

##### Introduction

Two applications that benefit from the speed and mass sensitivity of the competitive assay are discussed. The applications demonstrated are the determination of insulin content of single islets of Langerhans and quantitation of glucose-stimulated insulin released from single islets.

About one million islets of Langerhans are dispersed throughout the pancreas, but they make up only about 1% of the total mass of the pancreas. Islets are insulin secreting microorgans which contain approximately 3000 cells of 4 different types. 70-80% of the cells are  $\beta$ -cells which secrete insulin in response to glucose (59). The other cell types secrete glucagon (a peptide that counteracts insulin and raises blood sugar), pancreatic polypeptide (a peptide which regulates secretion of digestive enzymes), or somatostatin (a peptide that inhibits the release of all islet hormones).

Studies of insulin secretion are biomedically important because Type II diabetes mellitus, which afflicts 75-90% of all diabetics, is caused by inadequate insulin secretion (60). The underlying causes of decreased insulin secretion are not known, but it is not due to a loss in the number of  $\beta$ -cells within the islets. Since an islet represents the smallest completely functional unit for insulin regulation, insulin secretion studies at the single islet level are of special interest. These studies are made difficult by the lack of techniques

suited for small scale analysis. Previous work at the single islet level utilized perfusion techniques to collect eluent fractions. These fractions were then analyzed by RIA or ELISA (61-63). Although these methods provide adequate sensitivity, they are slow, labor intensive procedures with analysis times over 1 day. The most common RIA procedures utilize a 3-24 h preincubation with antibody followed by an overnight incubation with the radioisotope (64). A gamma counter is then used the next day after an hour of sample preparation to read the radioactivity. The sensitivity this technique is about 50 pM. The ELISA technique (64) involves several washes and a preincubation of several hours to immobilize antibody on the surface of microtitre plates. The samples are then incubated overnight. The next day, further washes and a 4 h incubation are required for reaction with the enzyme to be used for detection. The optical densities of the samples can then be read automatically with an ELISA reader. The sensitivity for this assay is about 10 pM and has the added advantage of not using radioisotopes and the potential for automation of some steps. It is apparent that a more rapid analysis would be advantageous for islet research. The applications presented here demonstrate the feasibility of performing such an analysis.

### Experimental

CZE. Separations were performed in 50  $\mu$ m i.d., 350  $\mu$ m o.d. fused silica acrylamide coated capillaries. They were either prepared as described in Chapter 3 or purchased from Beckman (neutral eCap, Catalog # 477441, Palo Alto, CA). The CZE apparatus used was as described previously with the Ar<sup>+</sup> laser used as the excitation source. The conditions were as developed in Chapter 3 for the coated capillaries. The

electrophoretic buffer was 0.02 M tricine pH 8 with NaOH. The applied voltage was +29 kV with the injections being made at the grounded end. Hydrodynamic injections were made from microvials by raising the vial 2.5 cm for 2.5 s. This gave injection volumes of 0.3 nL using the Hagen-Pouiselle equation for calculation (49).

The Beckman P/ACE System 2200 was also used to demonstrate the potential for automation of the analysis. Coated capillaries were used with the conditions described previously.

Chemicals. All reagents used were as described previously in Chapter 2. Fab was made from the anti-insulin with the  $K_b = 5 \times 10^7$  L/mol. The FITC-insulin was purified and the third fraction used as described in Appendix D. The internal standard was prepared as described in Chapter 3. The Ringer buffer solution used for the islet incubations was made from chemicals obtained from Sigma and Fisher. The cell culture media was purchased from Gibco (Grand Island, NY).

Calibration plots. Calibration plots were made by preparing solutions containing 50 nM IS, 100 nM FITC-insulin, 100 nM Fab and 0 to 100 nM human insulin. For the islet extraction experiments, the solvent was 0.02 M Tricine adjusted to pH 8.0 with NaOH. For the islet secretion experiments, the calibration solutions were prepared in a Ringer biological buffer solution (135 mM NaCl, 5.5 mM KCl, 1 mM MgCl<sub>2</sub>, 2 mM CaCl<sub>2</sub>, 20 mM HEPES, and 3 mM glucose and adjusted to pH 7.35). Standards were mixed and incubated as before with curves being constructed as described in the competitive assay section.

Islet insulin content determinations. Rat islets were isolated using standard methods (65) by Ms. Lan Huang. Prior to use, islets were stored in RPMI 1640 culture medium in an incubator for up to 1 week with media being replaced every 2-3 days. Freshly isolated islets were transferred from culture medium in 10  $\mu$ L aliquots and placed into a dish containing 5 mL distilled water to remove buffer. Single islets were transferred in 10  $\mu$ L volumes to conical minivials using a micropipette. The islets were disrupted by sonication for 15 min after which 25  $\mu$ L of an acid ethanol solution (0.18 M HCl in 96% v/v ethanol) was added. They were vortex mixed and left to extract overnight at 0°C in the refrigerator. Extracted samples were blown to dryness under a stream of He and reconstituted to a final volume of 100  $\mu$ L with 0.02 M tricine pH 8.0 containing 100 nM FITC-insulin, 100 nM Fab and 50 nM IS. The peak area ratios of the FITC-insulin to IS were compared to a standard calibration curve prepared in the tricine buffer for quantification. Blank samples were conducted by performing the same steps in a vial containing no islet to ensure the changes in peak size seen were not due to artifacts.

Insulin secretion measurements. The time dependence of insulin secretion from single islets was determined as follows. After 7 to 8 days in culture, single islets were selected from culture medium, placed in a dish containing a Ringer buffer (3 mM glucose) and pre-incubated for 1 h at 37 °C. A single islet was then micropipetted in a volume of 2  $\mu$ L into a conical glass minivial. A high glucose Ringer buffer solution also containing IS, FITC-insulin and Fab fragment was added so that the resulting solution contained 50 nM IS, 100 nM FITC-insulin, 100 nM Fab and 16 mM glucose in a total volume of 10  $\mu$ L.

The solution was mixed and incubated at 37 °C. Injections were made directly from the incubation solution at 5 min intervals onto the CE capillary.

The effect of glucose concentration on single islet insulin secretion was determined as follows. Islets were selected and pre-incubated as above after 1 to 2 days in culture. Low glucose determinations were made by incubating the islet in 2 µL of 3 mM glucose Ringer buffer for 5 min. The solution was then gently removed with a micropipette and mixed with 8 µL of the Ringer buffer containing IS, Fab, and FITC-insulin so that the final reagent concentrations were 50 nM, 100 nM and 100 nM respectively. This solution was injected onto the CZE for analysis. The same islets were then treated with a 16 mM glucose Ringer solution using an identical protocol for analysis. The  $\text{Ca}^{2+}$ -dependence of the insulin release was determined in an identical fashion except that the islets were first exposed to a  $\text{Ca}^{2+}$ -free Ringer solution containing 16 mM glucose and then exposed to a regular Ringer buffer containing 16 mM glucose.

### Results and Discussion

Islet insulin content. Competitive immunoassay electropherograms from islet extracts and a blank sample are shown in Figure 4-1a. Even for this complex sample the electropherograms are simple, showing only IS and FITC-insulin peaks along with a few reagent impurities. The islet itself contributed no new peaks. Because of the simplicity of the electropherogram, it was possible to use short columns and analysis times as shown in the figure. Figure 4-1b shows the results of a similar experiment performed on the commercial instrument. Since the commercial instrument allowed for a shorter inlet to detector distance, migration times could be decreased to as low as 30 s. With its

autoinjection capabilities, the use of the commercial instrument demonstrates the possibility of enhanced sample handling by automation of the analysis in both the preparation of the calibration curve and in sample analysis.

The average value for total insulin content of single islets was  $35 \pm 4$  ng (n = 6). Results for the individual islets are listed in Table 4-1. This value is in good agreement with previous RIA analyses of freshly isolated islets in terms of amount and standard deviation as shown in Table 4-2. For our analysis, the islet extract was diluted to 100  $\mu$ L, yet only 0.3 nL was injected. Therefore a minute fraction, approximately 0.0003%, of the islet sample was injected for this determination. This fraction corresponds to less than 1% of a single  $\beta$ -cell. Thus, with appropriate sample handling techniques, this assay could be used for determination of insulin in single cells as well.

Table 4-1. Insulin content results.

Islet	Insulin Content ng/ islet
1	26
2	50
3	51
4	46
5	25
6	31

Table 4-2. Comparison of results of insulin content of rat islets.

Insulin Content	Method	Reference
$35 \pm 4$ ng/islet	CE-immunoassay	present
$356 \pm 66.3$ ng/10 islets	RIA	66
$310 \pm 48$ ng/10 islets	RIA	67
$470 \pm 25$ ng/10 islets	RIA	68
$49 \pm 3$ ng/islet	RIA	69

Insulin secretion. The insulin secretion experiments required injection of the sample out of the high salt Ringer buffer onto the capillary containing an electrophoretic

buffer of low salt content. Conditions such as these are not favorable because the salt gradient causes a lower electric field in the sample region which leads to peak broadening. This condition seemed to be particularly problematic when using the acrylamide coated capillaries. Peaks were found to be very broad and tailed causing quantitation to be irreproducible. Also, there was often a "shelf" following the FITC-insulin peak. This irreproducibility was especially disturbing because preliminary experiments that had been carried out on the uncoated capillaries showed a reduction in the numbers of theoretical plates but no other adverse effects of this buffer system. Unfortunately, those conditions did have an irreproducibility problem due to adsorption. In order to overcome this problem, it was necessary to have an extremely well-coated capillary. Only one such column was made that could be used even though suitable results could be obtained injecting from the tricine buffer on the other columns. All of the work for secretion experiments was carried out on this column or with the Beckman neutral eCap columns. Three of the neutral eCap columns were tried and used successfully. However, it was necessary to let them equilibrate in the tricine buffer for 1-4 days before they could be used. It was found that these columns were only good for 1-2 days of use once they were conditioned. A 15 min base (0.1 M NaOH) rinse was used once to successfully regenerate a column for another day of use.

Figure 4-2 summarizes results for measurement of insulin secretion from single islets during static incubations with glucose. As demonstrated by the first two pairs of columns in Figure 4-2, incubations with higher concentrations of glucose and for longer times resulted in significant increases in the amount of insulin secreted. The average

amount of insulin released in 3 mM glucose buffer after 5 min was  $0.8 \pm 0.2$  ng ( $n = 3$ ).

These islets then released an average of  $3.0 \pm 0.5$  ng of insulin upon stimulation with 16 mM glucose for 5 min. Individual islet results for 5 min incubations are found in Table 4-3.

Table 4-3. Results of the effects of glucose concentration.

Islet	3mM Glucose ng insulin	16 mM Glucose ng insulin
1	0.48	3.42
2	1.03	3.33
3	0.86	2.28

In the time effect study (Table 4-4), islets showed an average increase of 170% in the amount of insulin released at 10 min compared to 5 min. It is difficult to compare these values to literature values since experimental conditions vary; however, the values shown here are in line with previous reports using static incubations and RIAs. For example, after 60 min incubations in 16 mM glucose, rat islets have been reported to secrete  $32 \text{ ng} \pm 2.3$  ng of insulin/ 10 islets (70).

Table 4-4. Results of time release study.

Islet	t = 5min ng insulin	t = 10 min ng insulin	Content
1	-	2.1	17
2	-	2.4	-
3	1.0	1.4	20.2
4	0.7	4.9	24.6
5	1.1	1.6	54

\* - indicates value not obtained.

In comparing results from the experiment testing the effect of glucose concentration and the experiment testing the effect of stimulation time, it is apparent that a 5 min incubation in 16 mM glucose stimulated significantly more insulin secretion in the former case than in the latter (see Figure 4-2). This difference is attributed mainly to the

difference in the age of islets. The islets for time dependent experiments were 7-8 days in culture while for the glucose concentration studies the islets were 1-2 days in culture. The difference may also be due in part to differences in islets from isolation to isolation and to slight differences in the incubation conditions.

The glucose-stimulated insulin secretion measured by these experiments is strongly dependent on  $\text{Ca}^{2+}$  as shown in the third pair of columns of Figure 4-2. In these experiments, islets were incubated with 16 mM glucose for 5 min in  $\text{Ca}^{2+}$  free buffer. After 5 min, the  $\text{Ca}^{2+}$  concentration was raised to 2.4 mM and the islets incubated another 5 min. The  $\text{Ca}^{2+}$  dependence demonstrates the release measured is physiological as it is well known that glucose-stimulated insulin secretion requires  $\text{Ca}^{2+}$  in the external medium.

Table 4-5.  $\text{Ca}^{2+}$  Release Data.

Islet	$\text{Ca}^{2+}$ Free ng insulin	2.4 mM $\text{Ca}^{2+}$ ng insulin
1	0.0	2.4
2	0.0	3.4
3	0.6	3.8

The speed with which the insulin determinations can be made by this method allows time-resolved insulin secretion measurements to be made in the microenvironment around the islet as illustrated in Figure 4-3. In this experiment, insulin secretion was measured every 5 min from a single islet over a 20 min period. The amount of insulin released into the medium slows down after 10 min. The leveling off of insulin secretion can be due to either consumption of glucose in the medium or a depletion of the releasable pool of insulin in the islet. On average, it was found that after 10 min of incubation, only 8.2% of the total insulin in an islet was released. This value is in agreement with other

studies which have shown that with static incubations only about 10% of the insulin in an islet can be released (70).

The data reported here are performed in a static system but demonstrate the feasibility of performing on-line immunoassays on microscale samples with this approach. Automation of the system and the use of perfusion techniques are planned which will allow more detailed studies of insulin secretion at the single islet level. A single islet isolated in a perfusion chamber will be placed in a stream of buffer carrying glucose and the immunoreagents. Systematic injections will be made every few seconds onto the CE capillary by means of an interface between the systems. In this way, time resolved changes in the insulin secretion will be able to be measured. It should also be possible to study other systems with similar techniques.

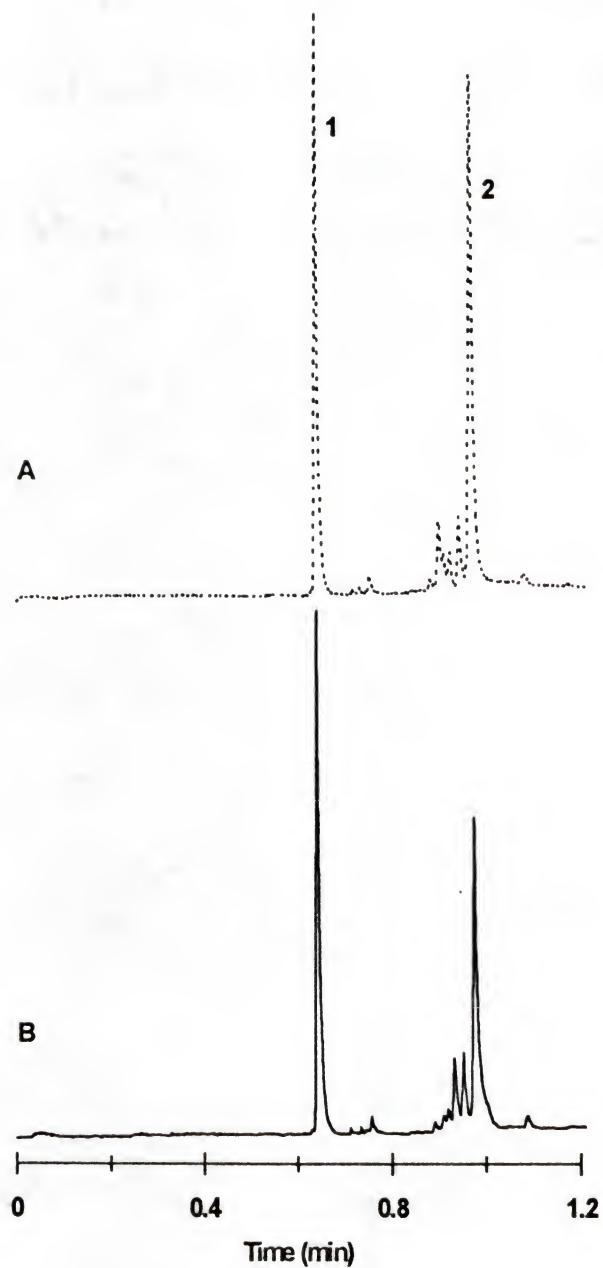


Figure 4-1. Islet insulin extracts. Electropherograms of blank (B) and single islet insulin extract (A) containing 100 nM FITC-insulin (peak 2), 100 nM Fab, and 50 nM internal standard (peak 1) performed on the in-house system.

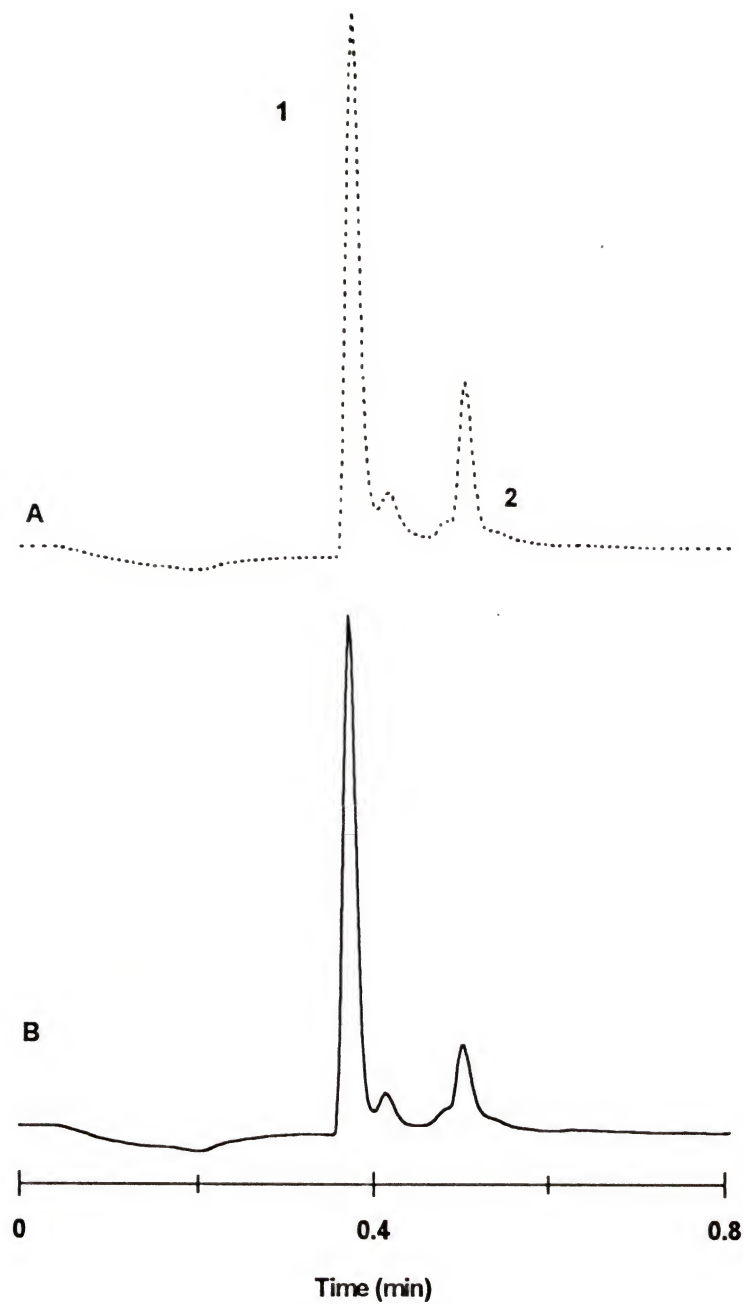


Figure 4-1 (continued). Electropherograms of blank (B) and single islet insulin extract (A) performed on the commercial instrument.

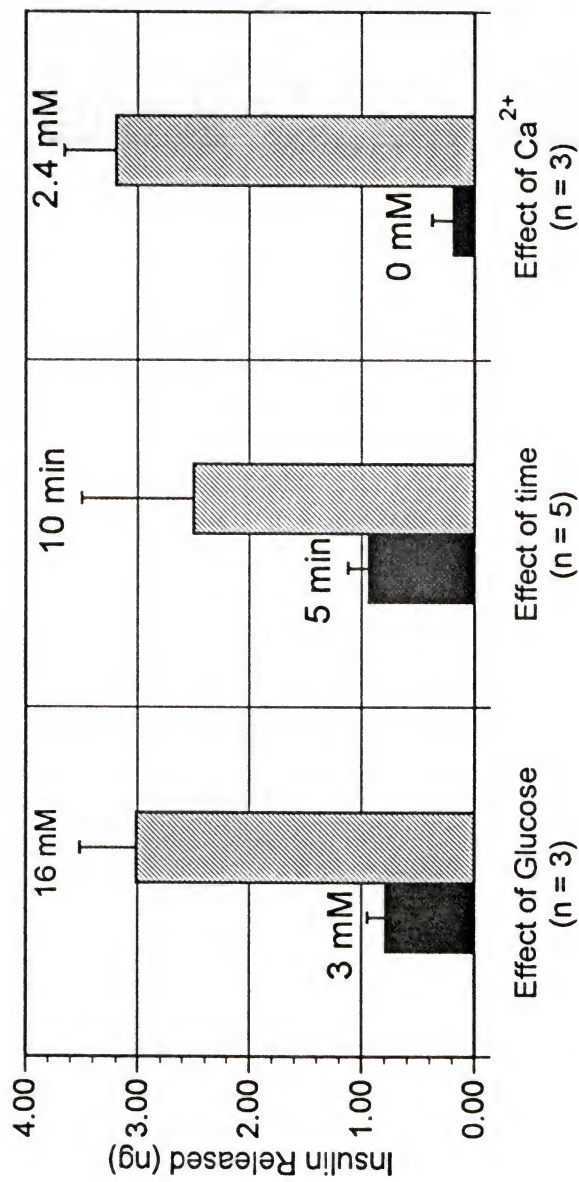


Figure 4-2. Results of insulin secretion experiments as described in the text. Unless shown otherwise, the glucose concentration was 16 mM for all stimulations. Error bars represent 1 standard deviation.

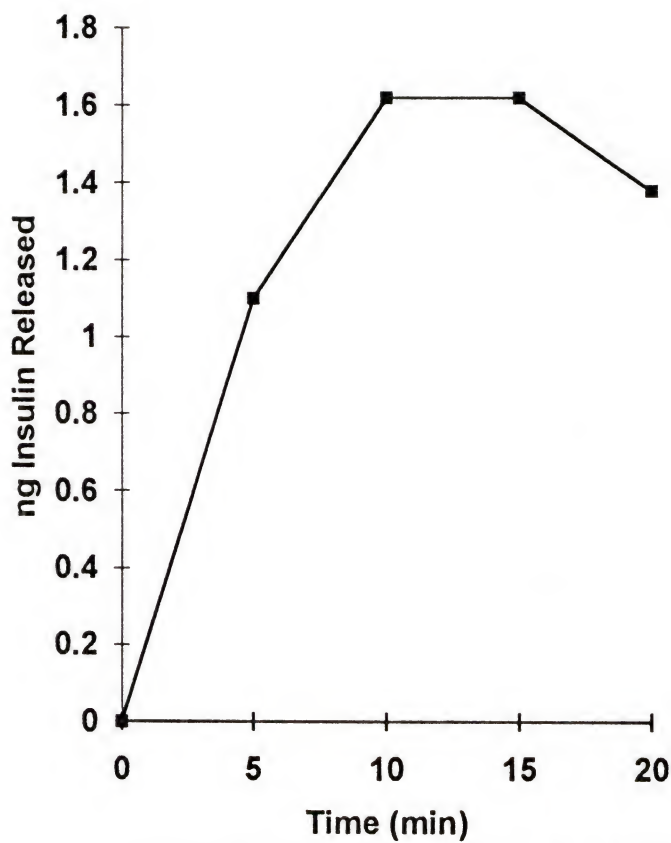


Figure 4-3. Insulin secretion as a function of time from a single islet. At  $t = 0$  the glucose concentration at the islet was raised from 3 mM to 16 mM.

## CHAPTER 5 APPLICATION II DETERMINATION OF BINDING CONSTANTS

### Introduction

Methods for studying binding phenomena are usually concerned with measuring either the unbound (free) and/or bound form of protein and determining the affinity constant using a mathematical model such as the one developed by Scatchard (71). Scatchard's theory, which was originally developed for the binding of proteins to small molecules and ions, uses the equilibrium of the reaction to develop a relationship between the amount of antigen bound to the antibody. The equilibrium expression can be written as Equation 5-1 based on the following relationship



$$K = \frac{[A \cdot Ab]}{[A] [Ab]} \quad \text{Equation 5-1}$$

Using the law of mass action, the total antibody concentration can be written as

$$[Ab^0] = [Ab] + [A \cdot Ab]$$

The equilibrium expression can then be rewritten as

$$K([Ab^0] - [A \cdot Ab]) = \frac{[A \cdot Ab]}{[A]}$$

By letting B and F represent the bound ( $[A \cdot Ab]$ ) and free ( $[A]$ ) amounts of insulin respectively, the equation for the Scatchard plot can be written as

$$\frac{B}{F} = -K_B + K [Ab^0]$$

Thus a plot of the B/F ratio versus the bound concentration of antigen should give a straight line with a slope of  $-K$ . The x intercept should equal the total concentration of binder.

These assays are generally used to characterize the affinity of drugs and proteins for their receptors and to determine the number of binding sites available (1). They are performed using competitive RIA procedures and take several hours to complete due to the necessary incubation steps. These methods quantitate the amount of bound ligand and from that determine the amount of free ligand. There is much debate in the literature over the validity of such results as many plots are non linear and need to be corrected for nonspecific binding or were generated under nonequilibrium conditions (72-74). Another problem lies in the statistical nature of the plot in that random error can occur in both the x and y directions.

This chapter discusses the use of a CE format for determining the binding constants of antigens for antibodies using the Scatchard technique. There are several advantages of using a CE technique to determine binding constants. First, minuscule amounts of protein and ligand are required as injection volumes are in the nL range. Second, it can be applicable to more than one type of compound at a time as long as the separation of all compounds is possible. Third it does not require the use of radioactive

tracers. Fourth, there is a savings in time due to the short run times and the possibility for automation. And finally, there is a possibility for improvement in validity as these separations are not based on a solid-phase interaction system.

As mentioned in the introduction, studying binding interactions with CE using Scatchard analyses has been demonstrated by other groups. Several different formats have been used. In one report, a study of protein-drug binding was conducted based on commonly used chromatographic procedures for doing such evaluations (17). The different techniques included the Hummel-Dreyer method, the vacancy peak method and the frontal analysis method. It was found that CE is a suitable technique for such studies as long as the drug and protein have different electrophoretic mobilities and the lifetime of the complex is stable on the timescale of the separation.

In another approach, interactions between oligonucleotides and synthetic peptides derived from human serum amyloid P component were characterized (23). From a solution containing free and peptide-bound oligonucleotides, the free nucleotides were separated by electrophoresis from the complex which was not detected. The decrease in the peak size for free ligand as a function of receptor concentration was used to quantitate the concentrations of bound and free ligand.

In a novel method, termed affinity capillary electrophoresis, the change in migration time of a receptor was monitored as a function of the concentration of ligand added to the migration buffer (16, 18-22, 24, 75). These measurements were made by measuring the changes in migration time versus another protein with similar migration that does not bind. As more ligand was added, the migration time of the receptor increased

until a saturating amount was added. A Scatchard type plot was then made using the migration differences, not peak areas, to determine the binding constant. Studies using ACE have included binding constants of benzene sulfonamides to carbonic anhydrase B (18, 20), NAD<sup>+</sup> and NADPH to glucose-6-phosphate dehydrogenase (18) and vancomycin to small peptides under multiple antigen and competitive formats (21, 22, 74). Comparisons with conventional assay determinations was in good agreement (18, 74). It was also reported to have been used for an antibody, but no data was shown (18). In another study, ACE was used to determine kinetic and equilibrium constants for binding of arylsulfonamides to bovine carbonic anhydrase (19). A similar approach was used to monitor protein-sugar interactions using some  $\beta$ -galactose-specific lectins and lactobionic acid as protein and sugar models, respectively (23). Association constants of monovalent interactions could be obtained from the slope of a plot of the migration differences between the protein and complex (determined as the migration time at the plateau) versus the concentration of lactobionic acid in the buffer.

In this work, a Scatchard analysis is used to determine the binding affinity of a labeled antigen (FITC-insulin) for the antibody (Fab). The affinity of unlabeled antigen (insulin) for the antibody is also determined using a competitive assay format. A competitive format can be used as long as the assumption that the tracer antigen binds with the same affinity as unlabeled antigen is valid (51).

### Experimental

CZE. Separations were performed on the CZE apparatus as described in Chapter 2 with the Ar<sup>+</sup> laser as the excitation source. The capillaries were 10  $\mu$ m i.d. and 350  $\mu$ m

o.d. The 150  $\mu$ m o.d. capillaries could not be used under these conditions because they frequently broke under high voltages. This breakage was the result of arcing through the capillary wall. The capillaries were pretreated by rinsing under pressure with 1 M NaOH for at least 1 hour followed by H<sub>2</sub>O and migration buffer for 15 min each. The migration buffer was 0.02 M tricine/ 0.2 M Na<sub>2</sub>SO<sub>4</sub> pH 8. The applied separation voltage was -29 kV giving a current of 15  $\mu$ A. Hydrodynamic injections were made at the grounded end by raising the vial 5.5 cm for 7 s. The injection volume for these capillaries was approximately 5 pL.

The Beckman P/ACE System 2200 was used to demonstrate automation of the analysis. With this system, the acrylamide coated capillaries were used with the conditions as described in Chapter 3.

Solution preparation. The solutions for binding constant determinations of FITC-insulin to Fab in the 10  $\mu$ m capillaries contained 500 nM Fab and FITC-insulin concentrations ranging from 100-500 nM. For the determination of binding constants to unlabeled insulin, solutions contained 500 nM each of FITC-insulin and Fab and human insulin concentrations ranging from 0-500 nM. These standard mixtures were prepared in 0.02 M tricine/ 0.2 M Na<sub>2</sub>SO<sub>4</sub> pH 8 buffer to a volume of 3 mL then mixed and injected. Scatchard plots were made after obtaining the peak areas for the bound and free FITC-insulin from the electropherograms.

Solutions used with the coated capillaries were prepared as above except the buffer was 0.02 M tricine pH 8. Each of these solutions also contained 50 nM of the internal standard prepared as described in Chapter 3.

Chemicals. All chemicals were obtained as described previously. The Fab was made from the HL111 antibody and FITC-insulin, purified as described in Appendix D, was used.

### Results and Discussion

FITC-insulin/Fab. It was desirable to use uncoated capillaries for this application because both the complexed and free forms of FITC-insulin could be detected in a single run. An example of an electropherogram for these conditions is shown in Figure 5-1. The first peak detected (B) is FITC-insulin bound to Fab and the second peak (F) is free FITC-insulin. Scatchard plots were made by evaluating the ratio of the peak areas for bound and free FITC-insulin. Figure 5-2 is an example of the resulting plot for the Scatchard analysis of Fab and FITC-insulin. The average  $K_b$  determined from the slopes of three of these plots was  $6.9 \pm 0.7 \times 10^7$  L/mol with an average correlation coefficient of 0.99. The average RSD for three runs of an individual sample was less than 10%. The  $K_b$  value is in good agreement with the literature value of  $5 \times 10^7$  L/mol for the binding constant of this antibody with insulin (43).

Insulin/Fab. As mentioned earlier, it is also possible to use competitive assays with Scatchard-type analysis to determine the binding constant of an unlabeled antigen for a receptor in the presence of the labeled antigen. A plot of this type is found in Figure 5-3. An average value of  $3.3 \times 10^7$  L/mol was obtained for a competitive Scatchard analysis for the human insulin. Again, this value is in reasonable agreement with the previously reported value (43).

Coated capillaries. Because the complex peak was not reproducible with the coated capillaries, a slightly different procedure was needed to obtain the amount of FITC-insulin bound in complex. A calibration plot was first constructed of normalized peak area versus concentration of FITC-insulin ranging from 0.5- 75 nM. By using this plot and the area of the free FITC-insulin determined from the electropherogram, it was possible to determine the concentration of FITC-insulin not bound in the complex. The concentration of bound insulin could then be determined by subtracting the free from the original concentration of FITC-insulin added to the solution. This method is similar to the idea used by Heegaard and Robey because the complex was not detected in their work (5-10). A Scatchard plot could then be constructed. Results performed with this method were only attempted once and gave a  $K_b = 2 \times 10^8$  L/mol. This value was a little higher than expected but perhaps with a better coating more reasonable results could be obtained. One possible reason for such a high value could be that the assumption that the binding constants of the labeled and unlabeled antibodies were equal was not valid.

In cases such where  $K_b^* \neq K_b$ , it is still possible to use a competitive assay to calculate  $K_b$  of the unlabeled antigen using another technique (19). To do this a Scatchard plot of bound labeled antigen/ unlabeled antigen concentration versus bound labeled antigen concentration is made and the slope is used to determine an apparent binding constant ( $K_b'$ ). The actual binding constant ( $K_b$ ) can then be calculated using the following equation

$$K_b = K_b' (1 + K_b^* [A^*])$$

where  $[A^*]$  is the fixed concentration of labeled antigen.

These results demonstrate the potential for automation because the coated capillaries can be used with the commercial CZE instrument with autoinjection capabilities. Besides the potential for automation, other benefits of this assay include a savings of time, due to short analysis times and incubation periods, and reagents as only femtogram quantities of both antibody and protein were required to do these analyses.

Benefits gained with using fluorescence detection are the possible determination of a wider range of binding constants than could be measured by UV detection. The reasoning for this is that for strong interactions even at low concentrations of ligand the unbound peptide may not be detectable by UV and a more sensitive detection scheme would be needed. This work is believed to be the first determination of binding constants by CE with fluorescently-tagged tracers.

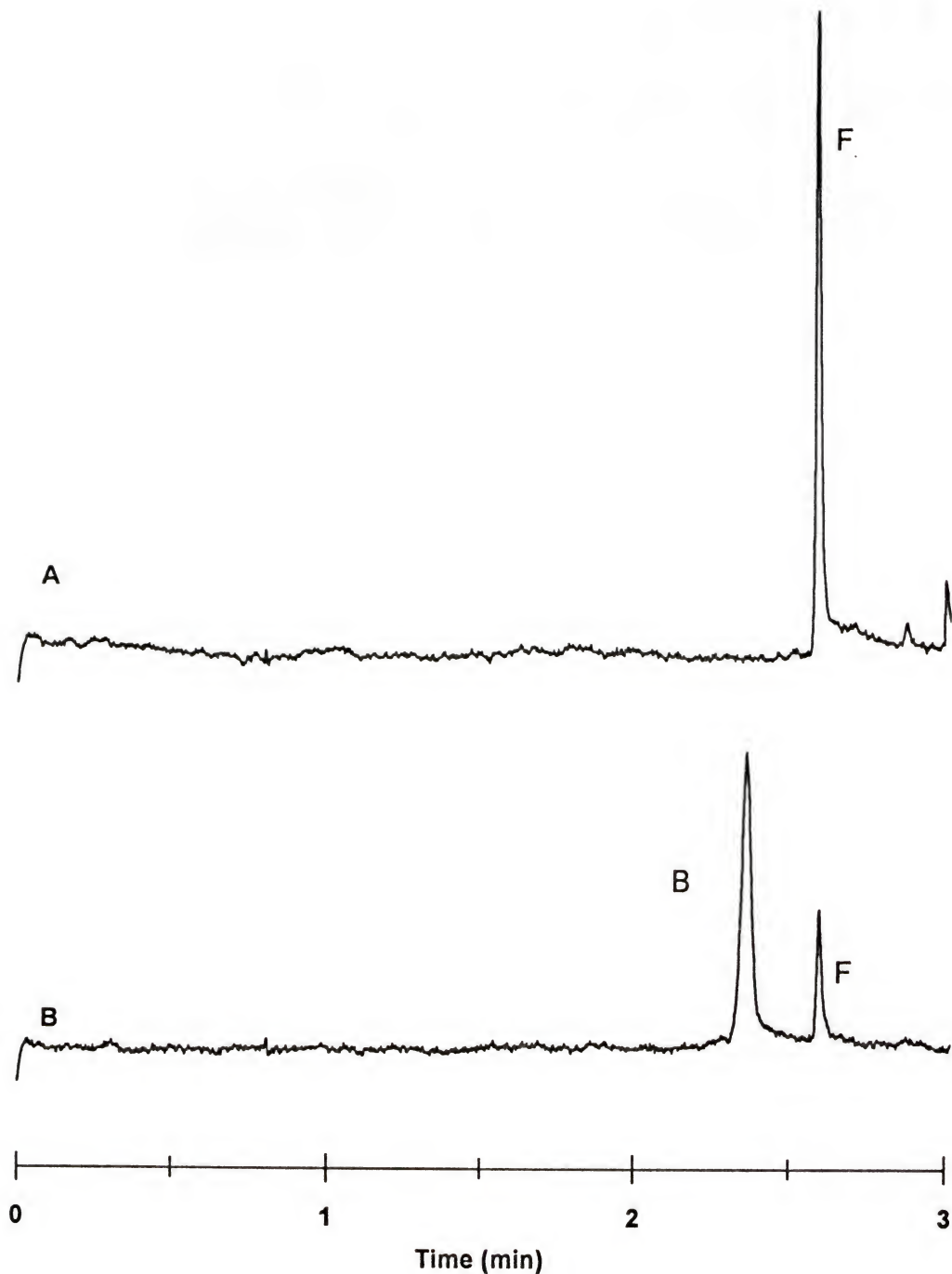


Figure 5-1. Electropherograms showing complex formation on an uncoated capillary using conditions described for Scatchard analysis in the Experimental Section. The upper electropherogram (A) is of an injection of 500 nM FITC-insulin (peak F). The lower electropherogram (B) shows FITC-insulin/ Fab complex (peak B) upon addition of 500 nM Fab.

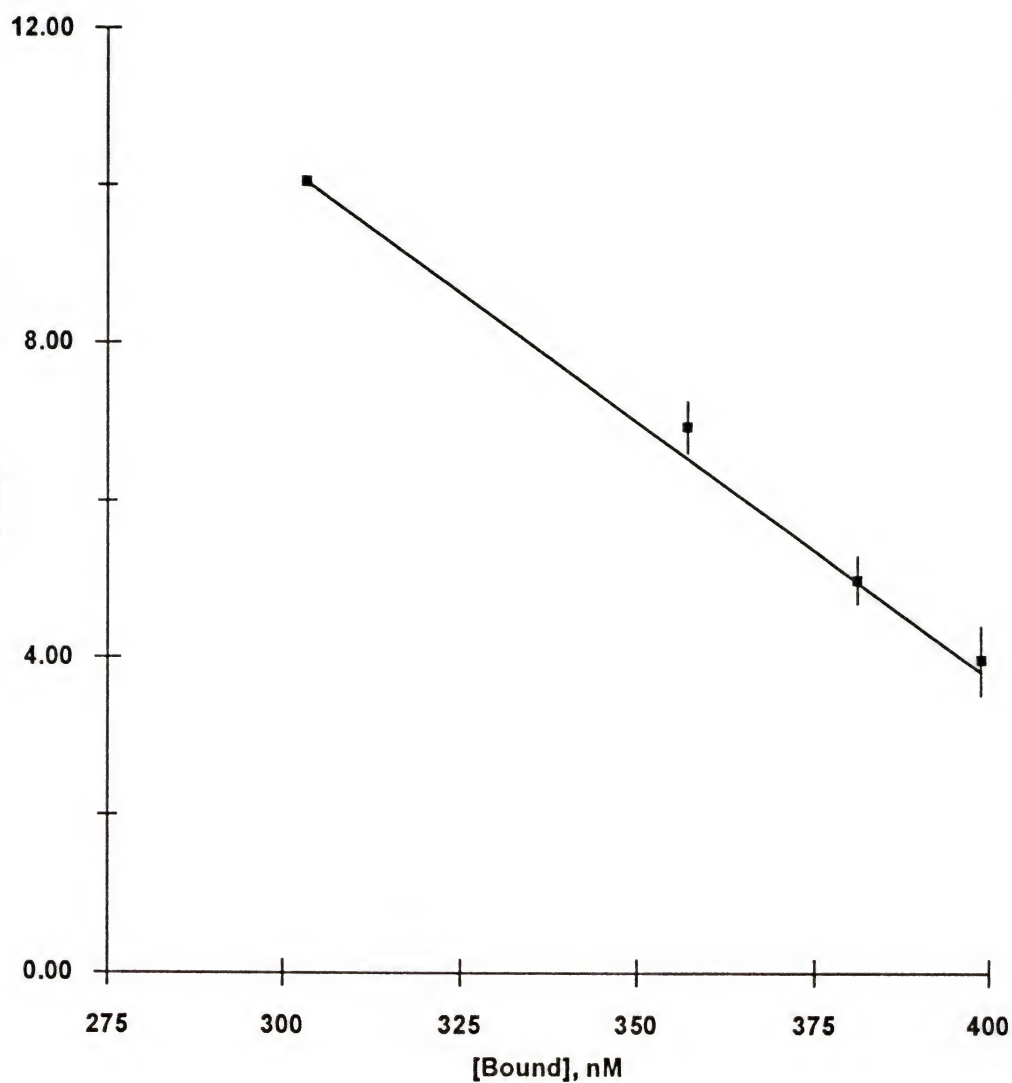


Figure 5-2. Scatchard plot estimating the  $K_b = 6.6 \times 10^7$  for FITC-insulin/Fab. The line drawn is the linear least squares fit with  $R^2 = 0.997$ . Data points are an average of 3 runs and error bars are 1 standard deviation.

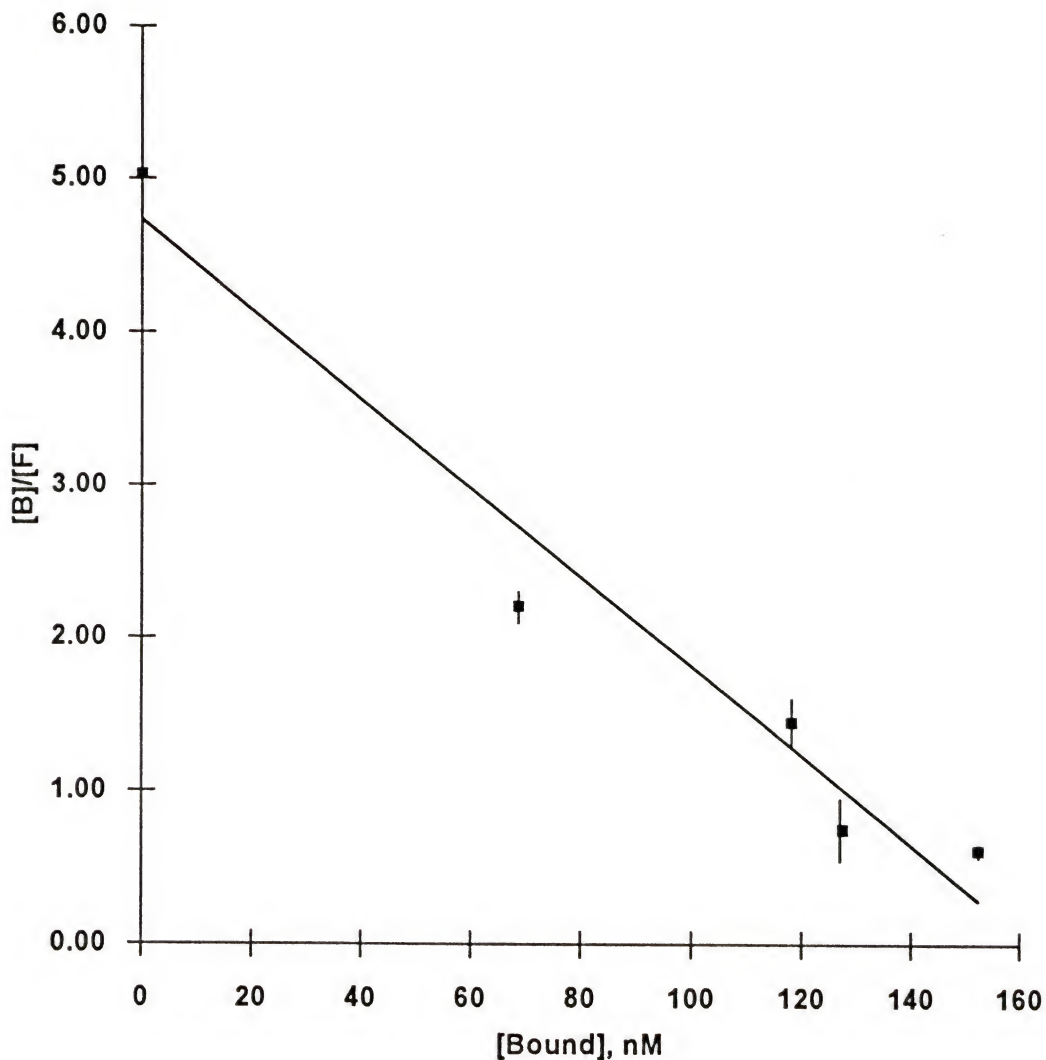


Figure 5-3. Scatchard plot estimating the  $K_b = 2.9 \times 10^7$  for unlabeled insulin/Fab. The line drawn is the linear least squares fit with  $R^2 = 0.99$ . Data points are an average of 3 runs and error bars are 1 standard deviation.

## CHAPTER 6 CONCLUSIONS AND FUTURE WORK

Performing immunoassays by capillary zone electrophoresis with laser induced fluorescence detection are possible as long as the complex is stable on the time scale of the separation. Run times as short as 30 seconds can be achieved and lengthy incubation periods are not necessary at least with this antibody. Both noncompetitive and competitive formats are feasible. The noncompetitive format was demonstrated by detecting antibody using labeled antigen. With this format, detection limits of 0.15 nM for Fab have been achieved with a mass LOD of 15 zeptomoles, assuming 0.1 nL injected. Further improvements in LOD of about another order of magnitude should be achievable with the current detection system. Further work is needed with the labeling of an antibody for the direct analysis of antigen. Purification of the IAF labeled Fab' fragments needs to be performed so that better separations can be achieved. It may be necessary to use capillary IEF to perform the separation if adequate resolution is not achieved between the complex and the labeled Fab'. A separation based on the pI of these species has proven possible using conventional IEF techniques.

Detection limits for the competitive assay were 3 nM and 0.3 attomoles for the concentration and mass of insulin, respectively. These values were found to be limited by the binding constant of the antibody. Further improvements could be attained by using an antibody with higher binding and an epitope for insulin in a location away from the

fluorescent labels. Alternatively, a different labeling scheme for the insulin could be developed to label insulin in a different region so that antibodies currently available with higher binding constants could be used. Although this technique does not compare in terms of concentration detection limits with the conventional immunoassay techniques, an improvement in mass detection is attained.

The use of the competitive assay to quantitate insulin extracted or secreted from single islets of Langerhans gave results comparable to those published using other techniques. This method provides a more rapid and potentially automatable format for performing these types of analyses on small samples in a microenvironment. Further work is needed for detecting insulin release from an islet in a time resolved fashion using the perfusion arrangement as discussed in Chapter 4. These experiments would allow for more information on the release of insulin to be attained.

Results for using the noncompetitive or competitive format for Scatchard analyses showed the potential for studying binding data.  $K_b$  values near those expected were achieved for the insulin and anti-insulin tested. This technique has a major advantage over conventional RIA procedures in terms of time and the capability of doing multiple antigens. Future work needs to include multiple antigens and the use of the competitive format for antigens with known differing binding constants.

The major limitation in performing analysis with CZE immunoassays is the adsorption of proteins and the potential losses to the capillary surface. With current research in column coating technology and the availability of more commercial columns, this problem should be eventually overcome. Overall, CZE immunoassays are fast, have

low mass detection limits, and are capable of studying binding and kinetic data. With the design of different antibody/antigen systems, there are a wide range of potentially useful microscale applications.

## APPENDIX A PREPARATION OF Fab FRAGMENTS

Antibodies can be digested with the protease papain to isolate the Fab fragments.

Papain is a proteolytic enzyme that cleaves the antibody on the amino-terminal side of the disulfide bonds that hold the two heavy chains together (45). (See Figure 1-6.) Therefore, digestion releases two Fab domains and one Fc fragment per antibody. Mouse immunoglobulins of the type used in this work are resistant to secondary cleavage so this reaction is easily performed without degradation and loss of product.

A commercially available Fab preparation kit was used to prepare the fragments (Catalog No. 44885 G, Pierce Chemical Co., Rockford, IL). It is designed for generating and isolating Fab fragments from mouse and human IgG using immobilized papain. The papain was supplied as a 50% slurry in glycerol and water and was immobilized on a crosslinked 6% beaded agarose gel for easy separation from the reaction mixture. The reported loading was 250  $\mu$ g of enzyme/mL of gel. The digestion buffer was prepared using cysteine monohydrate monohydrochloride and a phosphate buffer pH 10.0. For purification of the product, the kit contained an Immunopure IgG binding buffer and 2.5 mL prepacked Affinity columns of immobilized protein A. The typical binding capacity is 6-8 mg for mouse IgG/mL of gel in these columns. The Fc fragment of IgG binds to protein A, therefore cleaved Fc and any undigested antibody are retained by these

columns. The Fc portion and undigested antibody can then be recovered if desired using an ImmunoPure Elution Buffer provided with the kit to release them from the column.

The antibody was used directly as obtained in the phosphate buffered saline. The instructions provided with the kit were followed with only a few minor modifications.

*Initial Preparation:*

- 1) The digestion buffer was prepared by dissolving 42 mg cysteine-HCl in 12 mL of the supplied phosphate buffer. The pH was adjusted to  $7.0 \pm 0.2$  with NaOH.
- 2) The papain was equilibrated by mixing in a 16 x 100 mm glass test tube 0.5 mL of the 50% slurry and 4 mL of the digestion buffer. The papain was separated from the buffer using a serum separator plunger provided with the kit. This plunger forces the liquid through a membrane by compressing the gel in the bottom of the tube. The buffer was decanted off and another 4 mL wash was performed. The immobilized papain was then resuspended in 0.5 mL of the digestion buffer.

*Generation of Fragments:*

- 3) 0.5 mL of the antibody (approximately 5-25 mg) were added to the immobilized papain.
- 4) The reaction was incubated overnight ( $t = 12-15$  hours) while stirring at  $37^{\circ}\text{C}$ . This was accomplished using an air driven stir plate immersed in a water bath. This reaction was originally monitored by CZE with UV detection to determine the incubation times for the best results.
- 5) The next day the sample was recovered using the separator tube and decanted into a clean vial. The papain was washed with 1 mL of the binding buffer for maximum

recovery. The wash buffer was then combined with the sample to give a total volume of 2 mL.

*Fab Purification:*

- 6) An immobilized protein A column was equilibrated with 13 mL of the binding buffer after pouring off the 0.2% azide storage solution. ( NOTE: This can take 1-2 hours depending on the column.)
- 7) The sample was then applied to the column and allowed to drain completely through before fraction collection began. The AffinityPak columns are equipped with a unique flow device which enables the flow to stop when the liquid level reaches the frit at the top of the gel bed.
- 8) The column was then washed with 6 x 1 mL fractions of the Immunopure binding buffer. Each fraction was collected in a separate vial for UV monitoring at 280 nm.
- 9) The absorbance was read for each fraction using a Spectrophotometer at 280 nm. The cuvettes used were 1 cm pathlength minivials.
- 10) The Fab fragments were normally find in the first 3-4 fractions. The concentration was determined after combining fractions containing Fab fragments using a Beer's law calculation and an  $\epsilon = 1.42 \text{ mg mL}^{-1} \cdot \text{cm}^{-1}$  (46) Typical absorbance readings were 0.3-1.00 giving concentrations ranging from 0.2- 1 mg/mL (4-20  $\mu\text{M}$ ) depending on the concentration of the original antibody solution. (A 1 mL volume of antibody solutions as dilute as 1 mg/mL were used successfully with this kit.)

*Column Regeneration:*

- 11) If desired, the Fc and undigested IgG can be eluted from the column by collecting 1 mL fractions using the Immunopure Elution buffer and reading the absorbance to locate the fragments.
- 12) The column was regenerated by washing with 10 mL of 0.1 M citric acid adjusted to pH 3.0. For storage, 10 mL of 0.02% sodium azide solution were passed through the column and place in the refrigerator when about 3 mL remained. Columns were used up to ten times as recommended by the manufacturer.

Solutions of Fab fragments were stored as obtained in the binding buffer with 0.1% sodium azide added to prevent bacterial growth. Typically solutions lasted about 2 weeks before signs of growth were observed and a fresh batch was then made.

## APPENDIX B ADSORPTION

### Capillary Adsorption

Adsorption of proteins to the interior walls of the capillary is a problem in CZE because it causes band broadening. This is due to the acidic silanol groups on the capillary surface which attract negative regions on the proteins. Therefore, several methods have been developed to circumvent this problem. They include 1) manipulation of the buffer pH, 2) chemical modification of the surface, and 3) dynamic modification of the capillary surface by additives to the buffer. These techniques were taken into account when selecting buffer systems for the separations.

Several researchers have shown that by manipulating the buffer pH to extremely acidic or basic conditions the surface charges on the capillary can be modified and therefore reduce adsorption through charge repulsion. This was not considered as an option in this work because it has been found that undesirable consequences may occur in separations of biological compounds at these extreme pHs such as hydrolysis or denaturation of proteins (74). It was also not known what effect if any these conditions may have on complex formation. These extreme pH buffers work by reducing the electrostatic attraction of the proteins for the capillary surface. With a low pH buffer, the amount of negative charges found on the capillary surface will be greatly reduced due to a lower number of silanol groups. This significantly lowers the coulombic attraction of the

protein for the surface and therefore the amount of adsorption. High pH buffers serve to make both the surface and the solute negatively charged and therefore exhibit a repulsion for each other.

Chemical modification of the capillary's inner surface works through blockage of the surface silanol groups by reacting them with a polymer. Many such coatings exist but for ease of procedure and materials a coating with polybren (hexadimethrine bromide) was attempted. (Another coating which was found to work better was used later and is discussed in detail in Chapter 3.) This polymer formed a positively charged surface layer on the capillary which served to reverse the electroosmotic flow. The antibody should be negatively charged under the conditions employed and thus repulsed by the surface. In fact this is what occurred giving an efficient peak shape for the antibody but the insulin was broad and had a plate count of only a few hundred. The coating was applied by flushing the capillary with 0.1 M NaOH and H<sub>2</sub>O for 15 minutes. The capillary was filled with a 10% w/w solution of the polybren (Sigma) in DI H<sub>2</sub>O and left to coat overnight. The next day it was rinsed with the phosphate electrophoretic buffer and used. One problem with this coating is that it is known only to be stable in the pH 2-7 region and the buffer used was near this limit (pH 7). Another problem with this coating is that it slowly deteriorates with use therefore it is necessary to recoat the capillary each night. The deterioration problem was observed as extraneous peaks believed to be polymer passing the capillary window. Thus another technique was examined.

Dynamic modification of the capillary surface can be achieved by additives such as surfactants or simple salts in the migration buffer. The surfactant investigated was fluorad

(3M Company St. Paul, MN) which was found to give separations of basic proteins with efficiencies in excess of 300000 plates (75). It is positively charged and therefore attracted to the negatively charged capillary surface. This causes the formation of a double layer thus giving the capillary a positively charged surface and reverses the electroosmotic flow. The capillary was coated by dissolving 350  $\mu$ g/mL of the surfactant in a 0.05 M sodium phosphate pH 7 buffer. After cleaning, the capillary was rinsed with this solution until a stable baseline was obtained (about 2 hours). The surfactant coating buffer was then used as the migration buffer. A problem with using a dynamic modification procedure is that the presence of surfactant may cause problems with detection or disrupt complex formation between antibody and antigen. While this surface worked for the antibody, the insulin was not always detected.

Another way to decrease interactions between the capillary surface and a protein is to add high amounts of salt to the buffer. This technique minimizes adsorption by creating a competition between the positively charged alkali metal in the buffer and the protein for the capillary surface. Therefore, several salts were added to the 0.05 M sodium phosphate buffer. It is desired to use the lowest amount of salt possible to decrease the conductivity of the solution and therefore reduce the current. This prevents the generation of heat and allows higher voltages to be used giving faster more efficient separations. The best results in terms of plate counts, 11000 and 8000, for the antibody and insulin respectively, were obtained with the addition of 0.1 M  $K_2SO_4$  to the phosphate buffer. Therefore all proceeding work with the whole antibody used 0.05 M sodium phosphate/ 0.1 M  $K_2SO_4$  pH 7.5 as the electrophoretic buffer.

### Capillary Cleaning

During the course of this work it was discovered that the inner surface of the fused silica varied from batch to batch. This led to difficulties related to the cleaning the surface before it could be used. Most CE procedures use 15 minutes rinses of 0.1 M NaOH and DI H<sub>2</sub>O at the start of each day. This appeared to be acceptable when pretreating the 50  $\mu$ m i.d. capillaries, but more stringent procedures needed to be employed with smaller i.d. capillaries used later in this work. At first the typical procedure seemed adequate but more and more often problems were encountered with poor peak shapes, compound retention and irreproducible run times. Other rinses were attempted found in other protocols such as with acids (1M HCl) or organics (methanol/acetonitrile). These are believed to dissolve any metals or organics that may be deposited during the manufacturing process. The organic rinses never improved results but occasionally an hour long acid rinse did help. After much experimentation with times and concentrations, the best rinsing procedure was found to be 1-3 hours with 1 M NaOH followed by 15 min of H<sub>2</sub>O and migration buffer. The capillary was tested after each hour of base rinse with an injection of the FITC-insulin. If efficiencies of over 20000 plates were obtained, the capillary was used, if not the rinsing was continued. If after 3 hours the capillary was not useable, it was discarded because further improvements were seldom obtained. After the initial cleaning, daily rinses of just 15 minutes each with the 1M NaOH, DI H<sub>2</sub>O and buffer were employed. A simple 1-2 min buffer rinse between runs also seemed to improve reproducibility of peak areas and shapes. This was accomplished by coupling a piece of fused silica placed in a high pressure bomb to the separation capillary with a small piece of

Teflon tubing. All capillaries were left with ends submersed in buffer reservoirs for overnight storage so as not to let them dry out. Most capillaries could be used for 1-2 weeks before being replaced.

#### Vial Adsorption

One final problem to address in dealing with adsorption was the loss of sample to the sample vial. Originally, small sample volumes (100-500  $\mu$ L) were prepared in 500  $\mu$ L conical glass minivials to conserve sample. However, as the concentration of the assay was lowered from the  $\mu$ M to the nM range, a problem was detected in the decrease of peak areas over time and poor reproducibility (RSDs as high as 25%). This problem indicated loss of sample to the vial because mixing of new samples gave the original peak areas. To try and circumvent this problem, the vials were coated with Sigmacote (Sigma). This is a special silicone solution in heptane that forms a tight microscopically thin film on glass. It was thought that by blocking the surface with this layer the proteins would no longer adsorb. However, samples injected out of these vials gave peak areas barely detectable indicating increased adsorption. Silanized minicentrifuge tubes (Fisher) were also tried for similar reasons but the results were no better.

Another attempt was to add 1% (w/v) bovine serum albumin (BSA) to the 0.05M phosphate/0.025 M sulfate buffer used to prepare the samples. BSA is a very adsorptive protein used in many assays to coat surfaces to block them adsorbing the protein of interest. Results under these conditions were unfavorable to the presence of excess peaks indicating binding with the FITC-insulin and/or complex.

Next, a 0.05% (v/v) Tween 20 solution in the phosphate/sulfate buffer was prepared. Tween is a surfactant which is often used to decrease adsorption of proteins to surfaces. Peak areas were more reproducible but bound/free ratios were smaller than those originally detected from samples injected from in the minivials. This indicated some interference with the immunoaffinity interactions that would effect the sensitivity of the assay. Finally it was found that by increasing the amount of sample prepared to 3-4 mL that RSDs of injected samples were less than 5% over time. This was attributed to having a smaller amount of solution exposed to the vial surface. Therefore, all samples were prepared in 3 mL volumes.

## APPENDIX C DETECTOR OPTIMIZATION

The alignment of the epillumination system was performed by viewing the fluorescence through the microscope eyepieces. To align the laser beam, it was first directed into the back of the microscope chamber with the lens holder removed so that the beam could be centered by viewing it on the inner wall of the microscope. This alignment was done either by moving the beam director mirrors or by shifting the microscope if necessary. When the laser beam was centered on front wall of the microscope chamber, the optics holder was replaced and the beam was directed down onto the microscope stage onto a fluorescent card. The beam director mirrors were then moved until the brightest pin spot of fluorescence was in the middle of the view through the spatial filter port. When this initial alignment was finished, a capillary was placed in the capillary holder on the stage and flushed with a fluorescent solution under pressure so precise alignment with the capillary in place could be performed. The capillary was brought into view using the XYZ positioner of the microscope and focused. The aligned view through the 0.4 NA lens gave the appearance of a cross (as noted in the Hernandez paper) (40). This cross was reportedly due to the collection of light in both the orthogonal and parallel directions. This cross was centered while viewing through the spatial filter port as this filter was not in total alignment with the bull's eye as seen through the eyepieces.

After alignment, the settings for the spatial filter were optimized. S/N measurements were taken using various slit settings and it was found that a 1 mm width by 2 mm length gave the largest S/N ratio. These settings were just to the inside of the inner diameter of the capillary. It was found to be essential to have the settings within the i.d. of the capillary to decrease scatter from the inner boundary. Another consideration was the o.d. of the capillary used. It was found that the amount of background scatter was about the same for a 350 vs. 170 o.d. capillary. The smaller capillaries were usually used because they provided much more flexibility for injections using the short lengths employed in these works.

Once the laser was optimized, a limit of detection for FITC labeled arginine was acquired for comparison to previously reported findings with a similar system (40). The derivatization was done using an excess of arginine to fluorescent reagent. 1 mL of a 1 mg/mL solution of arginine in 0.2 M sodium carbonate pH 9.0 was mixed with 1 mL of a  $2.1 \times 10^{-4}$  M FITC (isomer I, Sigma) prepared in the same buffer. The reaction was left for 4 hours in the dark. The FITC-arginine was then diluted for injection onto the CZE. A 90 cm, 25  $\mu$ m i.d. capillary was used with a 40 mM carbonate electrophoretic buffer pH 10. The electric field strength was 225V/cm and injections were performed for 7 s at a voltage of 10 kV. The excitation source was the He-Cd laser. The limit of detection obtained was 100 pM based on 2 times the S/N ratio. A factor of about 10-fold higher was expected from the published results of 3 pM due to the use of the 442 nm line of the He-Cd laser versus the 488 nm line of an Ar<sup>+</sup> laser used in the paper (40). The difference was attributed in part to capillary i.d. because a 25  $\mu$ m was used as opposed to the 50  $\mu$ m

i.d. used in the paper (40). A larger i.d. would allow for larger injection volumes, at least a factor of 2, and possibly more fluorescent light to be collected.

To try and improve the LOD, a Liconix laser stabilizer was obtained and placed in-line with the laser to try and reduce background noise caused by fluctuations in the laser power. Signal to noise readings were taken while a fluorescent solution was pumped through a capillary aligned on the stage. No change was seen in the peak to peak noise with the stabilizer on or off, therefore; it was not used further. It appears that the main source of noise for this system is due to scatter from the capillary surface and to the choice of electrophoretic buffer. Originally, the phosphate/sulfate buffer gave the lowest amount of background noise but it was found that the 0.02 M tricine buffer used with the coated capillaries significantly lowered the background.

Once it was assessed that the system was working as expected, an optimization to obtain a lower LOD was attempted by using the 543.5 nm line of a 0.5 mW green helium-neon laser (Melles Griot, Irvine, CA) to excite rhodamine. Tetramethylrhodamine isothiocyanate (TRITC) (Sigma) has an excitation maximum of 544 nm and was used to derivative arginine following the same method as for the FITC-arginine. With this laser, a 546 nm band pass filter was used for excitation with 560 nm long pass and 580 nm band pass filters used for emission. The dichroic mirror had a cut off of 560 nm. An LOD of 10 nM was obtained for this system under the CE conditions as given above.

In order to use this system with the assay, it was first necessary to derivatize insulin with TRITC. A variation of the method referenced by Sigma for FITC labeling was used (76). Bovine insulin (5.5 mg) was dissolved in 1 mL of H<sub>2</sub>O by addition of

drops of 1M HCl. 1 M NaOH was then used to neutralize to pH 7 while testing with pH paper. This solution was combined with 1 mL of 280  $\mu$ M TRITC dissolved in 0.06 M carbonate buffer pH 9. The reaction was allowed to proceed for 4 hours in the dark. LC purification was then used under the conditions as given for the purification of FITC insulin in Appendix D. LC fractions were collected and those at 5 and 10 minutes were found to be fluorescent using CZE and determined to contain insulin by peak shifting upon addition of Fab. Problems arose in trying to determine the concentration of the TRITC-insulin and finding a suitable way for storage as degradation usually occurred after a few days in solution. Therefore, this system was not used; and an Ar<sup>+</sup> laser was obtained to use its 488 nm line to excite FITC because the FITC-insulin could be obtained commercially in a stable form.

As mentioned earlier, this laser is well suited for excitation of FITC at its excitation maximum of 495 nm. After alignment of this laser, the laser power was optimized in the range of 0-20 mW by electrophoretically pumping a solution of FITC-arginine through the capillary. The signal, background and RMS noise were measured at 2 mW power intervals. A plot of S/N ratio versus laser power began to level off at about 10 mW, therefore the laser was operated at this power for future experiments (Figure C-1). Above this point, the curve began to flatten mostly because of a leveling off of the signal which could be caused by quenching of the fluorescence as the molecules reached saturation.

A comparison of the LODs using the Ar<sup>+</sup> versus the He-Cd laser revealed a factor of about 8 was gained using the 488 nm line. An LOD of about 13 pM based on 2 times

the S/N for FITC-arginine was obtained with the Ar<sup>+</sup> system. An example of electropherograms for FITC-arginine under identical conditions except for the excitation source is shown in Figure C-2 and demonstrates the improvement in the LOD. The LOD for FITC-insulin under similar conditions was expected to be higher because as much as 50% quenching can occur upon derivatization with larger proteins. It was determined fluorimetrically that the best LOD for the FITC-insulin expected would be 30 pM under these conditions, therefore this set a limit for our assay LOD.

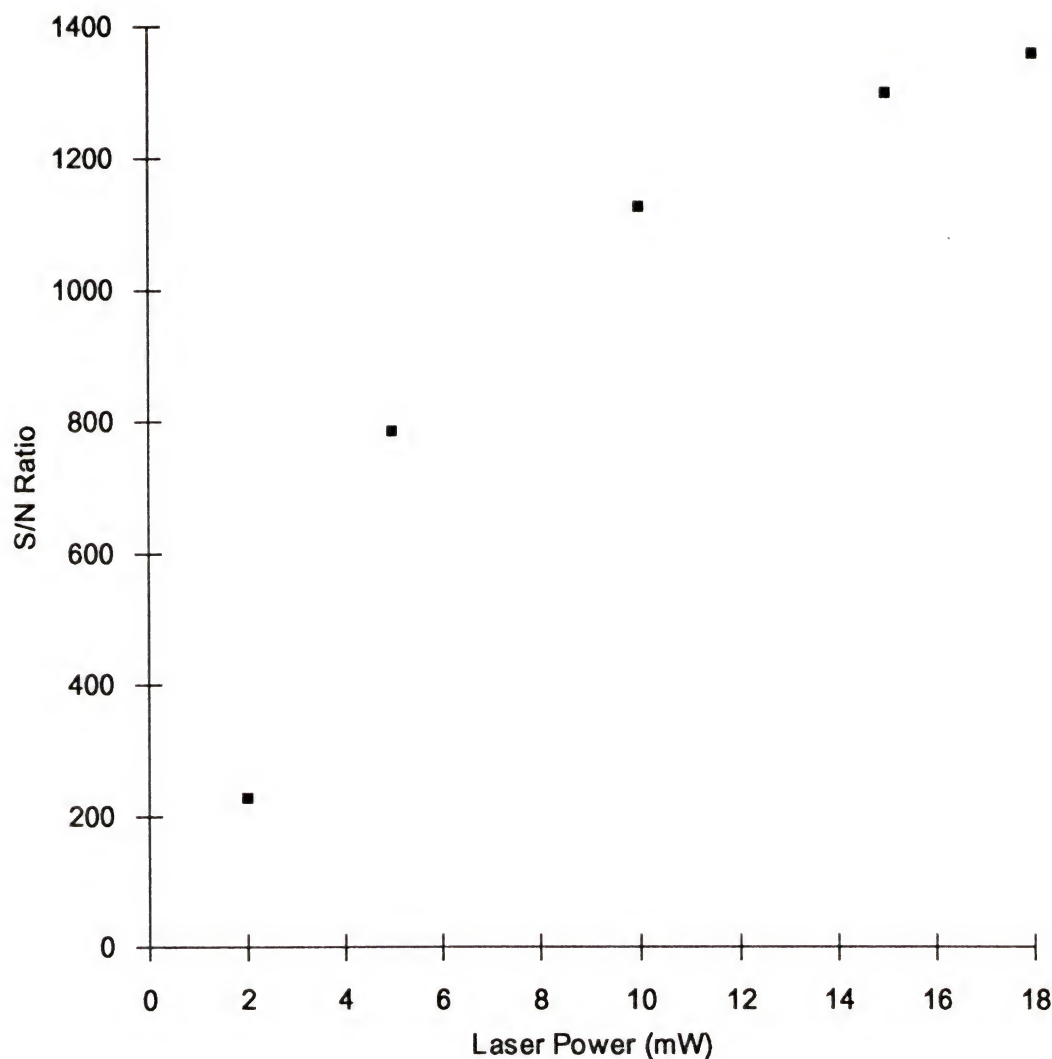


Figure C-1. S/N ratio plot for determination of optimum laser power for the  $\text{Ar}^+$  laser.

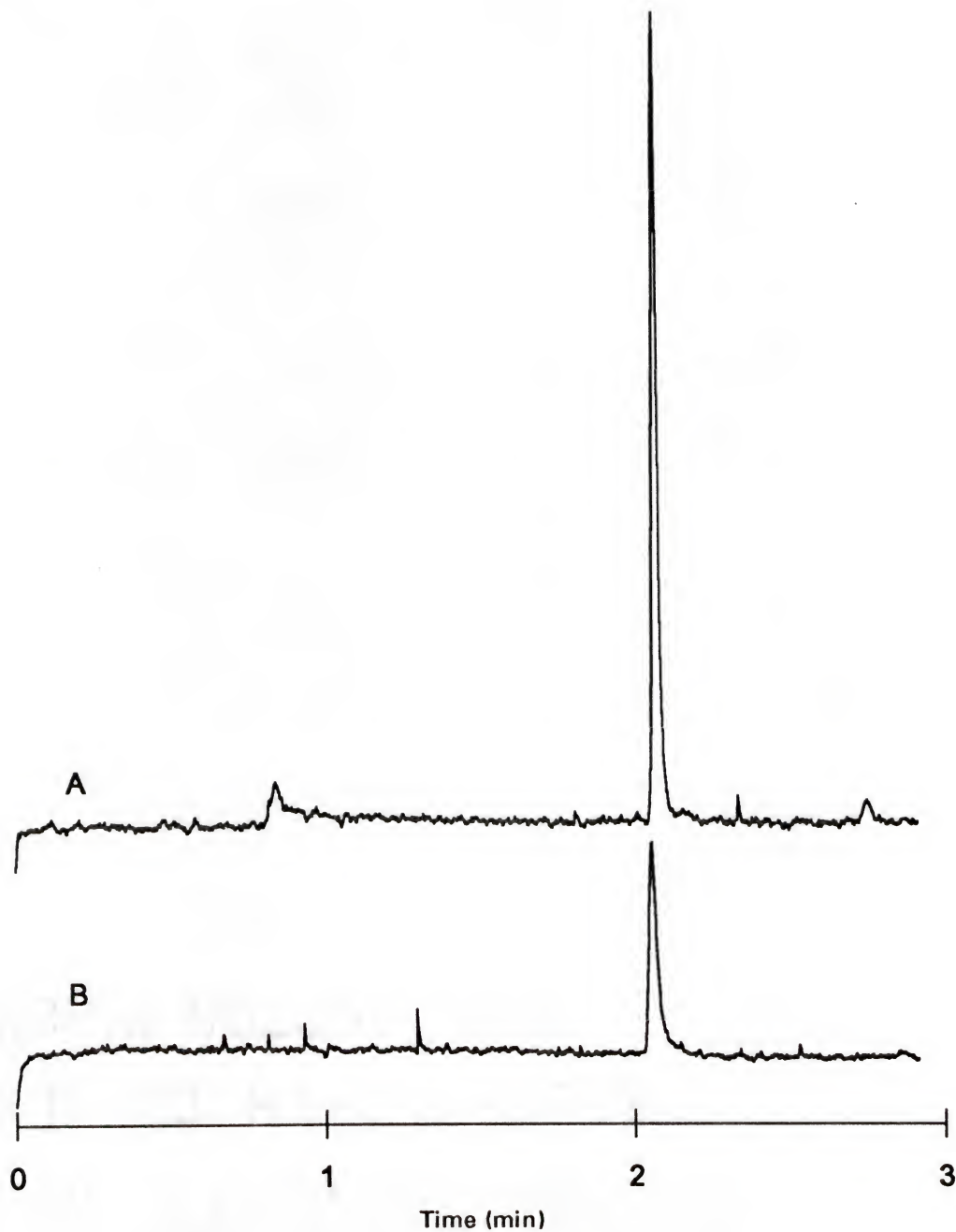


Figure C-2. Electropherograms of 10 nM FITC-arginine using the  $\text{Ar}^+$  laser (A) and the He-Cd laser (B) as the excitation sources. Conditions were as follows: 0.05 M phosphate/ 0.025 M sulfate pH 7.5 buffer; 30 cm 25 mm i.d. capillary 15 cm to window, -13 kV with a 10 s gravimetric injection.

## APPENDIX D FITC-INSULIN PURIFICATION

The FITC-insulin used in this work was obtained from Sigma and was in three forms due to multiple labeling sites. The method used to label it was developed by Tietze and co-workers (76). They found that most derivatives contained from 1.2-1.8 bound fluorescein groups/ mole of insulin. The most common labeled group was the chain B amino terminal phenylalanine group. It was also believed that the A chain amino terminus glycine may be tagged. A label may possibly be located at the B29 lysine amino acid as it contains an amino group which is available in the 3-D structure.

Because of its multiple forms, the FITC-insulin was purified using high performance liquid chromatography (HPLC) for improvement of the assay. For the separation, the FITC-insulin was dissolved in 0.1% trifluoroacetic acid to a concentration of at least 350  $\mu$ M. A 100  $\mu$ L aliquot of this solution was injected onto an HPLC system (SSI pump model 222C and 232C gradient mixer, Scientific Systems, Inc., State College, PA). The separation utilized a Vydac C-4 protein column with an isocratic mobile phase mixture of 70:30 0.1% trifluoroacetic acid: acetonitrile. UV-Vis detection was performed at 210 nm with a rise time of 1 s (Spectra Physics, Fremont, CA). The output of the detector was connected to an HP 3394A integrator (Hewlett Packard, Avondale, PA). One mL fractions were collected with an Isco Retriever 500 fraction collector (Isco, Inc., Lincoln, NE). Concentrations were estimated using UV-VIS absorption (HP 8450A,

Diode Array Spectrophotometer) and comparison to a Beer's law plot for the unpurified insulin.

Figure D-1 illustrates the three forms of the FITC-insulin in both a chromatogram and an electropherogram. The first eluted peak in the chromatogram is believed to be unlabeled insulin as its retention time corresponds to injections of unlabeled bovine insulin. The next two peaks (labeled 1 and 2) are believed to be the singly labeled forms of the FITC-insulin and the last peak (labeled 3) is the doubly labeled form. This conclusion was drawn based on the order of elution on both the HPLC and CE systems. With one FITC group, the singly labeled insulins would be less retained by the LC column due to lower amounts of hydrophobicity than with two labels. The CE migration order also supports this conclusion because the singly labeled forms would have a greater mobility towards the cathode as they would only contain 1 negative charge. The doubly labeled form would migrate much slower because it contains two negatively charged FITC groups.

Typical results for the absorbance readings of the fractions are found in the following Table D-1. Concentrations of about 3  $\mu\text{M}$  were normally obtained for the fraction concentrations. Fraction 3 was used for all purified work because it gave the best separation and the best binding to the insulin.

Table D-1. FITC-insulin absorbance readings.

[FITC-Insulin] $\mu\text{M}$	Absorbance ( $\lambda=280 \text{ nm}$ )
10	0.24
5	0.12
2.5	0.055
1	0.020
0.5	0.010
fraction 1	0.09
fraction 2	0.05
fraction 3	0.06

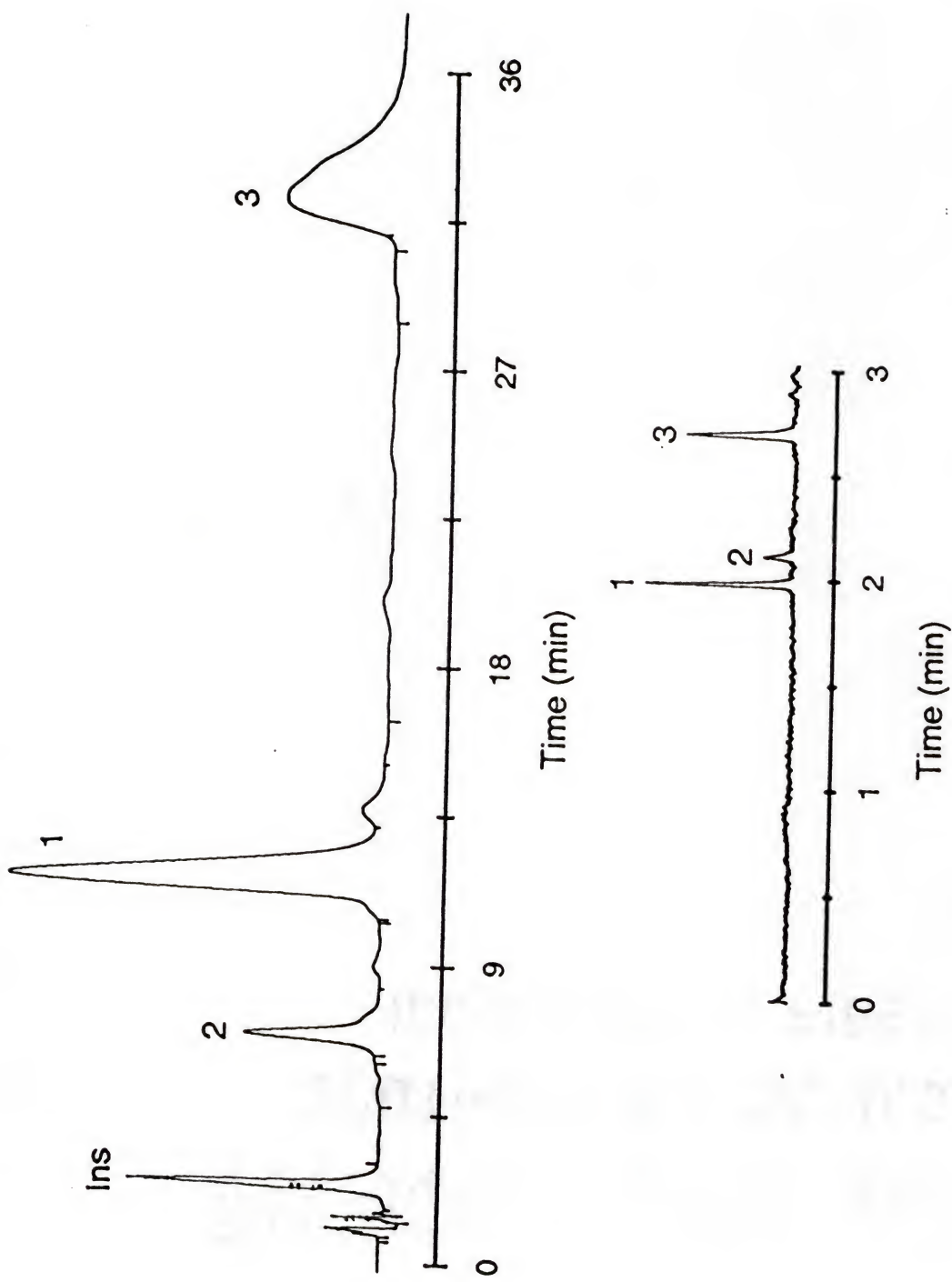


Figure D-1. Purification of FITC-insulin by HPLC. Peaks of corresponding insulin forms are labeled in the chromatogram (upper) and electropherogram (lower).

## REFERENCES

- 1) Butt, W.R.; Ed. *Practical Immunoassay*; Marcel Dekker: New York, 1984.
- 2) Wei, A.P.; Herron, J.N. *Anal. Chem.* **1993**, *65*, 3372.
- 3) Van Dyke, K.; Van Dyke, R. *Luminescence Immunoassay and Molecular Applications*; CRC Press, Inc.: Boca Raton, 1990.
- 4) Christopoulos, T.K.; Diamandis, E.P. *Anal. Chem.* **1992**, *64*, 342.
- 5) Song, M.I.; Iwato, K.; Yamada, M.; Yokoyama, K.; Takeuchi, T.; Tamiya, E.; Karube, I. *Anal. Chem.* **1994**, *66*, 778.
- 6) Brown, L.L.; Plant, A.L.; Horvath, Y.; Durst, R.A. *Anal. Chem.* **1990**, *62*, 2587.
- 7) Hage, D.S.; Kao, P.C. *Anal. Chem.* **1991**, *63*, 586.
- 8) Riggin, A.; Regnier, F.E.; Spartsman, J.R. *Anal. Chem.* **1991**, *63*, 468.
- 9) de Alwis, W. U.; Wilson, G. S. *Anal. Chem.* **1985**, *57*, 2754.
- 10) de Alwis, W. U.; Wilson, G. S. *Anal. Chem.* **1987**, *59*, 2786.
- 11) Hage, D.S.; Thomas, D.H.; Beck, M.S. *Anal. Chem.* **1991**, *65*, 1622.
- 12) Halsall, H. B.; Heineman, W. R.; Jenkins, S. H. *Clin. Chem.* **1988**, *34*, 1701.
- 13) deFrutos, F.C.; Paliwal, S.K.; Regnier, R.E. *Anal. Chem.* **1993**, *65*, 2159.
- 14) Jorgenson, J.; Lukacs, K.D. *Anal. Chem.* **1981**, *53*, 1298.
- 15) Lauer, H.H., Memanigell, D. *Anal. Chem.* **1986**, *58*, 166.
- 16) Chu, Y.H.; Avila, L.Z.; Biebuyck, H.A.; Whitesides, G.M. *J. Med. Chem.* **1992**, *35*, 2915.
- 17) Kraak, J.C.; Busch, S.; Poppe, H. *J. Chromatogr.* **1992**, *608*, 257.

18) Avila, L.Z.; Chu, Y.H.; Blossey, E.C.; Whitesides, G.M. *J. Med. Chem.* **1993**, *36*, 126.

19) Gomez, F.A.; Avila, L.Z.; Chu, Y.H.; Whitesides, G.M. *Anal. Chem.* **1994**, *66*, 1785.

20) Chu, Y.H.; Whitesides, G.M. *J. Org. Chem.* **1992**, *57*, 3524.

21) Chu, Y.H.; Avila, L.Z.; Biebuyck, H.A.; Whitesides, G.M. *J. Org. Chem.* **1993**, *58*, 648.

22) Honda, S.; Taga, A.; Suzuki, K.; Suzuki, S.; Kakehi, K. *J. Chromatogr.* **1992**, *597*, 377.

23) Heegaard, N.H.; Robey, F.A. *Anal. Chem.* **1992**, *64*, 2479.

24) Carpenter, J.L.; Camilleri, P.; Dhanak, D.; Goodall, D. *J. Chem. Soc., Chem. Commun.* **1992**, *11*, 804.

25) Akashi, M.; Sawa, T.; Babe, Y.; Tsuhako, M.J. *J. High Resolut. Chromatogr.* **1992**, *15*, 625.

26) Sawa, T.; Akashi, M. Baba, Y.; Tsuhako, M. *Nucleic Acids Symp. Ser.* **1992**, *27*, 51.

27) Baba, Y.; Tsuhako, M.; Sawa, T.; Akashi, M. *J. Chromatogr.* **1993**, *636*, 113-23.

28) Baba, Y.; Tsuhako, M.; Sawa, T.; Akashi, M.; Yashima, E. *Anal. Chem.* **1992**, *64*, 1920.

29) Nielsen, R. G.; Rickard, E. C.; Santa, P. F.; Sharknas, D. A.; Sittampalam, G. S. *J. Chromatogr.* **1991**, *539*, 177.

30) Schultz, N.M.; Kennedy, R.T. *Anal. Chem.* **1993**, *65*, 3161.

31) Rosenzweig, Z.; Yeung, E.S. *Anal. Chem.* **1994**, *66*, 1771.

32) Shimura, K.; Karger, B.L. *Anal. Chem.* **1994**, *66*, 9.

33) Skoog, D.A., Leary, J.J. *Principles of Instrumental Analysis*, 4th ed.; Saunders College Publishing: Forth Worth, 1992.

34) Yeung, E.S.; Wang, P.; Li, W.; Giese, R.W. *J. Chromatogr.* **1992**, *608*, 73.

35) Wu, S.; Dovichi, N. *J. Chromatogr.* **1989**, *480*, 141.

36) Sweedler, J.V.; Shear, J.B.; Fishman, H.A.; Zare, R.W. *Anal. Chem.* **1991**, *63*, 496.

37) Fuchigami, T.; Imasaka, T.; Shiga, M. *Anal. Chim. Acta* **1993**, *282*, 209.

38) Chan, K.C.; Janini, G.; Muschik, G.M.; Issaq, H.J. *J. Liquid Chromatogr.* **1993**, *16*, 1877.

39) Lee, T.T.; Yeung, E.S. *J. Chromatogr.* **1992**, *595*, 319.

40) Hernandez, L.; Escalona, J.; Joshi, N.; Guzman, N. *J. Chromatogr.* **1991**, *559*, 183.

41) Hollenberg, M.D. ed. *Insulin, Its Receptor and Diabetes*; Marcel Dekker, Inc.: New York, 1985.

42) Smith, L. *Am. J. Med.* **1966**, *40*, 662.

43) Schroer, J.A.; Bender, T.; Feldmann, R.J.; Kim, K.J.; *Eur. J. Immunol.* **1983**, *13*, 693.

44) Haughland, R.P. *Molecular Probes: Handbook of Fluorescent Probes and Research Chemicals*; Molecular Probes: Portland, 1992.

45) Harlow, E.; Lane, D. *Antibodies: A Laboratory Manual*; Cold Spring Harbor Laboratory, 1988.

46) Chaiken, I.; Rose, S.; Karlson, R. *Anal. Biochem.* **1992**, *201*, 197.

47) Wimalasena, R.L.; Wilson, G.S. *J. Chromatogr.* **1991**, *572*, 95.

48) Richard, R.F.; Rosenstein, R.W.; Konigsber, W.H. *Immunoglobulins*; Litman, G.W.; Good, R.A., eds.; Plenum: New York, 1978.

49) Giddings, J.C.; *Unified Separation Science*; John Wiley & Sons, Inc.: New York, 1991.

50) Parham, P. *J. Immunol.* **1983**, *131*, 2895.

51) Means, G.; Feeney, R., Eds. *Chemical Modifications of Proteins*; Holden Day, Inc.: New York, 1971.

52) Odell, W.D., Franchimont, P. Eds. *Principles of Competitive Protein Binding Assays*; John Wiley & Sons: New York, 1983.

53) Hjerten, S. *J. Chromatogr.* **1985**, *347*, 191.

54) Schmalzing, D.; Piggee, Frantisek, F.; Carrilho, E.; Karger, B.L. *J. Chromatogr.* **1993**, *652*, 149.

55) Stefansson, M.; Novotny, M. *Anal. Chem.* **1994**, *66*, 1134.

56) Towns, J.K.; Regnier, F.E. *Anal. Chem.* **1991**, *63*, 1126.

57) Hjerten, S.; Kiessling-Johansson, M. *J. Chromatogr.* **1991**, *550*, 811.

58) Hayes, R.L.; Goswitz, F.A.; Pearson Murphy, B.E. *Radioisotopes in Medicine: In Vitro Studies*, 1968.

59) Orci, L.; Vassalli, J. D.; Perrelet, A. *Scientific American* **1988**, *260*, 85.

60) Unger, R. H. *Science* **1991**, *251*, 1200.

61) Gilon, P.; Shepherd, R.M.; Henquin, J.C. *J. Biol. Chem.* **1993**, *268*, 22265.

62) Bergsten, P.; Hellman, B. *Biochem. Biophys. Res. Comm.* **1993**, *192*, 1182.

63) Bergsten, P.; Hellman, B. *Diabetes* **1993**, *42*, 670.

64) Webster, H.V.; Bone, A.J.; Webster, K.A.; and Wilkin, T.J. *J. Immuno. Meth.* **1990**, *134*, 95.

65) Wolheim, C.B.; Meda, P. Halban, P.A. *Meth. Enzy.* **1990**, *192*, 188.

66) Sandler, S.; Andersson, A.; Hellerstrom, C. *Endocrinology*, **1987**, *121*, 1424.

67) Andersson, A. *Diabetologia*, **1978**, *14*, 397.

68) Stridsberg, M.; Berne, C.; Sandler, S.; Wilander, E.; Oberg, K. *Diabetologia*, **1993**, *36*, 843.

69) Bjork, E.; Kampe, O.; Andersson, A.; Karlsson, F.A. *Diabetologia*, **1992**, *32*, 490.

70) Sandler, S.; Bendtzen, K.; Eizirik, D.L.; Welsh, M. *Endocrinology*, **1990**, *126*, 1288.

71) Scatchard, G. *Ann. N.Y. Acad. Sci.* **1949**, *51*, 660.

72) Scheinberg, I.H. *Science* **1982**, *215*, 312.

73) Klotz, I.M. *Science* **1982**, *217*, 1247.

74) Munson, P.J.; Robard, D. *Science* **1982**, *220*, 979.

75) Liu, J.; Volk, K.J.; Lee, M.S.; Pucci, M.; Handwerger, S. *Anal. Chem.* **1994**, *66*, 2412.

76) Malik, A.; Zhao, Z; Lee, M.L. *J. Microcol. Sep.* **1993**, *5*, 119.

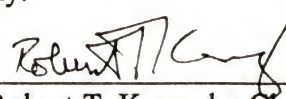
77) Emmer, A.; Jansson, M.; Roerade, J. *J. Chromatogr.* **1991**, *547*, 544.

78) Tietze, F.; Mortimore, G.E.; Lomax, N.R. *Biochim. Biophys. Acta*, **1962**, *59*, 336.

## BIOGRAPHICAL SKETCH

Nicole Marie Schultz was born December 18, 1966 in Hagerstown, Maryland. She received a Bachelor of Science in chemistry with a minor in mathematics from James Madison University in May 1988. For a period of two years, she worked for Program Resources Inc. as a research technician in the Chemical Synthesis and Analysis division. While in this position, her primary duties were in the HPLC analysis of biological samples. With an interest in separations being obtained, she decided to attend graduate school in the area of analytical chemistry. In August of 1990, she began her graduate career at the University of Florida department of chemistry and awaited the arrival of her advisor Dr. Robert T. Kennedy. She completed her research and obtained her Doctorate of Philosophy in analytical chemistry in December of 1994.

I certify that I have read this study and that in my opinion it conforms to acceptable standards of scholarly presentation and is fully adequate, in scope and quality, as a dissertation for the degree of Doctor of Philosophy.

  
\_\_\_\_\_  
Robert T. Kennedy, Chairman  
Assistant Professor, Chemistry

I certify that I have read this study and that in my opinion it conforms to acceptable standards of scholarly presentation and is fully adequate, in scope and quality, as a dissertation for the degree of Doctor of Philosophy.

  
\_\_\_\_\_  
Anna Braijter-Toth  
Associate Professor, Chemistry

I certify that I have read this study and that in my opinion it conforms to acceptable standards of scholarly presentation and is fully adequate, in scope and quality, as a dissertation for the degree of Doctor of Philosophy.

  
\_\_\_\_\_  
James D. Winefordner  
Graduate Research Professor,  
Chemistry

I certify that I have read this study and that in my opinion it conforms to acceptable standards of scholarly presentation and is fully adequate, in scope and quality, as a dissertation for the degree of Doctor of Philosophy.

  
\_\_\_\_\_  
David E. Richardson  
Associate Professor, Chemistry

I certify that I have read this study and that in my opinion it conforms to acceptable standards of scholarly presentation and is fully adequate, in scope and quality, as a dissertation for the degree of Doctor of Philosophy.

  
\_\_\_\_\_  
Kenneth B. Sloan  
Associate Professor, Medicinal  
Chemistry

This dissertation was submitted to the Graduate Faculty of the Department of Chemistry in the College of Liberal Arts and Sciences and to the Graduate School and was accepted as partial fulfillment of the requirements for the degree of Doctor of Philosophy.

December 1994

---

Dean, Graduate School